tecnun
Universidad
de Navarra

Escuela de Ingenieros

Reader Architecture Characterization for Chipless Wireless Sensors Applications

by

Fátima Villa González

Acknowledgements

I would like to express my sincere gratitude to:

Dr. Daniel Valderas, who guided and directed my Bachelor Thesis and encourages me to follow the path of research;

Dr. Iñaki Sancho, who supported my initial ideas and let me use his previous work to test my project;

Dr. Héctor Solar, who let me use his RF components to build the reader.

Dr. Noemí Pérez and Dr. Javier Díaz, who showed interest in improving the design and applications of the reader;

Mr. Javier Garcia, who helped fabricating the set up of the reader and the tag models;

Cao Wenda, who came from Beijing to carry out his undergraduate project in our department in Tecnun, helped me with my Bachelor Thesis and became a good friend;

Rubén Campo, who worked with me during his Bachelor Thesis, collaborated in the redaction of a paper presented in the Eucap 2017 and kept in touch to help me with my project;

Josu Catalina, who developed the first software version of the reader and will continue improving the current program, hopefully with successful results;

Miren Azcárate, Lucía Merino and Miguel Sanz, members of the Smarts Systems Lab in Tecnun, classmates and friends, who helped, supported and advised me;

Liang Yudu, who designed and fabricated chipless tags with resonators that I could use for testing the reader;

My brother Jose Mari, who read the whole report and corrected the grammatical errors with patience;

The rest of my family, who loves me and gives me the opportunity to continue studying what I like;

Contents

List of Figures

List of Tables

Chapter 1

Objectives

The main goal of this project is to design, implement and characterize a portable chipless reader for resonator chipless tags by comparing it with a non-portable chipless reader.

In laboratory settings, test equipment such as Vector Network Analyzers (VNAs), Signal Analyzers and Digital Storage Oscilloscopes (DSO) are used. However, it is not economical to use these expensive and heavy laboratory pieces of equipment for the real-world applications of chipless RFID systems. Therefore, apart from reducing the cost by using chipless technologies, it is essential to develop a low-cost reader device that makes the system even more inexpensive. This is basically done by replacing the large and bulky equipment with some commercial components that make the device light and portable. Concretely, the design of the reader presented in this document, implements a Wideband Synthesizer with Integrated VCO in order to replace the Signal Generator. The most challenging task is the correct synchronization of the new device with the rest of the elements of the reader. This is achieved by a new computer software specifically programmed to control the whole reader, which is based on a previous version.

The system's performance is tested with several chipless tags; resonators with different resonance frequencies. The obtained results are compared to the measurements taken with a VNA and with a previous version of the reader composed by laboratory instruments. The measurements are made with a gain/phase detector that sends its data to an Arduino. Moreover, the information is processed by a Visual Studio project written in C Language that also contains the software with the user interface to control the synthesizer from the computer and all the data processing and visualization algorithms.

The aim of the project is to describe the characterization of a reader based on frequency domain detection techniques and obtain the most accurate and effective performance of it to improve the previous version of the system and approach to an applicable device.

Chapter 2

State of the Art

Radio Frequency Identification (RFID) is a wireless communication technology that lets computers read the identity of electronic tags from a distance, without requiring a battery in the tags. The tags contain information, electronically stored in an application-specific integrated circuit (ASIC) whose design and fabrication makes them more expensive. Therefore, removing the ASICs by developing Chipless RFID systems can significantly reduce the cost of the tags.

The chipless RFID system, is a novel technology that uses frequency signatures for data encoding. It is a fully passive system, in fact, its operation is completely handled by the reader, and the tag does not have any control over the communication and does not need any power supply to operate.

This section contains an overview of the background, basis and state of the art of RFID technology, focusing deeper on chipless RFID technology.

2.1 Introduction to RFID Chipless Technology

Since radio frequency waves communication and the electronic components related to it improved significantly some years ago, previous objects and people identification methods based on printed codes and data processing, which required either contact with the identifier or visibility, have been replaced with some novel methods. These recent technologies are called Radio Frequency Identification (RFID) or Contactless Identification.

Some years ago, it was impossible to provide a remote power supply to the identifier, as it required a local power source like a battery. However, with the advances in integrated

circuits it has been achieved a contactless system using no batteries. However, even if no battery is present in RFID tags, the application-specific integrated circuit (ASIC) provides information for identification and sensing with digital resolution.

Basing on backscattered signal analysis and transmitted signal analysis, it is possible to eliminate the electronics of the tags and at the same time encode and transmit data, developing a chipless technology applicable in the readers.

2.2 Backscattered Signal Analysis

Backscattering is the reflection of waves or signals in the direction from where they came. It has important applications in different science fields and is often used in radar applications.

The contactless ID system relies on RF waves for data transmission between the data carrying device called the transponder or tag, and the interrogator, also known as the reader. Therefore, backscattering of signals to encode and transmit data is one of the main operation principles of the chipless RFID technology.
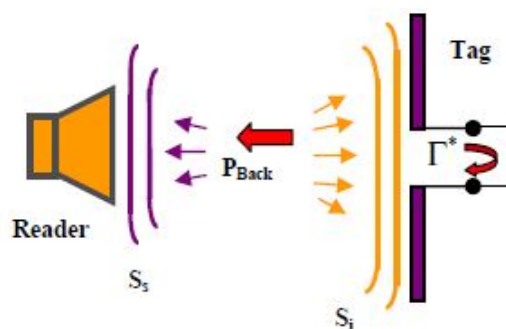
FIGURE 2.1: Backscattering in a passive chipless RFID system

2.2.1 Reflection Coefficient (S11)

The reflection coefficient is the ratio of the complex amplitude of the reflected wave to that of the incident wave, this is, it is a parameter that describes how much of an electromagnetic wave is reflected by an impedance discontinuity in the transmission medium.

The S11 is a complex number that indicates the ratio between the reflected and the incident signals. It is often represented on Polar Diagrams, Smith Charts or Log/Magnitude Graphs. Additionally, it is numerically written either in Cartesian or Polar Coordinates as it will be explained in another section, and it is sometimes called gamma (Γ).

In a system formed by two ports, Port 1 and Port 2, the S11 could be expressed as:

$$S11 = \frac{Wave\ into\ Port\ 1}{Wave\ out\ from\ Port\ 1} \tag{2.1}$$

This parameter is extracted with a set up where a transmitting antenna faces a target or sensor and a receiver antenna measures the reflected signal. The antenna that measures the backscattered wave can be either the same transmitting antenna (monostatic mode), or a different one (bistatic mode).

When measuring the S11, it must be taken into account that the surrounding environment of the antenna has an effect on it, even in the absence of a target. Therefore, it is necessary to apply a normalization factor to the reflection coefficient extracted by the reader. This procedure implies first measuring the S11 of the free space, without a tag in front of the antenna and subtracting it to the S11 measured when adding the tag. This way, the result obtained after the calibration is the normalized S11.

$$S11_{Normalized} = S11' - S11$$
$$|S11_{Normalized}|\angle\varphi_{Normalized} = |S11'|\angle\varphi' - |S11|\angle\varphi \tag{2.2}$$

Where S11' is the reflection coefficient of the system with the tag and S11 is the reference reflection coefficient (S11 of the environment).

2.2.2 The Friis Transmission Equation

The Friis Transmission Equation (2.3) gives the power received by one antenna under idealized conditions, given that another antenna some distance away is transmitting a known amount of power.

$$P_r = P_t G_t G_r (\frac{\lambda}{4\pi R})^2 \tag{2.3}$$

P_r is the received power, P_t is the transmitted power, G_t is the gain of the transmitting antenna, G_r is the gain of the receiving antenna, λ is the wavelength and R is the distance between antennas. The factor $(\frac{\lambda}{4\pi R})^2$ is the free-space loss factor. It reflects two effects: (1) the decrease in the power density due to the spherical spread of the wave through the term $\frac{1}{4\pi R^2}$, and (2) the effective aperture dependent on the wavelength as $\frac{\lambda^2}{4\pi}$.

If the transmission line introduces losses in addition to those of the antenna system, these need to be taken into account as well.
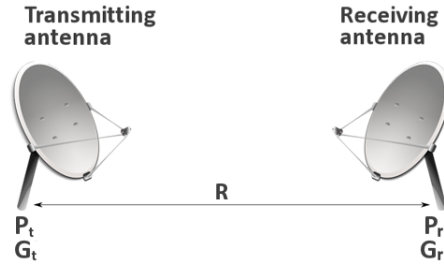
FIGURE 2.2: Transmitter-Receiver Configuration

In a system based on backscattering of signals, the Friis Equation must be applied twice; from the transmitting antenna to the tag and from the tag to the receiving antenna. This is, in both directions of the communication.

2.2.3   Radar Range Equation (RRE)

The Friis equation (2.3) is considered the One-Way Radar Equation, which is then extended to the Two-Way Radar Equation.

The gain of the receiving antenna is affected by the Radar Cross Section, σ, which will be explained in the next section.

$$G_r = \frac{4\pi\sigma}{\lambda^2} \tag{2.4}$$

Replacing it in equation 2.3:

$$P_{reflected\ from\ target} = P_t G_t \frac{4\pi\sigma}{\lambda^2}(\frac{\lambda}{4\pi R})^2 = \frac{P_t G_t \sigma}{4\pi R^2} \tag{2.5}$$

The equation for the power reflected in the radar's direction is the same as equation 2.3 except that $P_t G_t$, which was the original transmitted power, is replaced with the reflected signal power from the target from equation 2.5. This gives:

$$P_{reflected\ received\ back\ at\ input} = \frac{P_t G_t \sigma}{4\pi R^2} \frac{G_r \lambda^2}{(4\pi R)^2} \tag{2.6}$$

If like terms are cancelled, the Two-Way Radar equation is obtained and the peak power at the receiver input is:

$$P_r = \frac{P_t G_t G_r \lambda^2 \sigma}{(4\pi)^3 R^4} \tag{2.7}$$

The Radar Range Equation (RRE) gives the ratio of the transmitted power to the received power, after it has been scattered (re-radiated) by a target of cross-section σ. According to the RRE,

$$\frac{Pr}{Pt} = \frac{G_t G_r \lambda^2 \sigma}{(4\pi)^3 R^4} \tag{2.8}$$

where P_r is the received power from the tag by the receiver antenna in watts, P_t is the transmitted power from the transmitter antenna, σ is the RCS of the chipless tag, R is the distance from the reader to the tag, G_r is the transmitting antenna gain, and G_r is the receiver antenna gain.

If the chipless tag reader uses the same antenna for transmitting and receiving (monostatic mode), the previous equation is reduced to:

$$\frac{Pr}{Pt} = \frac{G^2 \lambda^2 \sigma}{(4\pi)^3 R^4} \tag{2.9}$$

This equation can be directly related to the reflection coefficient S11.

$$|S11|^2 = \frac{G^2 \lambda^2 \sigma}{(4\pi)^3 R^4} \tag{2.10}$$

2.2.4 Radar Cross-Section (RCS)

The size and ability of a target to reflect radar signals in the direction of the radar receiver can be expressed a single term, σ, known as the Radar Cross-Section. The definition of RCS includes the fact that not all the radiated energy falls on the target. At the resonant frequency it is given by equation 2.11:

$$\sigma = 4\pi R^2 \frac{S_{tag}}{S_{reader}} \tag{2.11}$$

S_{reader} is the incident power density and S_{tag} is the power density at the receiver, determined by the following equations:

$$S_{reader} = \frac{P_{reader-T} G_{reader}}{4\pi R^2} \tag{2.12}$$

$$S_{tag} = \frac{P_{tag-T} G_{tag}}{4\pi R^2} \tag{2.13}$$

where $P_{reader-T}$ and P_{tag-T} are powers transmitted by the reader and scattered by the tag respectively, while G_{reader} and G_{tag} are the gains of the reader and tag antennas.
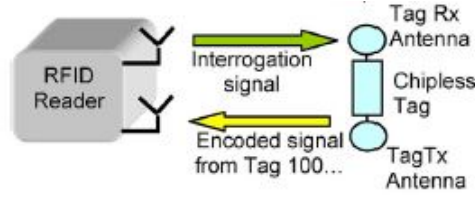
FIGURE 2.3: Schematic of the "reader-tag-reader" link

The power P_{tag-R} collected by the tag is defined as the product of the incident power density and the effective aperture of the tag.

$$P_{tag-R} = S_{reader} A_{etag} \tag{2.14}$$

with

$$A_{etag} = \frac{\lambda^2}{4\pi} G_{tag} \tag{2.15}$$

The backscattered power P_{tag-T} for backward link is shown in equation 2.16, where K is the transmission factor that describes the power dissipated in the tag antenna.

$$P_{tag-T} = P_{tag-R} K \tag{2.16}$$

with

$$K = |1 + \Gamma^*| \tag{2.17}$$

Γ is defined as the reflection coefficient, shown in Figure 2.1.

$$\Gamma^* = \frac{Z_a^* - Z_l}{Z_a + Z_l} \tag{2.18}$$

$Z_a = R_a + jX_a$ is the complex antenna impedance and Z_l is the complex load impedance, which is assumed to be 50Ω for a chipless tag.

$$K = \frac{4R_a^2}{|2Z_a|^2} \tag{2.19}$$

After replacing each term by its expression, the RCS (2.11) becomes:

$$\sigma = 4\pi R^2 \frac{P_{tag-T} G_{tag}}{P_{reader-T} G_{reader}} = A_{etag} G_{tag} K = \frac{\lambda^2}{4\pi} * G_{tag}^2 * K \tag{2.20}$$

If K is plugged in into the previous formula, the expression for the Radar Cross-Section is deduced.

$$\sigma = \frac{\lambda^2 G_{tag}^2 R_a^2}{\pi |2Z_a|^2} \tag{2.21}$$

Understanding the RCS behavior is important for the efficient design of chipless tags. It can be observed that the only parameter in the RCS equation (2.21) that has an effect on the phase φ_N of the S11 is K. From its formula (eq. 2.19) and using Euler's identity, the phase of K, and therefore the phase of the S11, can be deduced.

$$|S11|\angle\varphi_N = \arctan(\frac{\Im\sqrt{K}}{\Re\sqrt{K}}) \tag{2.22}$$

2.3 Transmitted Signal Analysis

The transmission of signals through the tag is also a significant technique in chipless systems. In fact, they rely on a similar theoretical background as the ones based on the reflection of waveforms, even though measured parameter is the forward transmission coefficient (S21), instead of the reflection coefficient (S11).

Therefore, in this section only the general concept of transmission coefficient will be explained, as the rest of equations and concepts related to power transmission are similar to the previous ones.

2.3.1 Forward Transmission Coefficient (S21)

The forward transmission coefficient is the ratio of the complex amplitude of the transmitted wave to that of the incident wave at a discontinuity in the transmission line.

$$S21 = \frac{Wave\ into\ Port\ 2}{Wave\ out\ from\ Port\ 1} \tag{2.23}$$

In a system formed by two ports, Port 1 and Port 2, the S21, is a complex number that indicates the ratio between the incident waveform and the one transmitted after passing through a tag, this is, the relationship presented in equation 2.23.

This parameter is extracted with a set up where a target or sensor is located between a transmitting and a receiving antenna, facing the first one (bistatic mode). The signal going through the tag will be measured by the antenna placed behind it.

As it happened for the reflection coefficient, S11, when measuring the S21, it is necessary to apply a normalization factor to the measured transmission coefficient. The rest of the equations describing the behaviour of waveforms across the system (power transmission, RCS and RRE) can be applied to the S21 the same way they were used with the S11. This is possible because the S11 and the S21 are closely related by the reflection coefficient Γ in equation 2.18. The transmission coefficient is defined as $1 + \Gamma^*$.

$$1 + \Gamma^* = \frac{2Z_a^*}{Z_a + Z_l} \tag{2.24}$$

In the following image there is a schematic of the S-parameters, where the forward reflection and the forward transmission coefficients (S11 and S21) are represented.
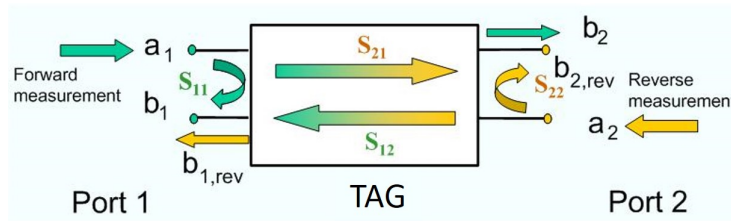
FIGURE 2.4: Representation of S-parameters

2.4 Operating Principle of the Chipless RFID System

2.4.1 Operation of the Chipless RFID Tag

The identification and extraction of data from the chipless tags that have no on-board ASIC is done by analyzing the signal that they reflect or back-scatter, based on the equations explained before. In the last years, some chipless tags have been developed, but most of them are still prototypes. The reader in this project is designed for extracting information from frequency domain based tags, concretely from resonator based chipless tags.

In terms of operating frequency, the system works in a very big bandwidth, greater than 500 MHz. The multiresonator based tag is a fully passive transponder that resonates at different frequencies of the operating frequency bandwidth, where every resonator is a bandstop filter. It uses amplitude attenuation and phase jumps in a continuous wave for encoding data.

Therefore, if the response of the filter in frequency domain is H(f), then the amplitude response A(f) and phase response ϕ(f) of a N resonance tag can be expressed as:

$$A(f) = \prod_{i=1}^{N} |H_n(f)| \tag{2.25}$$

and

$$\phi(f) = \sum_{i=1}^{N} \angle H_n(f) \tag{2.26}$$

Since the chipless tag is a passive structure, it is necessary to have an external source of electromagnetic signals for the interrogation of the tag. The sent wideband signal is captured by the tag and the resonators start resonating at the corresponding frequencies creating attenuations in the designed frequency. Moreover, phase jumps are also created at these frequencies. After that, the attenuated signal is retransmitted by the tag to the antenna of the reader. As it can be easily deduced, the absence resonator does not create either attenuation nor phase jumps. The signal received by the reader is the one that has a certain frequency signature determined by the tag, due to the presence and absence of bandstop filters. Depending on the combinations of resonant frequencies used in the tag, the frequency signature can vary. However, the tags used in this project resonate only at a single frequency, which will be detected by the reader.

The signal transmitted towards the tag is compared to the one received by the reader. The data corresponding to the gain $A(f)$ and phase $\phi(f)$ of both signals are analyzed by a differential gain/phase detector and based on this comparison, attenuations and phase jumps are identified with a hardware based process. The RF section outputs the gain and phase information of the tag and a microcontroller analyzes them. The operation of the chipless reader represented in Figure 2.6 will be explained in detail in chapter 3.
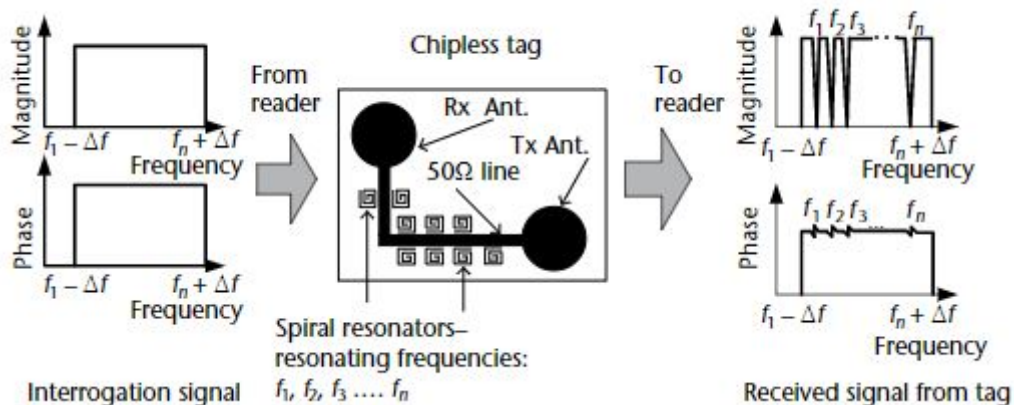
FIGURE 2.5: Operating Principle of the multiresonator based chiples Tags
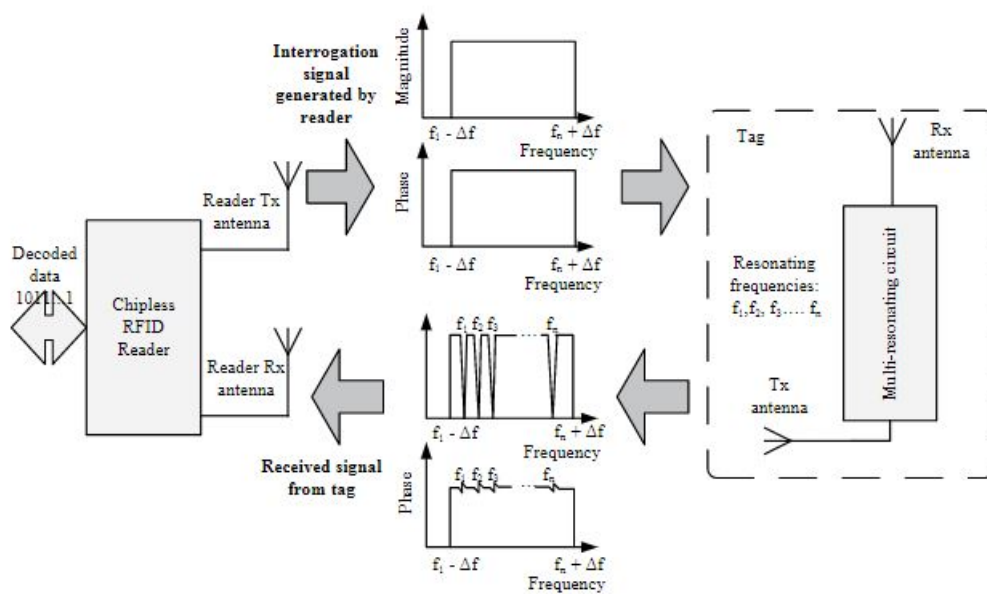
FIGURE 2.6: Operating Principle of the multiresonator based chiples RFID system

Chapter 3

Frequency Domain Chipless Tag Reader Operation

The designed reader detects the resonance frequency of the chipless tags. Its operation is presented in this chapter for a better understanding of its architecture and development.

The spectral signature detection process consists of two main stages: the generation of a wideband interrogation signal and the gain and phase detection.
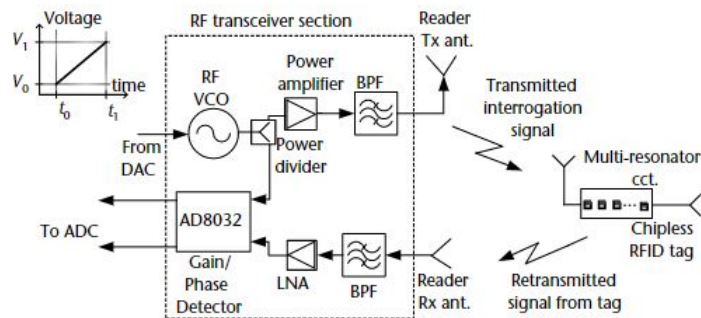
FIGURE 3.1: Block Diagram of a common Chipless RFID reader

A frequency sweep signal is generated by a VCO, passed through the tag and the retransmitted signal is captured by the receiving antenna. A reference signal is extracted directly from the output of the VCO using a power divider and it is fed to a gain/phase detector (GPD). With the use of the GPD, it is possible to extract both the amplitude and phase responses of the frequency signature of the tag and identify the amplitude differences and phase jumps that occur due to resonators of the chipless tag. The reliability of the readings depends on the ability to recover both amplitude and phase in the RF section of the reader. After this detection, the amplitude and phase signals are processed in a PC to extract the value of the resonance frequency.

3.1   Generation of a Wideband Interrogation Signal

The first step for the reader is the generation of an interrogation signal that covers the whole range of frequencies around the resonance of the tag. Such a wide band can be generated using a VCO (Voltage Controlled Oscillator), or as it will be explained later, using a PLL (Phase Locked Loop). When a voltage ramp is applied as the tuning voltage over a certain period of time T, the frequency output of the VCO varies over T from a frequency f_1 to f_2, generating a frequency sweep of a range between these two values. However, even if the sweep has a constant amplitude, it is not continuous, but stepped. It can be approximated to an ideal sweep by applying very small voltage steps, so that the output of the VCO is almost a linear voltage ramp. The resolution of the output of the VCO is decisive in the reader development, because it affects the value of the detected resonance frequency.

It is worth to mention, that if a PLL is used with the objective of generating the wideband interrogation signal, the conversion from voltage to frequency is done by the device, so only f_1, f_2 and the sweep spacing between those two frequencies need to be selected in its software.
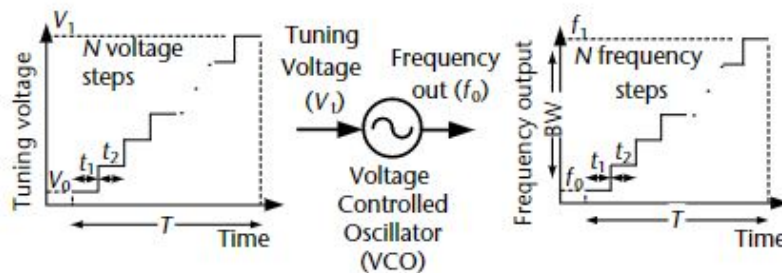
FIGURE 3.2: Generation of a wideband linear stepped frequency signal with a VCO

3.2   Process of Detecting the Features of Frequency Signatures

The attenuations and phase jumps introduced by the resonating circuit must be detected in order to identify the resonance frequency of the tag.

The identification of these features is done by using a gain/phase detection module. A diagram of this stage is shown in Figure 3.3. The transmitted signal, taken as a reference is compared with the signal received from the tag. The GPD outputs both the differences in amplitude and in phase between these two signals. At attenuated frequencies, the measured gain and phase measurements show peak values for the DC voltage outputs of the GPD. Information about the voltage values can be extracted from

the datasheet of the component with this functionality. The resonance frequencies are known, so these experimental peaks can be plotted or observed and it can be confirmed if they correspond to the theoretical ones. If there is no peak of amplitude information or a phase jump, it means that the tag does not resonate at that frequency.
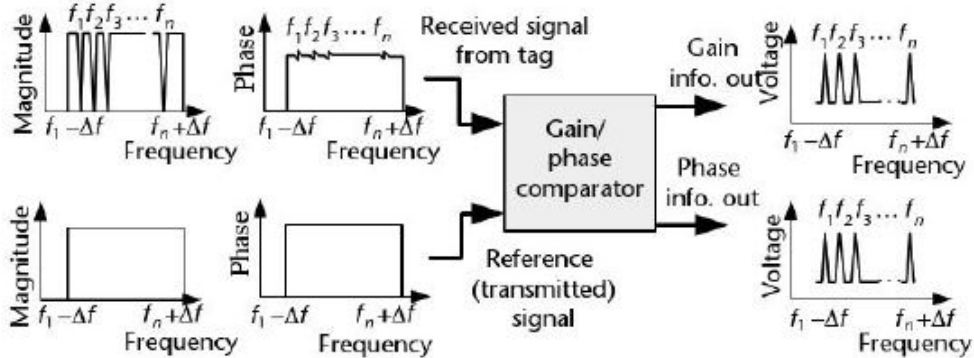
FIGURE 3.3: Identification of the frequency signature of the chipless tags by the reader

3.3 Block Diagram of the Chipless Tag Reader

The component-level block diagram of the designed reader is shown in Figure 3.4. It is quite different to the commercial readers' structure, but the operation principle is similar.
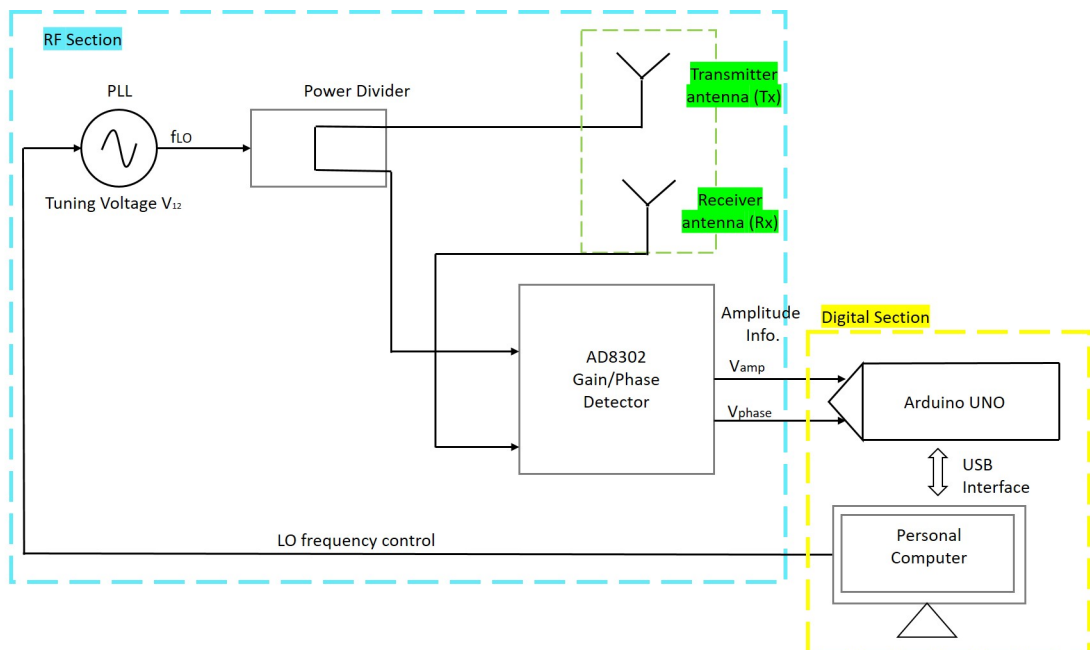
FIGURE 3.4: Block Diagram of the Chipless Tag Reader with two antennas, one for transmission and one for reception

There is a chance of using only a single antenna to transmit and receive the signals in the reader. In this case, instead of implementing a power divider, the component used

with a similar functionality would be a bidirectional coupler. The block diagram for this alternative configuration is presented in Figure 3.5.
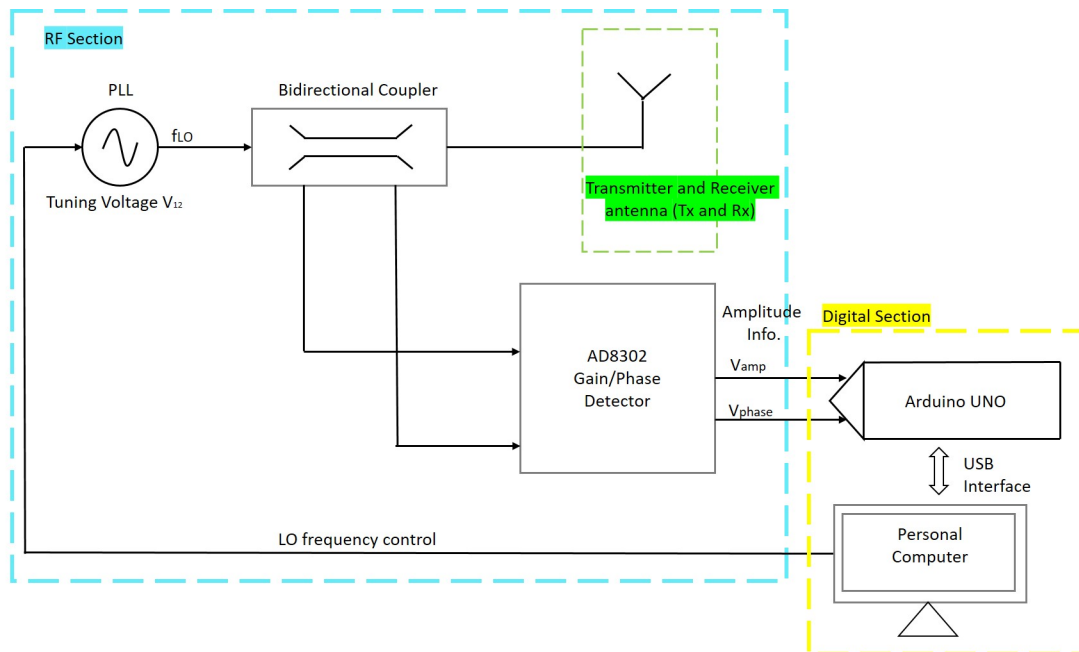
FIGURE 3.5: Block Diagram of the Chipless Tag Reader with a single antenna for transmission and reception

The operation of the digital part of the reader, this is, where the signal processing is done in order to identify and plot the frequency, will be explained in Chapter 4.

3.4   Operation Modes of the Chipless Tag Reader

Depending on the architecture of the chipless tag reader and on the location of the tag with respect to the reader's antennas, the device can operate in three different modes:

1. Bistatic Transmission Mode

2. Bistatic Reflection Mode

3. Monostatic Reflection Mode

The bistatic modes work when the reader is composed by two antennas, as it happens in Figure 3.4. Tx antenna is for the transmission of the interrogation signal, and Rx is for the reception of the signal coming from the chipless tag. If a single antenna is used by the reader to both, transmit and receive the signals, as in Figure 3.5, the reader is operating in a monostatic mode.

3.4.1 Bistatic Transmission Mode

The chipless tag reader operates in a Bistatic Transmission Mode when the tag is located between the Tx and the Rx antennas at the same distance of both of them.

FIGURE 3.6: Diagram of the antennas and tag for the Bistatic Transmission Mode

After the interrogation signal outputs the VCO, it goes through a power divider. The signal from one of the branches is directly sent towards the resonating structure, and the other one is used as a reference of the transmitted signal in the gain/phase detector. Once the interrogation signal hits the tag, it goes through it until reaching the receiving antenna of the reader positioned on the other side. The attenuated waveform detected by the Rx antenna is fed into the gain/phase detector to compare it with the reference.

Therefore, the parameter measured when using this configuration is the transmission coefficient S21. At this point, the digital section of the reader is in charge of the analysis of the signal, and the necessary information is extracted from it.

3.4.2 Bistatic Reflection Mode

The chipless RFID reader is said to work in a Bistatic Reflection Mode, if the Tx and the Rx antennas are located one on top of the other, both facing the tag, which is in the middle of them a certain distance away.
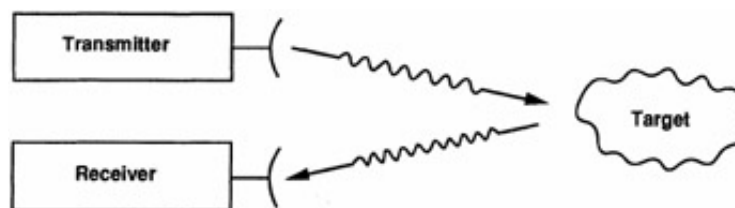
FIGURE 3.7: Diagram of the antennas and tag for the Bistatic Reflection Mode

The interrogation signal coming from the VCO goes through a power divider as it happened in the previous case. The outputs of both branches of the divider follow the same path as before, one goes towards the resonating structure, and the other one is inputted to the gain/phase detector. The signal that hits the chipless tag does not go

through it this time. Instead, it is backscattered by the resonator back to the way it came from. However, the Rx antenna is the one in charge of receiving the attenuated waveform and sending it to the gain/phase detector in order to compare it with the reference and operate.This operation mode is based on the reflection of signals, indeed, the measured and analyzed parameter is the reflection coefficient S11.

3.4.3 Monostatic Reflection Mode

For the Monostatic Reflection Mode, the reader only needs to implement a single antenna that acts as the trasmitter and the receiver. This TX and Rx antenna faces the chipless tag, as observed in Figure 3.8.
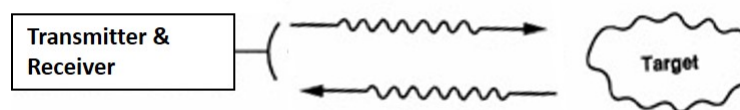
FIGURE 3.8: Diagram of the antennas and tag for the Monostatic Reflection Mode

This time, the block diagram of the reader is quite different from the previous one. It does not have a power divider, but a bidirectional coupler after the VCO. The interrogation signal goes through the coupler and its output is plugged into the antenna. The waveform goes towards the resonating structure and it is backscattered by it, back to the same antenna. The received attenuated waveform inputs the bidirectional coupler in the opposite direction. The two signals compared in the GPD are the coupled input signal and the coupled output signal, that correspond to the S11 between the transmitted and reflected signals. This way, two S11 values are compared and the gain/phase detector gives the appropriate voltage values to study in the digital section.

Example of a Monostatic Chipless RFID Reader

The following paragraphs describe the operation of a Monostatic Chipless RFID Reader developed and commercialized, which works within a low frequency range. A reader with a similar configuration was used to do several measurements of chipless tags with resonance frequencies around 20 MHz.The block diagram of the reader is shown in Figure 3.9.

The device contains a RF source that generates a frequency sweep in the 1-50 MHz range used as the interrogation signal. This waveform goes through a directional coupler

until it reaches a loop antenna that transmits it to a chipless RFID tag that resonates at certain frequencies. The tag sends back a response with the corresponding spectral signature to the antenna. Then, the signal is fed into the coupler in the opposite direction of the interrogation signal, but instead of going out through the input port, it outputs the device from the third port. This output is connected to a detector that samples and measures the power of the received signal, identifying the peaks in the amplitude.
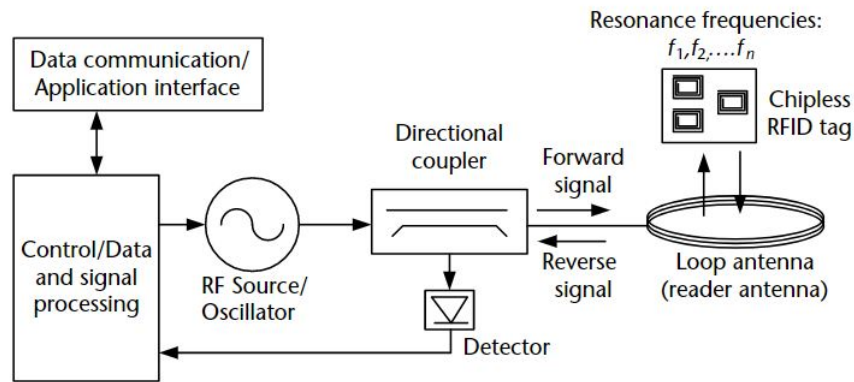
FIGURE 3.9: Diagram of the chipless RFID reader antennas and tag for the monostatic reflection mode of operation

The developed reader has the Monostatic Operation Mode block diagram, combined with the monostatic reader diagram, due to the fact that it uses a loop antenna as Tx and Rx.

Chapter 4

Frequency Domain Chipless Tag Reader Development

The design and development of the chipless RFID reader is done in two parts: the RF section and the digital section. Block diagrams in Figure 3.4 and Figure 3.5 show the general architecture of the reader for the three operation modes.

There are two versions of the reader developed with real components:the non-portable one and the novel portable one. The first version uses a signal generator as the interrogation signal source, and for the portable version, the heavy laboratory equipment is replaced by a PLL (Phase Locked Loop) that lightens the weight of the reader.

Some of the measurements to check that the device does a correct detection of the resonance frequency of the tags are made with the non-portable version, so its operation and the components that differ from the novel version are explained. Besides, both versions diverge in the software used in order to do the digital signal processing part; being MATLAB the software implemented in the non-portable version and C the programming language in Visual Studio for the portable one.

4.1 Design of the Chipless Tag Reader

The design of the reader is done in a single module or board where all the necessary components to fabricate the device are placed easing the connections. The platform contains both the power divider, necessary for the bistatic operation modes of the reader, and two bidirectional couplers that work at different frequency ranges, implemented with the aim of using the reader in the monostatic operation mode.

21
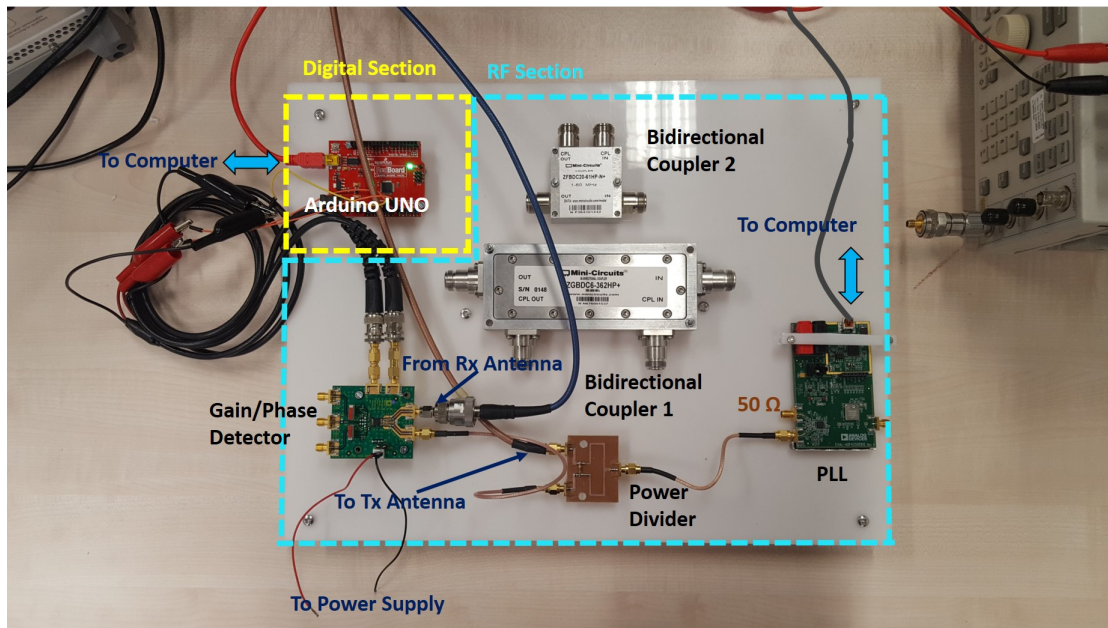
FIGURE 4.1: Chipless Tag Reader connected for the Bistatic Operation Mode
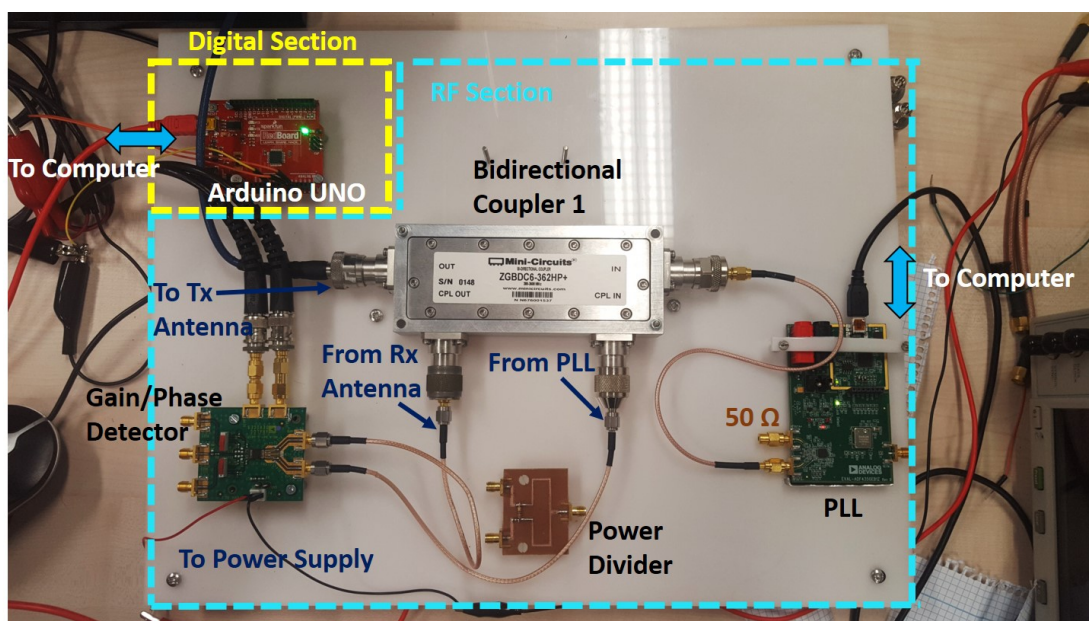
FIGURE 4.2: Chipless Tag Reader connected for the Monostatic Operation Mode

The reader with the connections for the Bistatic Operation Mode is shown in Figure 4.1 and the one for the Monostatic Mode is in Figure 4.2.

The RF section of the bistatic system consists of a Wideband Synthesizer with Integrated VCO (ADF4350 PLL), a power divider, a gain/phase detector (AD8302) and two antennas. On the other hand, the power splitter is replaced by a bidirectional coupler (ZGBDC6-362HP+ or ZFBDC20-61HP-N+) and one antenna is removed in the monostatic system. The PLL and the GPD are implemented with their corresponding evaluation boards, but in a future

design of the reader, they could all be set up in the same PCB, adding the necessary elements for their correct operation. Moreover, in order to power up the AD8302, there is an Agilent Power Supply (E3646A).

The Arduino UNO with a SparkFun RedBoard and the PC are considered part of the digital section.

The design supports the identification of the resonance frequency of chipless tags that resonate at a single value. To generate a frequency sweep covering the desired frequency range with the selected spacing between frequencies, the EVAL-ADF4350EB1Z Evaluation Board for Fractional-N/Integer-N PLL Frequency Synthesizer is used. This element is connected to the computer through the USB interface and it is controlled with its corresponding Analog Devices PLL software. When passing through the power splitter, half of the interrogation signal generated goes to the reader Tx antenna and half goes to the gain/phase detector unit. The waveform backscattered by the chipless tag is read by the Rx antenna and fed to the other input of the GPD. The two outputs of the AD8302 are read with two pins of the Arduino UNO and finally, the analog signal is converted into digital and sent to the PC for signal processing.

Furthermore, the technology operates over a wide frequency band of 2.5625 GHz (137.5 MHz to 2.7 GHz). The low frequency limit is set by the PLL and the upper limit is set by the gain/phase detector, even though the PLL is able to reach up to 4.4 GHz.

4.2 Components of the Novel Portable Version of the Reader

4.2.1 ADF4350 Wideband Synthesizer with Integrated VCO

The ADF4350 is the component that generates the interrogation signal (frequency sweep) that will be sent across the circuit.

It allows the implementation of fractional-N or integer-N phase-locked loop (PLL) frequency synthesizers if it is used with an external loop filter and an external reference frequency. These additional elements are included in the EVAL-ADF4350EB1Z evaluation board designed for the component, characterized in the next section.

The ADF4350 has an integrated Voltage Controlled Oscillator (VCO) with a fundamental output frequency range from 2200 MHz to 4400 MHz. Additionally, divide-by-1/2/4/8 or 16 circuits make it possible to generate RF output frequencies as low as 137.5 MHz. Therefore, the frequency range covered by the PLL goes from 137.5 MHz up to 4400

MHz. According to the RF output, four output power levels may be set. These levels give output power levels of -4 dBm, -1 dBm, $+2$ dBm, and $+5$ dBm, respectively.

Furthermore, there are a number of ways to match the output of the ADF4350 for optimum operation; the most basic is to use a 50 Ω. Nevertheless, the structure of the connections to the device can be examined using the evaluation board. The device operates with a power supply ranging from 3.0 V to 3.6 V. After the correct application of voltages to the supply pins, the 6 on-chip registers, which allow setting all the parameters specified in the data sheet of the component, must be written following the correct sequence (from register 5 to register 0).
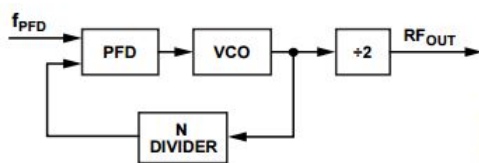
FIGURE 4.3: Loop Closed Before the Output Divider
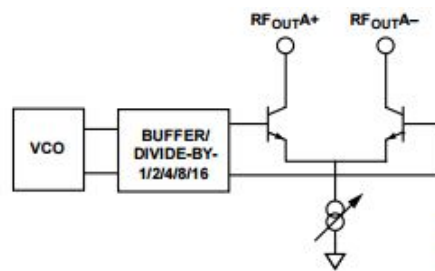
FIGURE 4.4: Output Stage of the ADF4350

4.2.2 EVAL-ADF4350EB1Z Evaluation Board

The EVAL-ADF4350EB1Z is the evaluation board used to evaluate the performance of the ADF4350 Fractional-N/Integer-N PLL Frequency Synthesizer with Integrated VCO.

Figure 4.5 shows a picture of the board. The hardware contains the ADF4350 synthesizer, a USB connector and related interface, a 25 MHz TCXO reference source, SMA connectors for the RF outputs, and reference signal plus headers for various signals and voltages. There is also a loop filter (35 kHz) on board. The package also contains Windows software to program the synthesizer from a PC.

FIGURE 4.5: Evaluation Board for the ADF4350

The board can be powered either from the USB port or via dc power connectors (4 mm banana connectors). In the designed reader, the board is connected to the PC. Therefore, the D6 LED will indicate that USB power is available, and D5 will indicate that the ADF4350 is powered. The evaluation board has two SMA output connectors (differential outputs). Only one port of the differential pair is used, so the other one is terminated with a 50 Ω load.

The set up of the board to visualize the generated signals is shown in Figure 4.6. For the chipless RFID reader, the optional reference connection is not used, neither the Spectrum Analyzer, as the RF output is fed to the power splitter.
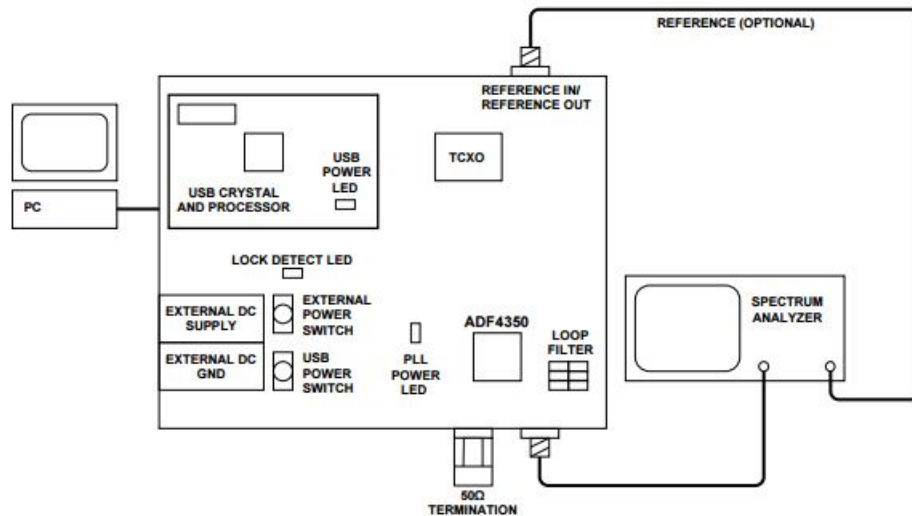
FIGURE 4.6: Set Up for the Evaluation Board
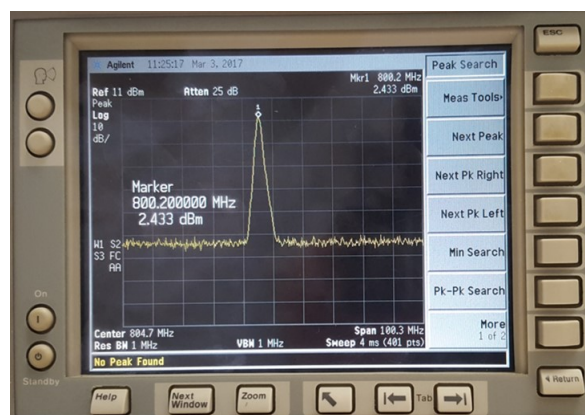
FIGURE 4.7: Tone of the Frequency Sweep Generated by the ADF4350 Evaluation Kit

The control software for the EVAL-ADF4350 accompanies the EVAL-ADF4350EB1Z on a CD. However, in order to be able to control the Arduino UNO at the same time as doing the frequency sweep, the source code of the evaluation board was downloaded from https://ez.analog.com/thread/13743 and run in Visual Studio 2015.

4.2.3 ADF4351 Wideband Synthesizer with Integrated VCO

The ADF4351 is a PLL of the same family as the The ADF4350, used to generate the frequency sweep that will be the interrogation signal. Both devices have a similar operation and are controlled with the same software. However, one of the main differences between them, which makes the AFD4351 slightly more useful, is that its frequency range is wider than for the ADF4350.

In fact, the frequency range covered by the PLL goes from 35 MHz up to 4400 MHz. This makes the device suitable for chipless tags with a low resonance frequency.

4.2.4 Power Divider

A power divider or power splitter is a passive device that couples a certain amount of the electromagnetic power flowing in one direction in a transmission line to a port, enabling the signal to be employed in another circuit.

The power divider used for the reader is composed by an input port P_1 and two output ports P_2 and P_3. When a signal enters port 1, it splits into equal-amplitude, equal-phase output signals at ports 2 and 3.
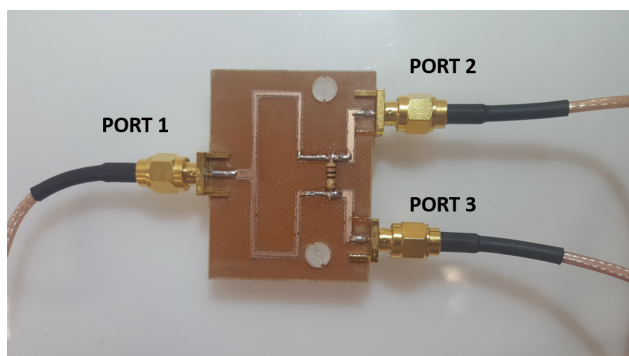
FIGURE 4.8: Power Divider

The characterization of the component was done by measuring the transmitted signal (S21) at a working frequency of 868 MHz between port 1 and port 2 and port 1 and port 3. The values are shown in Table 4.1.

S21 Measurements at 868 MHz in Ports 2 and 3		
Port	**Amplitude (dB)**	**Phase (º)**
Port 2	3,2	-148
Port 3	3,4	-149
Isolation	-24,65	164,8

TABLE 4.1: Characterization of the Power Splitter at 868 MHz

4.2.5 AD8302 RF/IF Gain and Phase Detector

The AD8302 is an integrated system for measuring gain/loss and phase by comparing two input signals. The input signals can vary from –60 dBm to 0 dBm in a 50 Ω system, from low frequencies up to 2.7 GHz. The device requires few external components and a supply of 2.7 V–5.5 V.

FIGURE 4.9: Evaluation Kit for the AD8302 Gain/Phase Detector

Moreover, the outputs are accurate measurements of gain (or loss) over a ±30 dB range scaled to 30 mV/dB, and of phase inside the range of $0^{\underline{o}}$– $180^{\underline{o}}$, scaled to 10 mV/degree. The phase and gain output voltages are available simultaneously.
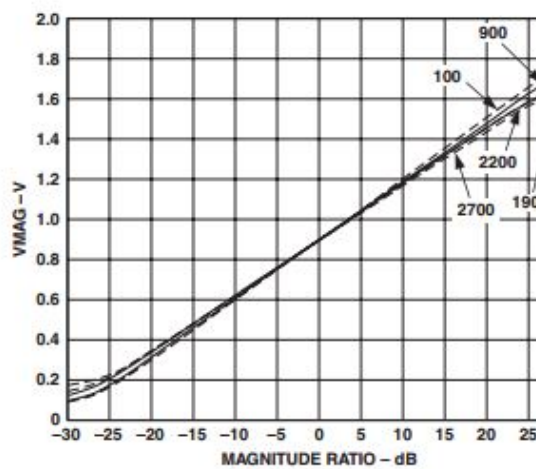
FIGURE 4.10: Magnitude Output (VMAG) vs. Gain (VINPA/VINPB)
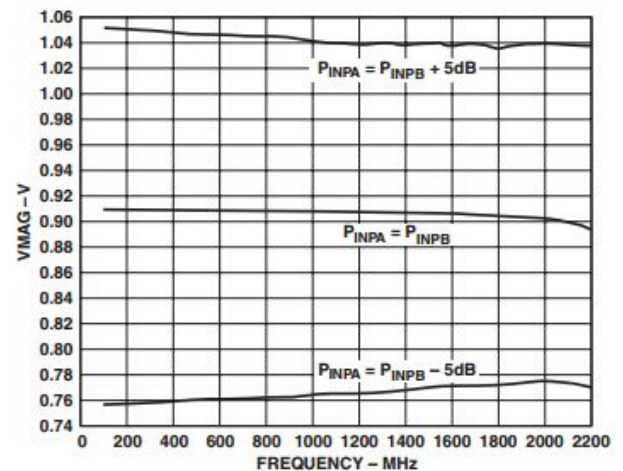
FIGURE 4.11: VMAG Output vs. Frequency

Based on the graphics, the measured voltage values at the output pins can be interpreted as amplitude values in dB and phase values in degrees. These operations are done in the source code of the PLL, in Visual Studio, after the Arduino reads the voltage from the corresponding pins and sends the data to the PC.
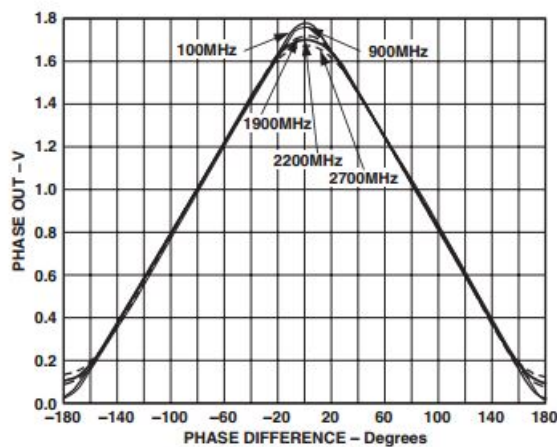
FIGURE 4.12: Phase Output (VPHS) vs. Phase Difference

4.2.6 ZGBDC6-362HP+ Bidirectional Coupler

A bidirectional coupler is an RF passive device used to couple a specific proportion of the power travelling in one transmission line out through another connection or port. Indeed, it is very useful to sample a small amount of power for measurement purposes in RF applications. It is a four port device that samples the signal on a through line, but in a way that discriminates between forward and reverse traveling waves. The four ports are generally:

1. Input (Port 1, Incident)

2. Transmitted (Port 2, Output)

3. Coupled (Port 3, Forward coupled port)

4. Isolated (Port 4, Reverse coupled port)

Typically, the main line that carries high power levels, is the one between ports 1 and 2. Ports 3 and 4 are more suited for lower powers as they only carry a small proportion of the main line power. Moreover, when the incoming signal is partially split between the output port and the coupled port, no signal appears at the isolated port.

Common desired properties for a bidirectional coupler are wide operational bandwidth, high directivity, coupling accuracy at the frequency band center (coupling factor), low main line and insertion losses, a high isolation between the input and isolated port and a good impedance match at all ports when the other ports are terminated in matched loads.
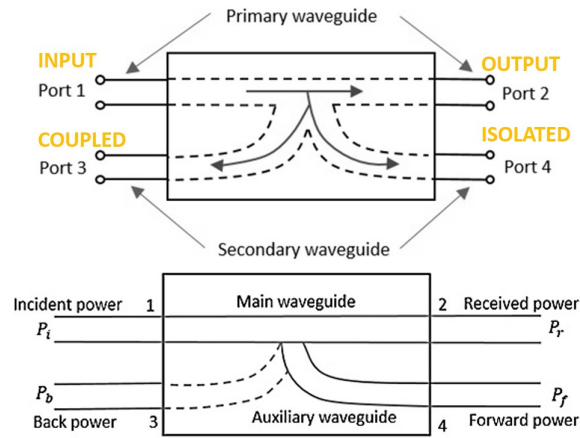
FIGURE 4.13: Diagrams of ports and powers in a bidirectional coupler

Mini-Circuits ZGBDC6-362HP+ Bidirectional Coupler works at a wide frequency range; from 380 MHz to 3600 MHz. According to its datasheet, it has a high directivity of 24.7 dB, a high power handling, 250 W and a low insertion loss of 0.20 dB.
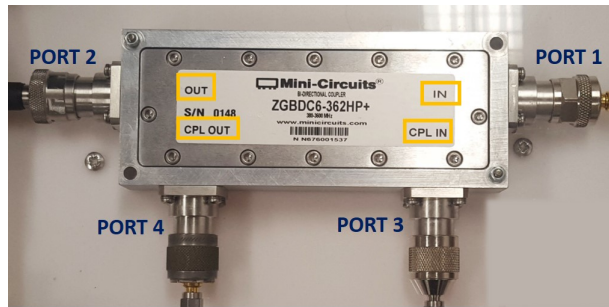
FIGURE 4.14: ZGBDC6-362HP+ Bidirectional Coupler

The characterization of the device at 868 MHz is shown in Table 4.2.

Characterization of ZGBDC6-362HP+ Bidirectional Coupler	
Feature	**Value**
Frequency Band	380-3600 MHz
Main Loss	0.2 dB
Coupling	6.6 dB
Directivity	26 dB
Return Loss	28.3 dB

TABLE 4.2: Characterization of ZGBDC6-362HP+ Bidirectional Coupler at 868 MHz

4.2.7   ZFBDC20-61HP-N+ Bidirectional Coupler

Mini-Circuits ZFBDC20-61HP-N+ Bidirectional Coupler works over a frequency range from 1 MHz up to 60 MHz. It has an excellent directivity of 30 dB, up to 25 W and a low main line loss of 0.10 dB. The characterization of the device at 20 MHz is shown in Table 4.3.

FIGURE 4.15: ZFBDC20-61HP-N+ Bidirectional Coupler

Characterization of ZFBDC20-61HP-N+ Bidirectional Coupler	
Feature	**Value**
Frequency Band	1-60 MHz
Main Loss	0.1 dB
Coupling	20.14 dB
Directivity	32 dB
Return Loss	38.8 dB

TABLE 4.3: Characterization of ZFBDC20-61HP-N+ Bidirectional Coupler at 20 MHz

4.2.8   Antennas

The antennas used in the reader are Type 1399.17.0028 planar directive antennas manufactured by Huber+Suhner. The S11 of these antennas measured with a VNA is shown in the plots in Figures 4.17 and **??**.

It can be observed that both antennas operate on a similar range from 750 MHz up to 900 MHz, so they are appropriate for the chipless tags used. Several characteristics of the antennas are indicated in Table 4.4.

FIGURE 4.16: Antenna 1 and 2
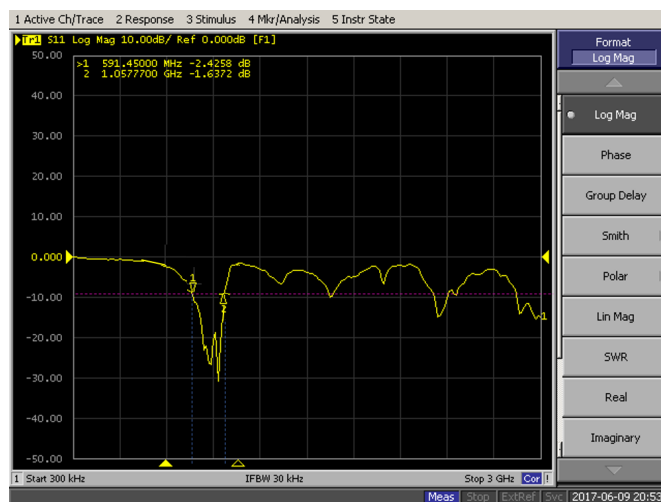
FIGURE 4.17: Working Frequency Range of the Antennas

Characterization of Antenna 1 and 2	
Feature	**Value**
Frequency	763 MHz to 985 MHz
Impedance	50 Ω
Polarization	Linear, Vertical
Gain	8 dBi
Maximum Power	75 W at 25$^{\text{o}}$
VSWR	1.8 @ 806-824 MHz
	1.5 @ 824-960 MHz

TABLE 4.4: Characterization of Antenna 1 and 2

4.2.9   Chipless Tags

The targets employed in order to test the reader are chipless tags known as resonator based chipless tags. Their operation was explained in Section 2.4.1. It is worth to mention that the resonating structures are based on LC elements and have only a single resonance frequency, which is the one identified by the reader.

The resonance frequency of the tags is determined by their capacitance, permittivity of the background material of the resonators and some additional parameters. That is the reason why these tags are easy to design, simulate and manufacture. It is important to characterize correctly each tag, because the performance of the reader will be tested based on the provided information.

778 MHz Aluminum Oxide Tag

This chipless tag is a 2 by 2 resonator matrix manufactured with Aluminum Oxide.

FIGURE 4.18: Aluminum Oxide Tag

The ideal resonance frequency of the tag is 777 MHz, as it can be observed in the CST simulation in Figures 4.19 and 4.20.
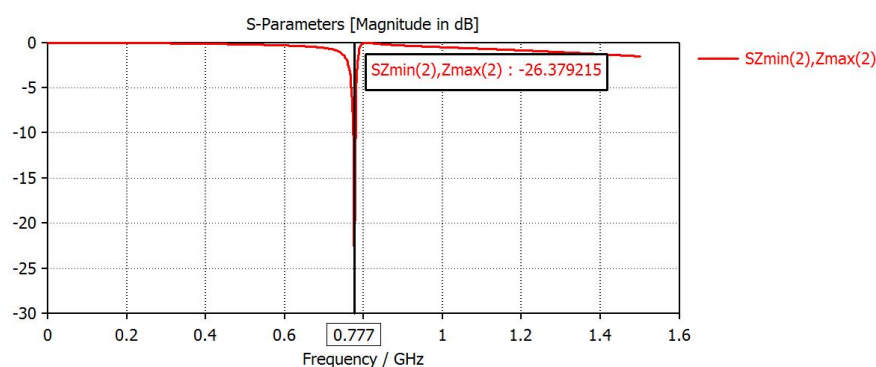
FIGURE 4.19: Gain Simulation of the Aluminum Oxide Tag
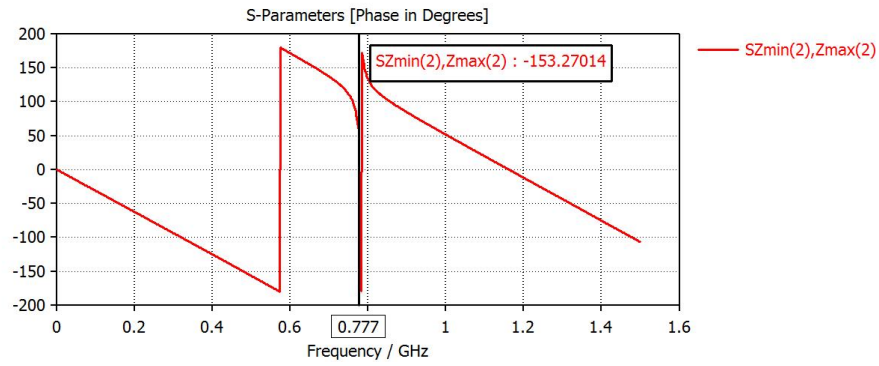
FIGURE 4.20: Phase Simulation of the Alumninium Oxide Tag

The resonance frequency is measured with the VNA. The bistatic transmission mode measurement set up is shown in Figure 4.22. The tag is located at 20 cm from each antenna, and the frequency sweep is from 700 MHz to 1000 MHz. The magnitude graph shows a peak at 778 MHz and the phase curve presents a jump at the same frequency.
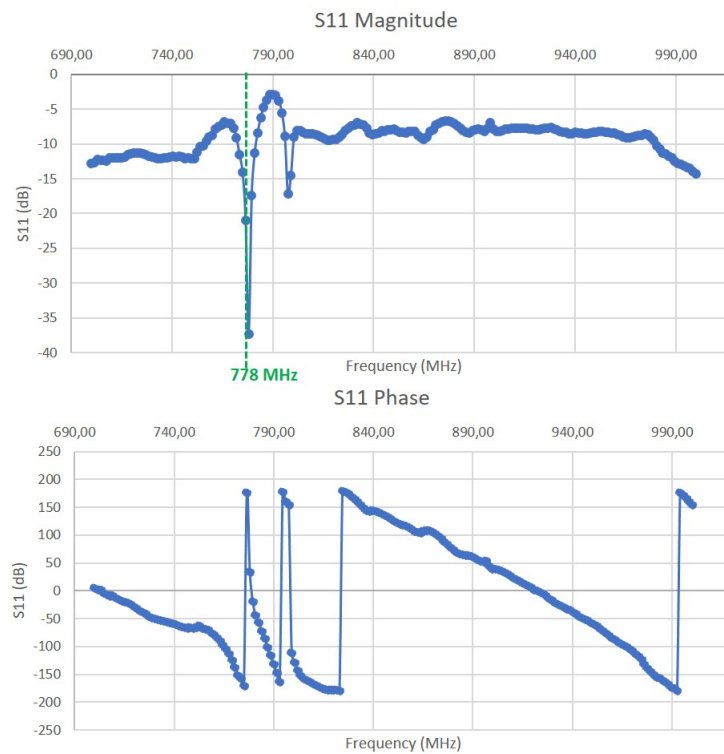
FIGURE 4.21: VNA Gain and Phase measurements of the Aluminimum Oxide Tag
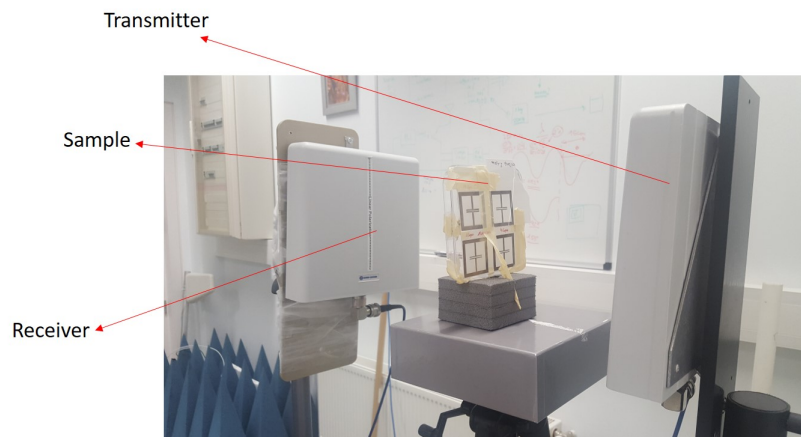
FIGURE 4.22: Set up of S11 Measurement of the Aluminum Oxide Tag with the VNA

810 MHz FR-4 Tag

This chipless tag is a 2 by 2 resonator matrix manufactured with FR-4. FR-4 is a composite material composed of woven fiberglass cloth with an epoxy resin binder that is flame resistant and has a permittivity of 4.3.

FIGURE 4.23: FR-4 Tag

The ideal resonance frequency of the tag is 820 MHz, as it can be observed in the CST simulation in Figure 4.24.

The resonance frequency has also been measured with the VNA. The bistatic transmission mode measurement set up is shown in Figure 4.26. The tag is located at 20 cm from each antenna, and the frequency sweep is from 500 MHz to 900 MHz. The S11 magnitude graph shows a clear peak at 810 MHz, and the phase plot also presents a phase-jump at that value.
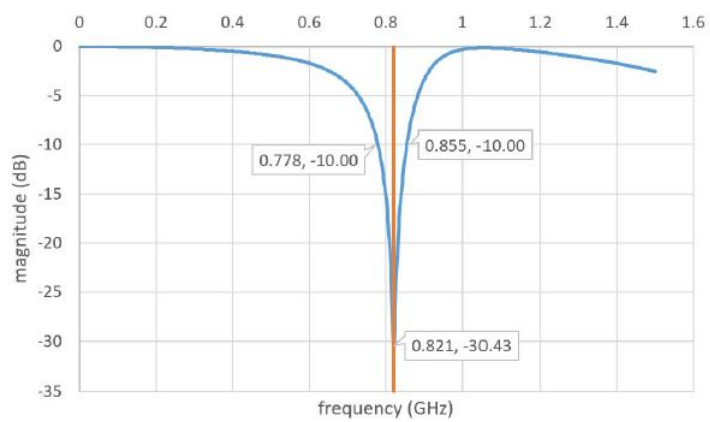
FIGURE 4.24: Simulation of the FR-4 Tag
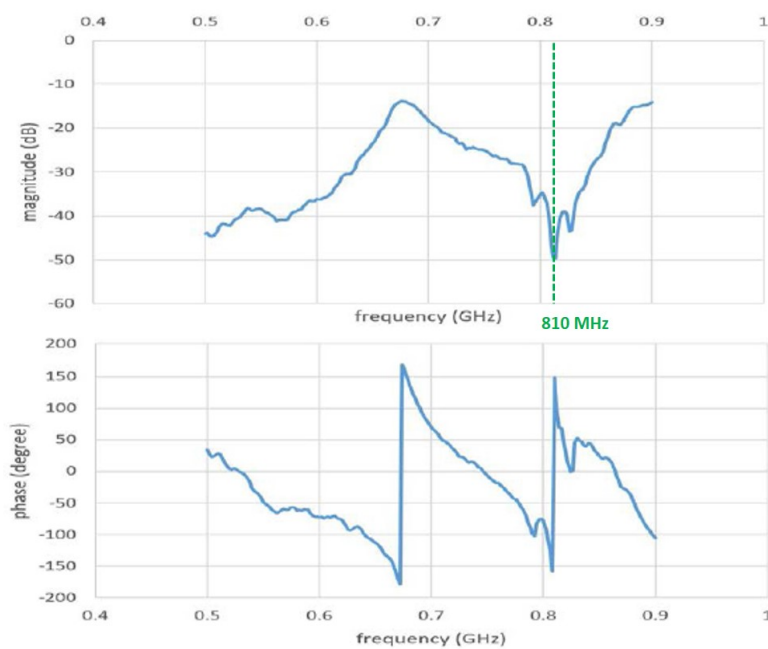
FIGURE 4.25: VNA Gain and Phase measurements of the FR-4 Tag
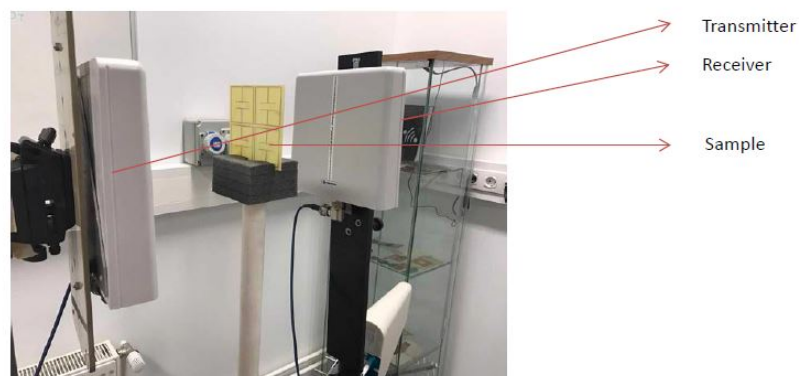
FIGURE 4.26: Set up of S11 Measurement of the FR-4 Tag with the VNA

Low Frequency Tags

These 3 tags are composed by an inductance; and their resonances frequency is measured by placing them facing a loop antenna, which acts as a wear and tear sensor. The operation mode is the monostatic reflection mode.

The resonance frequency of the tags is between 0 MHz and 40 MHz, concretely around the value of 20 MHz. The experimental values, the set up and the procedure followed in order to characterize each tag will be explained in Chapter 6.
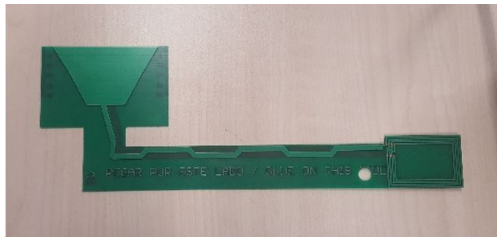
FIGURE 4.27: Tag 1

FIGURE 4.28: Tag 2

FIGURE 4.29: Tag 3

FIGURE 4.30: Loop Antenna

4.2.10 Agilent E3646A DC Power Supply

A power supply is an electronic device that converts one form of electrical energy to another. In this case, a DC power supply is one that supplies a constant DC voltage to its load. The Agilent E3646A is a 60-watt dual-output programmable power supply, with 30 to 100W of output power. It is used to power the AD8302 gain/phase detector. It is recommended to follow a certain procedure when using the power supply.

First, it is important to set the current limit of the E3646A Power Supply, so that the current coming out from it will not burn the AD8302 gain/phase detector's chip. In order to do that, it is necessary to:

1. Turn on the device

2. Press the Output on/off button

3. Press the Display Limit button

4. Press the voltage/current button

5. Adjust the maximum current

In this case, as the voltage supply for the gain/phase detector is 2.7 V, and the current that corresponds to it is 0.021 A, the current limit is set in 0.03 A. The output used is Output 1, and the steps to connect the positive and negative outputs safely are:

1. Connect the black wire to ground

2. Press the Output on/off button

3. Set the current limit

4. Connect the red wire

5. Raise the power up to 2.7 V (0.021 A)
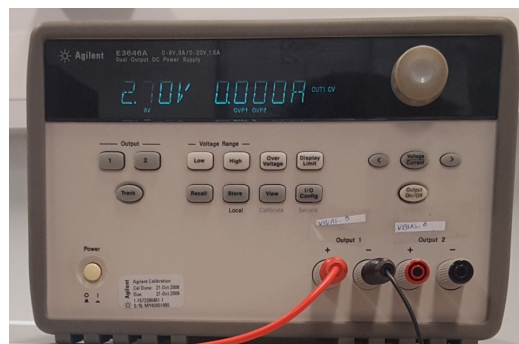
FIGURE 4.31: Agilent E3646A DC Power Supply

4.2.11 Agilent E5062A Vector Network Analyzer

A VNA is an instrument to measure the network parameters of electrical networks. Network analyzers are appropriate to measure S–parameters, this is, reflection and transmission between ports in different networks. They are mostly used at high frequencies and indicate both amplitude and phase properties. The specific equipment used is the Agilent E5062A Vector Network Analyzer, which works from 300 kHz to 3 GHz.

When a pair of antennas is connected to a VNA, a signal is emitted by one of the antennas and received by the other one. As the frequency sweep is from one predefined

value to another, the device creates a diagram on the screen of the VNA, which can be displayed on several types of plots. These two antennas are known as port 1 and port 2.

The VNA is used to characterize each tag, as their resonance frequency needs to be determined. Before doing any measurement, the VNA should be calibrated with the wires and connectors that will be used between the equipment and the antennas. Calibration is a procedure that takes into account the energy loss within the wires when testing. It includes short, open, load and through, as well as the enhanced response calibration. Frequency-sweeping range is set before calibration. The procedure followed for an S11 measurement with the VNA are:

1. Set the sweeping frequency of the VNA

2. Do the calibration

3. Do the whole set up and measure the distance between the two antennas

4. Do a measurement without the tag to get the effect of the environment and store the result

5. Put the tag between the antennas and remove the environmental influence to this measurement
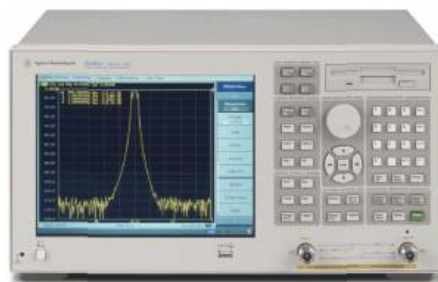
FIGURE 4.32: Agilent E5062A Vector Network Analyzer

4.2.12 Connections

The inter component connections in the RF section are fundamentally done via SMA connectors and wires. These are coaxial RF connectors with an impedance of 50 Ω. SMA is the main interface for the PLL, the power splitter and the GPD to communicate.

Bidirectional couplers are designed for N-type connectors.

Additionally, the RedBoard and the PLL are connected to the PC via USB (Universal Serial Bus) and in case the signal generator is used, it uses a USB GPIB connector to communicate with the computer.

FIGURE 4.33: USB GPIB Connector
of the Signal Generator
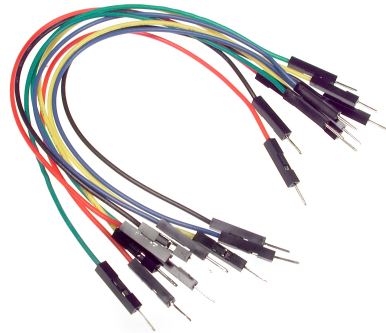
FIGURE 4.34: Jumper Wires

The gain/phase detector is connected to the analog headers of the SparkFun RedBoard programmed with Arduino UNO with jumper wires.

4.2.13 SparkFun RedBoard Programmed with Arduino UNO

Arduino is an open-source platform used for building electronics projects. It consists of a physical programmable circuit board (a microcontroller) and a software or IDE (Integrated Development Environment) that runs on the computer, to write and upload computer code to the physical board. Being open source implies that the schematics, hardware design files and source code are all available for viewing and modifying, so anyone can design and produce their own hardware versions. The SparkFun RedBoard is a microcontroller board that looks like an Arduino Uno, but it is modified.

The microprocessor on the boards is the ATmega328, it has 14 digital input/output pins and 6 analog I/Os. Furthermore, it operates at 5V, has an on-board 3.3V regulator and can be powered through USB, by connecting it to the PC.
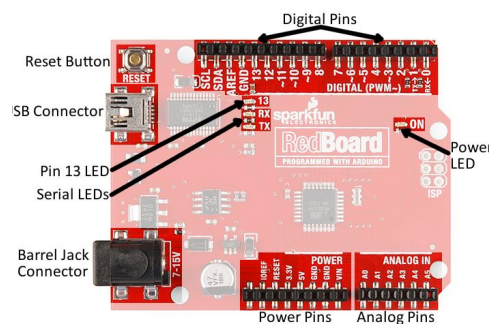
FIGURE 4.35: Basic Pins of the RedBoard Programmed with Arduino
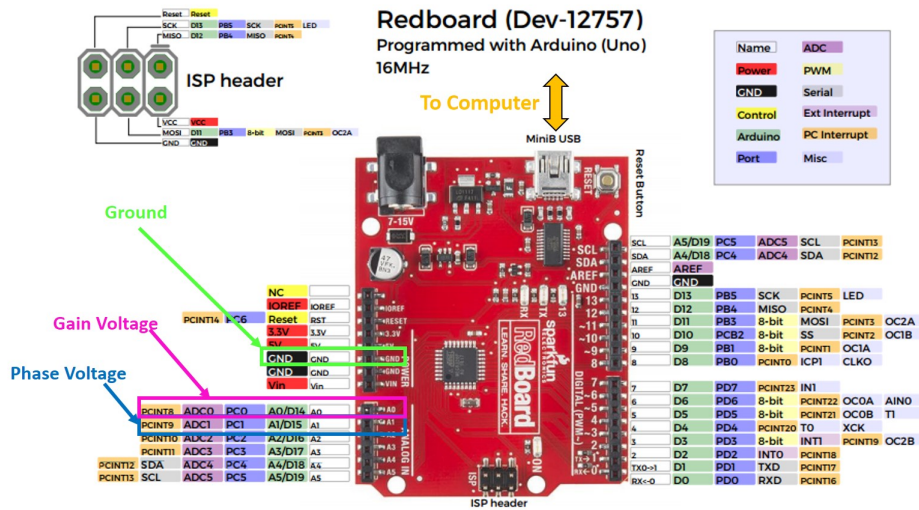
FIGURE 4.36: Graphic Datasheet of the RedBoard Programmed with Arduino

The function of the Arduino UNO in the reader is to convert the analog voltage at the gain and phase outputs of the AD8302 into digital data that can be analyzed and processed in the computer Visual Studio software. The six analog inputs on the analog header have analog-to-digital converters, so two of them are used to read in the analog voltage between 0 and 5V coming from the gain and phase outputs of the AD8302. The A0 pin is used to read the gain voltage and the A1 pin is used to read the phase difference voltage as it is shown in Figure 4.36 and 4.37.
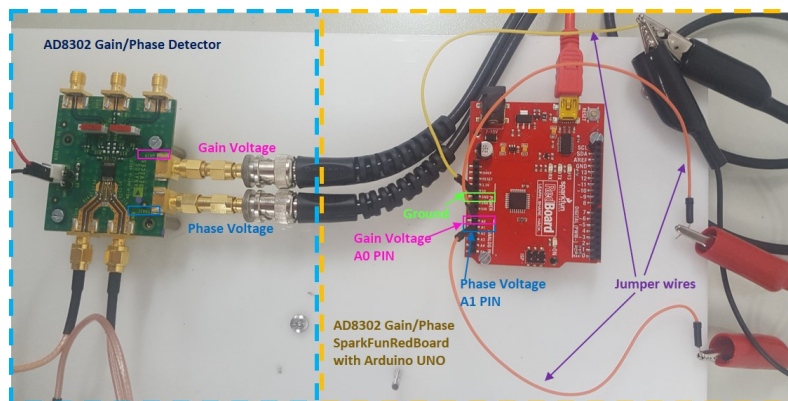
FIGURE 4.37: A0 and A1 pins to read Gain and Phase Voltages respectively

The Arduino IDE uses a simplified version of C++ programming language, however, the provided software is only used to set the data rate in bits per second (baud) for serial data transmission from the Arduino to the computer, which does not affect the synchronization with the PLL. The rest of the programming of the board is included in the C code of the software of the PLL in Visual Studio. The reason is that the reader must acquire the voltage corresponding to each frequency at the same time the sweep is being done, so a software where both devices are synchronized is needed.

4.2.14   Microsoft Visual Studio

Microsoft Visual Studio is an IDE from Microsoft used to develop computer programs for Microsoft Windows, as well as web sites, web apps, web services and mobile apps. It supports 36 different programming languages, among which C is included.

The version used to modify and run the software of the ADF4350 and program the Arduino UNO simultaneously is Visual Studio Professional 2015 with an update of the .NET Framework 4.5.2.
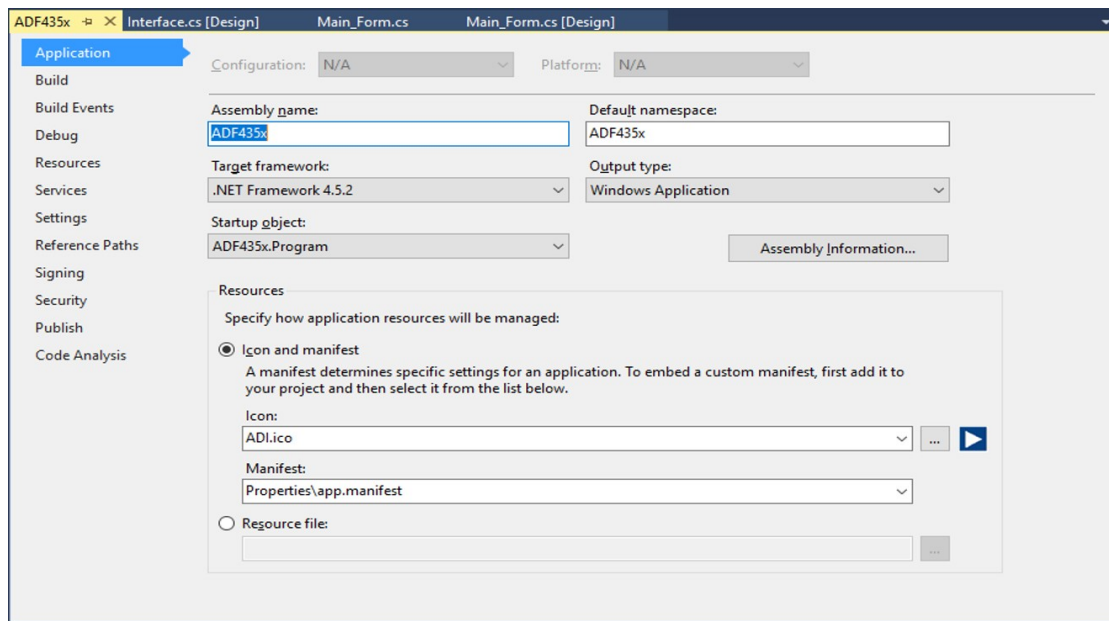
FIGURE 4.38: Interface of Visual Studio Settings of the Software Application

.NET Framework is a software framework developed by Microsoft that runs primarily on Microsoft Windows and that is used by most of the applications created for the Windows platform. It includes a large class library called Framework Class Library (FCL) that provides user interface, data access, database connectivity, cryptography, web application development, numeric algorithms, and network communications. Software is produced by programmers by combining their source code with .NET Framework and other libraries. Visual Studio can also be defined as an integrated development environment largely for .NET software produced by Microsoft.

Communication with the Arduino in Visual Studio

Visual Studio is not the default program for the PC to communicate with Arduino, so it is necessary to install a driver that allows the data acquisition from the external device. Concretely, the required tool is a .NET library for controlling an Arduino board directly through a USB connection. It allows to easily connect, drive and debug

an Arduino through a simple and highly Arduino syntax compatible request/response protocol running over the serial connection.

The installation of the ArduinoDrive library is done following the instructions of the website https://github.com/christophedieiricx/ArduinoDriver. The command in Figure 4.40 must be run in the Package Manager Console in Visual Studio.
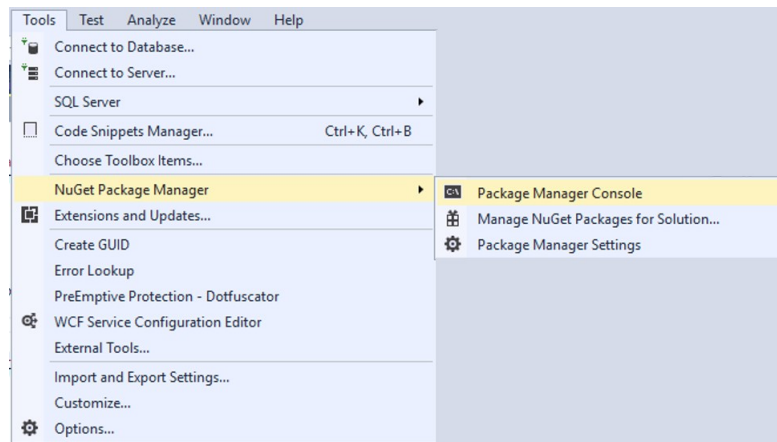
FIGURE 4.39: Package Manager Console Mode Set Up in Visual Studio

FIGURE 4.40: ArduinoDriver Installation Command in the Package Manager Console

When the code in Listing A.1 in the Appendix A is typed in any line of the code of the software, it creates an ArduinoDriver for a specific Arduino Model (in this case an UNO). The relevant COM port is autodetected. To send a message to the Arduino and receive a response the *Send* method on the driver is used. The typical Arduino library methods have these request/counterparts: AnalogReadRequest/AnalogReadResponse, AnalogWriteRequest/AnalogWriteResponse, DigitalReadRequest/DigitalReadResponse, DigitalWriteRequest/DigitalWriteResponse, PinModeRequest/PinModeResponse...

4.3 Components of the Non-Portable Version of the Reader

4.3.1 Agilent HP E4432B Signal Generator

RF signal generators are electronic laboratory devices that allow the user to test equipment, components, receivers and systems, such as antennas, with different waveforms and frequencies. The Agilent E4432B RF signal generator generates electronic signals in the digital domain for research, development and manufacturing applications. It covers a wide range of frequencies between 250 kHz and 3 GHz and outputs powers of +13 to

–136 dBm. Besides, it includes a sweep mode with a frequency step operation, which was the function used in the chipless RFID reader to do some tests.

Even if the main goal in the reader design was to replace this big and bulky signal generator by the PLL in order to develop a portable device, for the first non-portable version, the signal generator was connected to the PC via USB GPIB connector and controlled with MATLAB to do the desired frequency sweeps.

FIGURE 4.41: Agilent HP E4432B Signal Generator

Communication with the Signal Generator

The aim of this section is to illustrate how to communicate with this instrument via a GPIB controller using the VISA standard provided by Agilent Technologies in MATLAB. Virtual Instrument Standard Architecture (VISA) is a standard defined by Agilent Technologies and National Instruments for communicating with instruments regardless of the interface. The Instrument Control Toolbox software in MATLAB supports the GPIB using the VISA standard. Communication is established through a VISA instrument object created in the MATLAB workspace. The VISA-GPIB object will allow to use the VISA standard to communicate with the E4432B Function Generator.
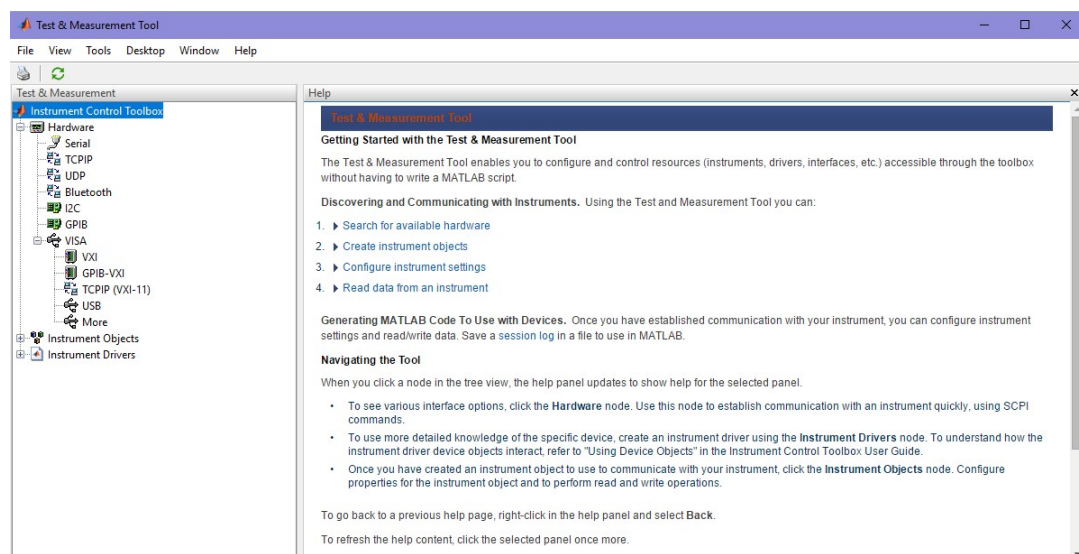
FIGURE 4.42: Instrument Control Toolbox Interface in Matlab

First of all, when opening the *Instrument Control Toolbox* the *More* tab must be clicked within the VISA section on the panel on the left side of the screen. This node is for communicating with generic VISA instruments as it scans for installed Generic VISA Resources. The *Instrument Control Toolbox* explains step by step how to establish the communication.

1. Click *Scan* in the lower-right of the center panel. Scanning returns each Generic VISA resource installed on the system. The *More* node adds a sub-node for each resource found by the scan.

2. Expand the *More* node and select the resource to use.
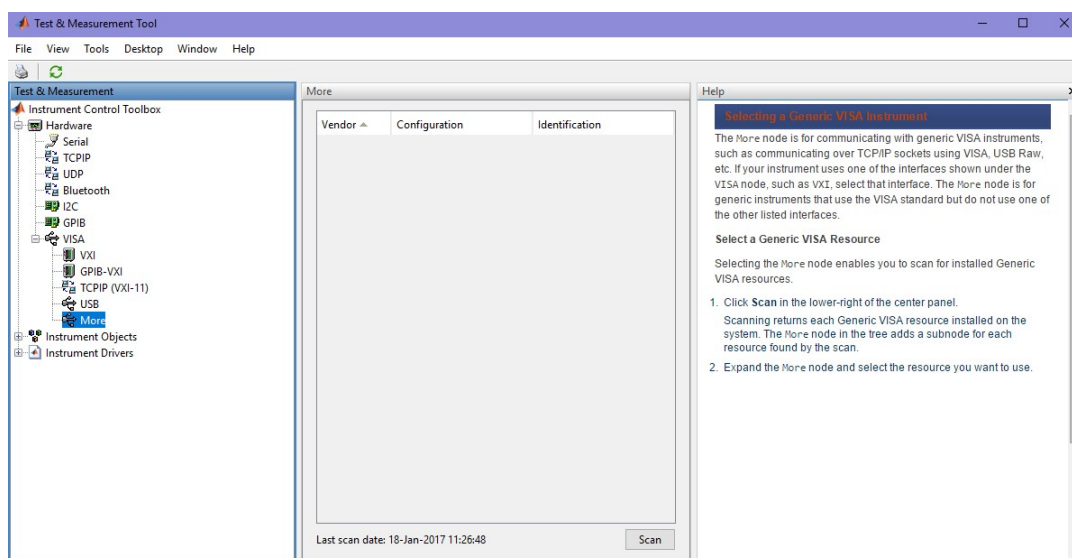
FIGURE 4.43: *More* node in the *Instrument Control Toolbox* Interface in Matlab

The function generator is the GPIB0::17::INSTR resource found by the scanner. Now it is possible to enable communication with the instrument identified at that node.

1. Click *Connect* to establish a connection with an instrument.

2. Click the *Communicate* tab to specify the data to read and write.

3. Click the *Configure* tab if the instrument communication settings want to be changed.

4. Optionally click the *Session Log* tab and click *Save Session* to save the instrument control session. This saves the current session in file, which can be run from MATLAB to recreate the session programmatically.

5. Click *Disconnect* to close the connection to the instrument.

Instead of saving the session, the MATLAB code generated when connecting with the instrument is copied onto the .m file that runs the GUI software programmed to do the frequency sweep. The section called *Communication with Instrument Software* is then modified to tell the E4432B to do the frequency sweep.

The MATLAB code generated for the communication is presented in Listing A.2 in the Appendix A.

4.3.2   MATLAB

MATLAB (MATrix LABoratory) is a programming language developed by MathWorks, that allows matrix manipulations, plotting of functions and data, implementation of algorithms, creation of user interfaces, and interacting with programs in other languages.

The portable version of the reader with the PLL does not use MATLAB, but the previous design composed by the signal generator is based on a MATLAB software that lets the user select three different measurement modes in an interactive interface.

When opening the file Guilector.m, a GUI (Guided User Interface) appears on the screen. On the upper side, there is a *Mode* tab. When clicking on it, the *Frequency Sweep Mode* must be selected. It is the most significant mode in the development of the portable version of the device, shown in Figure 4.46.

The interface gives the chance to select the range of frequencies for the sweep. In addition, it allows to compare graphically and numerically the measurements done with the signal generator to the ones done with the PLL in the Visual Studio software. The communication among the Arduino, the gain/phase detector and the signal generator is very slow, so it takes a long time to do exact measurements with a small spacing between frequencies.
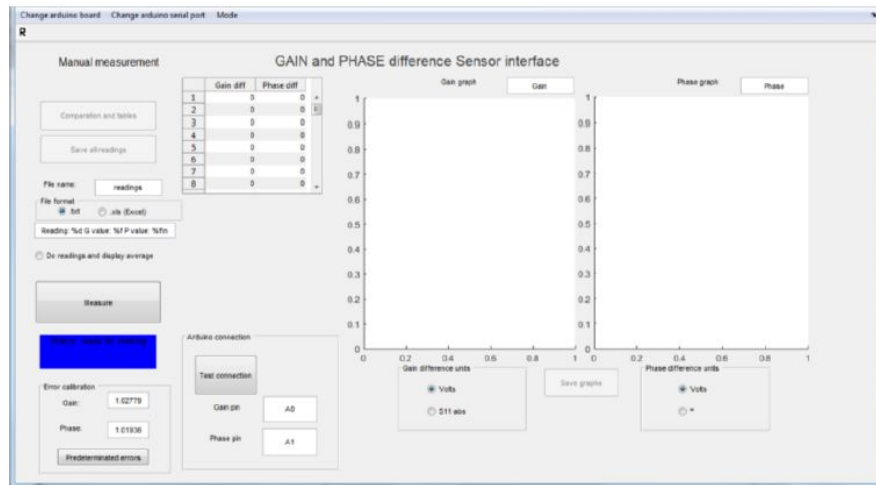
FIGURE 4.44: Matlab Interface for the Discrete Reading Mode
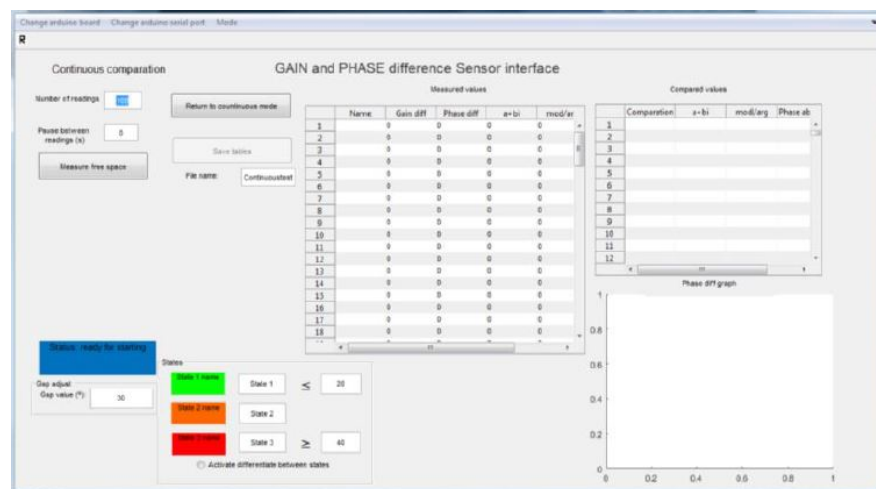
FIGURE 4.45: Matlab Interface for the Continuous Reading Mode
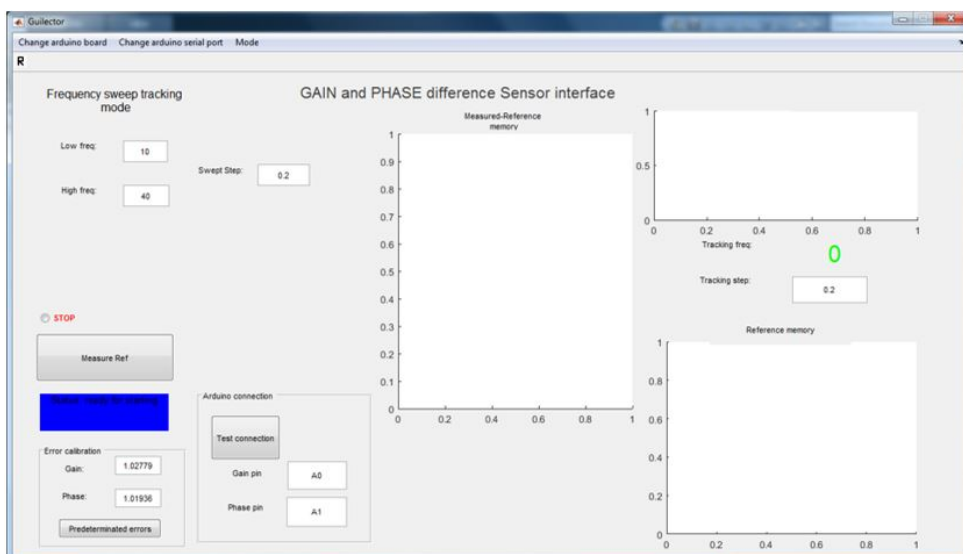
FIGURE 4.46: Matlab Interface for the Continuous Sweep Mode

Chapter 5

Operation of the Digital Section of the Chipless Tag Reader

5.1 General Operation of the Digital Section

The digital section of the chipless RFID reader is formed by an Arduino UNO with a SparkFun RedBoard and a PC. The latter controls the entire operation of the reader, which can be divided into three functions:

1. Transmitter Control (PLL control)

2. Receiver Control (Arduino control)

3. Signal Processing and Data Decoding (Visual Studio software in C language)

The procedure and sequence of operation of the digital part of the reader was implemented directly on a the ADF435x software in C language run in Visual Studio. The flowchart of the whole controlling algorithm and data processing algorithm is shown in Figure 5.1
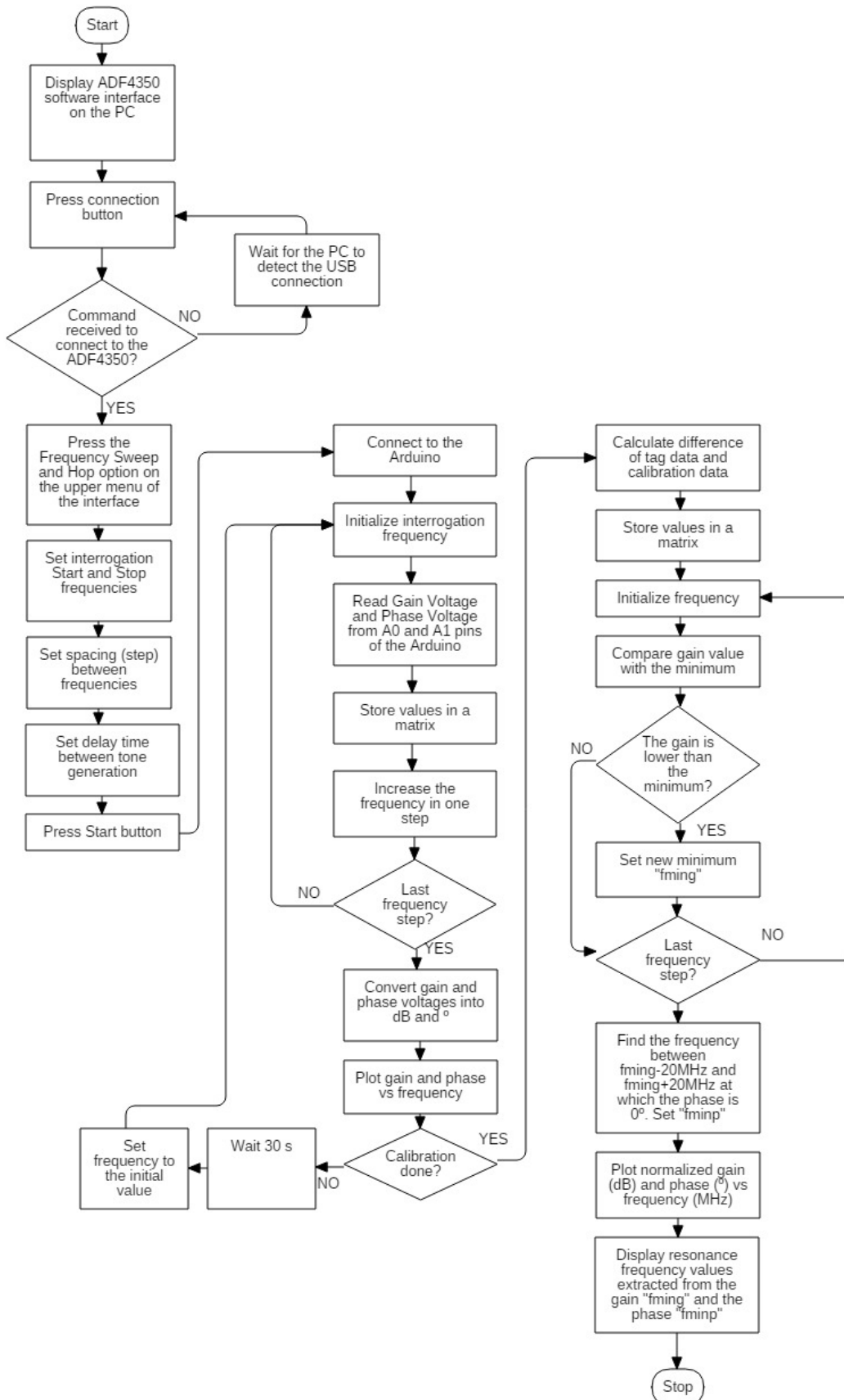
FIGURE 5.1: Flowchart of the signal processing function of the reader that identifies the resonance frequency of chipless tags

5.2 Control of the PLL

The Evaluation Board of the ADF4350 Wideband Synthesizer with Integrated VCO is controlled with the user interface of the Microsoft Visual Studio Application called ADF435x. This section describes the first part of the flowchart diagram, where a reference frequency sweep for the free space calibration is carried out by the PLL and a similar sweep done with the tag located in front of the reader antennas. The main goal of this device is to generate an interrogation signal as fast as possible from a start frequency up to a stop frequency set by the user. The step between frequencies is also defined in the interface, as well as some other relevant parameters.

The first step is to press the *Run* button of the Visual Studio environment. The user interface of the ADF4350 and ADF4351 will appear.
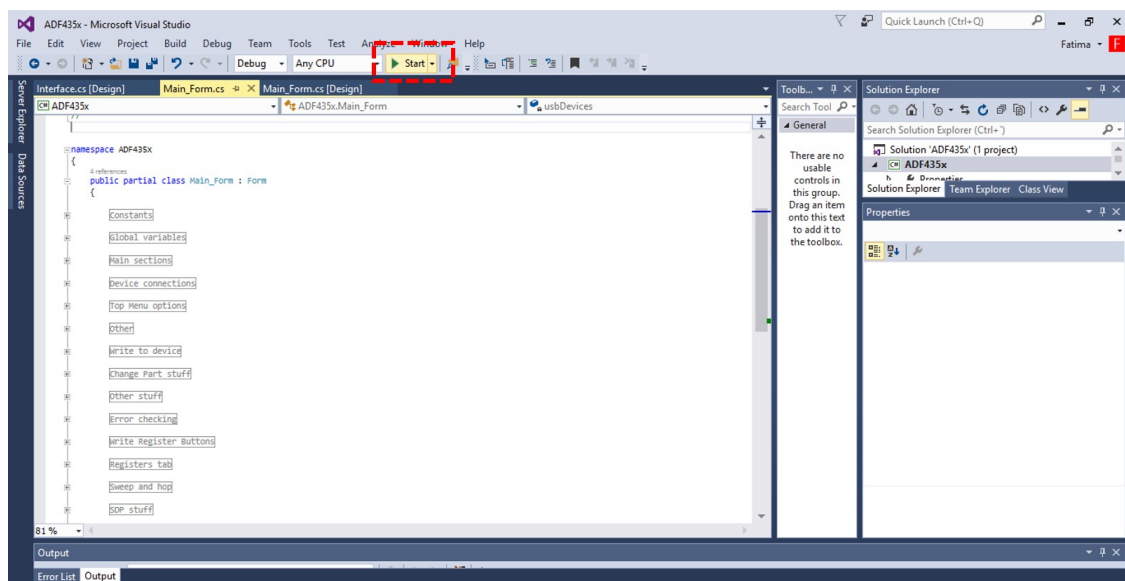
FIGURE 5.2: Visual Studio Environment to run the ADF435x Software

In the front panel, the radio button that says ADF4350 must be selected and the *Connect* button must be pressed. The Main Panel is used to generate individual tones, so the reader does not implement any function from this subsection, but the one to set the RF Output Power. The most significant interface is the one observed in Figure 5.5, as it makes it possible to determine the parameters for the frequency sweep and start it. The parameters that can be selected in the Sweep and Hop panel are:

1. Start Frequency (MHz) & Stop Frequency (MHZ)

2. Step (MHz)

3. Time Delay (MHZ)
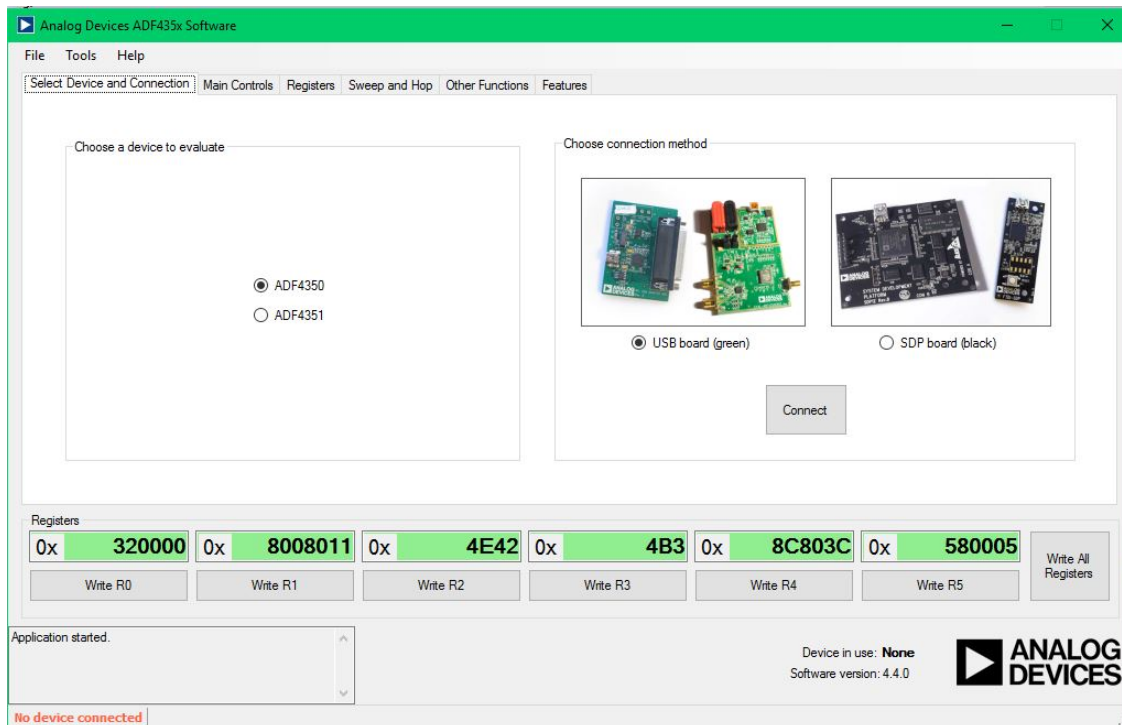
FIGURE 5.3: Front Panel of the Evaluation Board Software
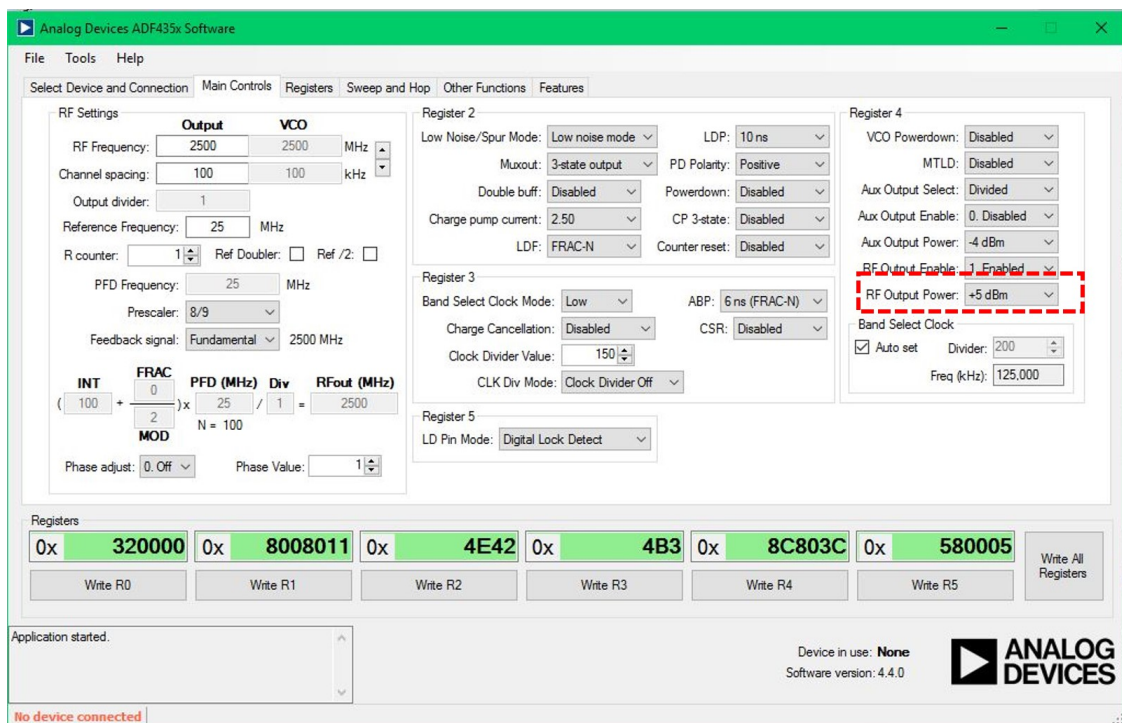
FIGURE 5.4: Main Panel of the Evaluation Board Software

Once the *Start* Button is pressed, the frequency sweep starts and the Arduino UNO begins converting the analog voltages coming from the gain/phase detector into digital values.
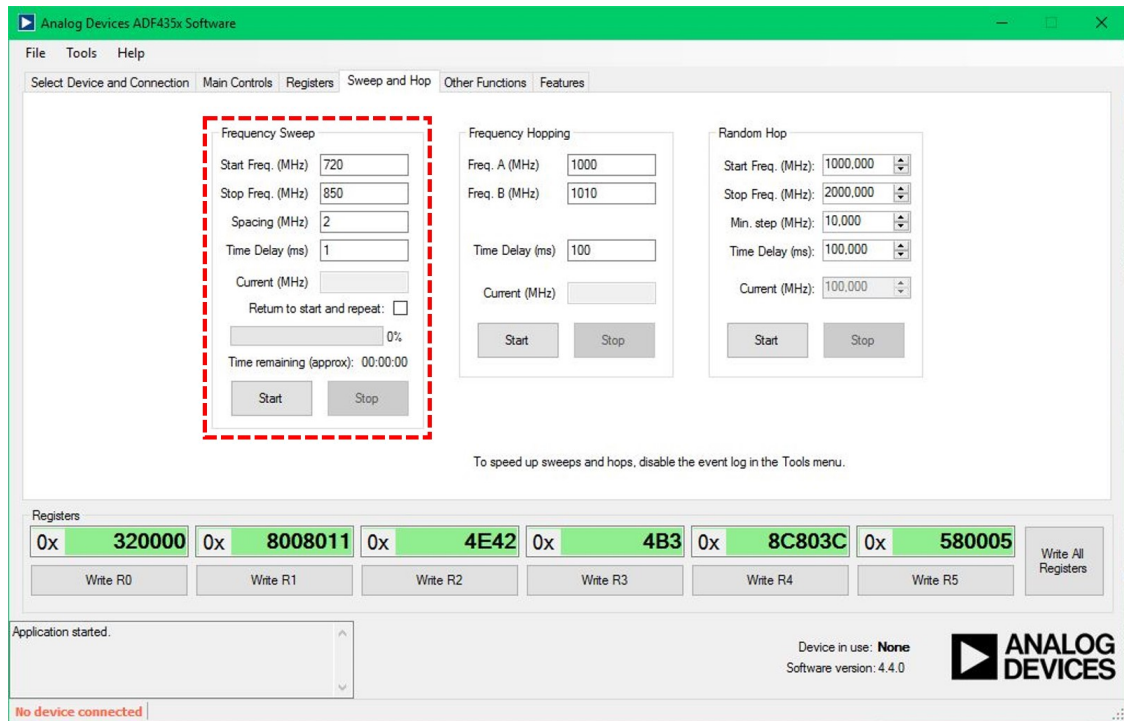
FIGURE 5.5: Sweep and Hop Panel of the Evaluation Board Software

5.3   Control of the Arduino

The main function of the Arduino UNO in the reader is to convert the analog voltage at the gain and phase outputs of the AD8302 into digital data that can be analyzed and processed in the computer Visual Studio software.

Each time the PLL generates a tone at a certain frequency, the created Arduino Driver sends a request to the hardware. The gain and phase outputs connected to the RedBoard at A0 and A1 pins are transferred to Visual Studio with the *AnalogReadRequest()* function.

In Listing A.3, *vg* and *vf* are the variables that store a mean of four measurements done consequently in the A0 (*ping*) and A1 (*pinf*) pins in a respective way. The number of readings is set to four but a single reading could be done in case the speed of the reader needs to be increased. These variables will be used for the steps corresponding to Signal Processing and Data Decoding in the flowchart.

5.4   Obtaining the Gain in dB from Voltage Output

The voltage output from the gain output is a value between 0 and 1.8 V. The set up for this procedure is shown in Figure 5.6 and Figure 5.7, which consists of the PLL doing a

frequency sweep from 200 MHz up to 2500 MHz with a step of 50 MHz and a power of 5 dBm. It is connected to the power divider, from which the two halves of the split signal go out with the same power ($P1 = P2$). They are fed into the GPD inputs through two equal length wires ($L1 = L2$), so that the signal is not attenuated more in one of them, and so that they have the same phase when reaching the AD8302.
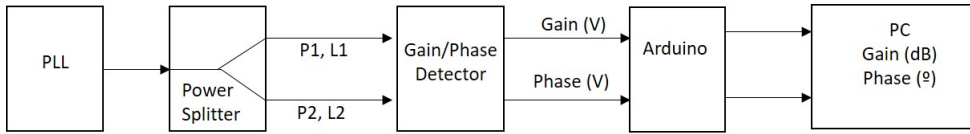
FIGURE 5.6: Diagram to convert gain and phase voltages into dB and degrees
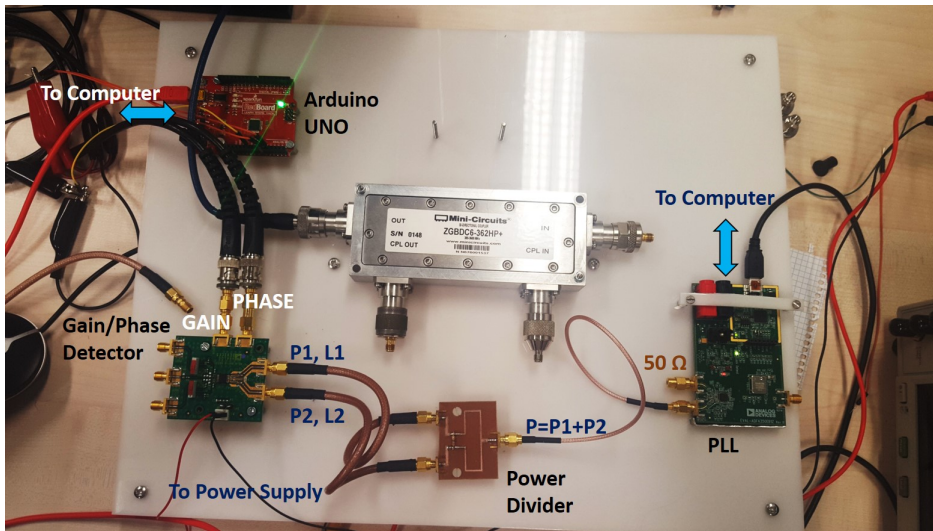
FIGURE 5.7: Set up to convert gain and phase voltages into dB and degrees

The gain output is connected to the RedBoard and its A0 pin is read in Visual Studio with the *AnalogReadRequest()* function. The values are converted into voltages with Equation 5.1, due to the fact that the Arduino is powered with 5 V.

$$vg = vg \frac{5}{1023} \tag{5.1}$$

where vg is the voltage read in A0 pin corresponding to the gain. This value is plotted in Figure 5.8 as a function of the frequency. As it can be observed, according to Figure 4.10 and Figure 4.11 in the AD8302 datasheet, if the input signals have the same power, the measured voltage should be around 0.91 V. The experiment shows a higher voltage, also verified by a multimeter, so this value needs to be adjusted in the software. The procedure followed to to this error correction is to multiply the read voltage by a factor of 0.94.

$$vg = 0.94 \frac{5}{1023} vg \tag{5.2}$$
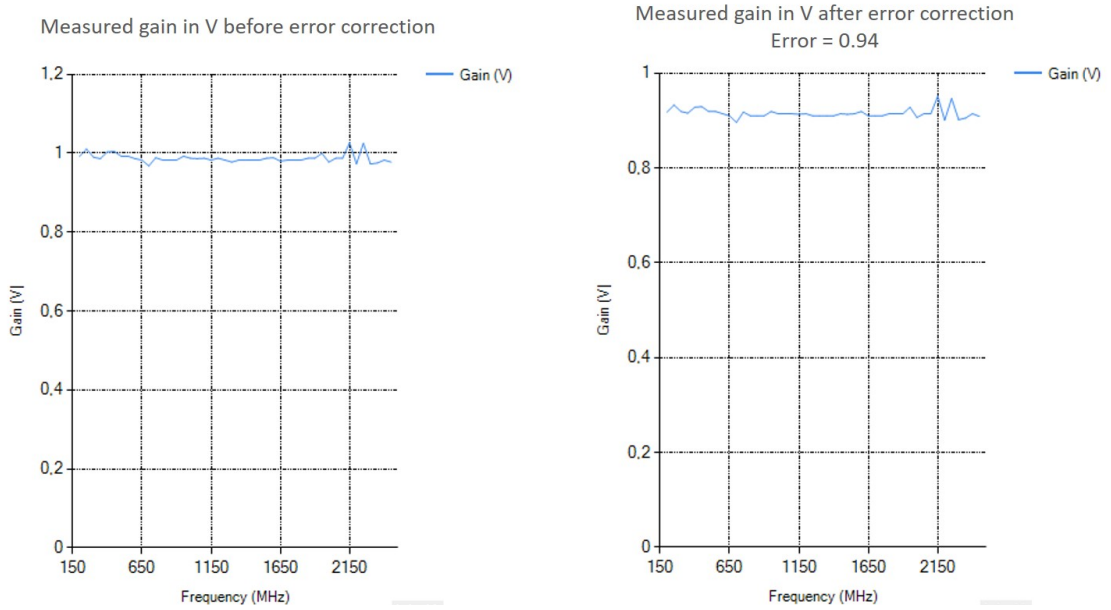
FIGURE 5.8: Gain (V) vs. Frequency graphs with and without the voltage adjustment

The voltage is converted into dB with a linear equation based on the values of the graphs in Figure 5.12, where 0.03 is the slope of the gain graph.

$$Gain(dB) = \frac{vg - 0.9}{0.03} \qquad (5.3)$$
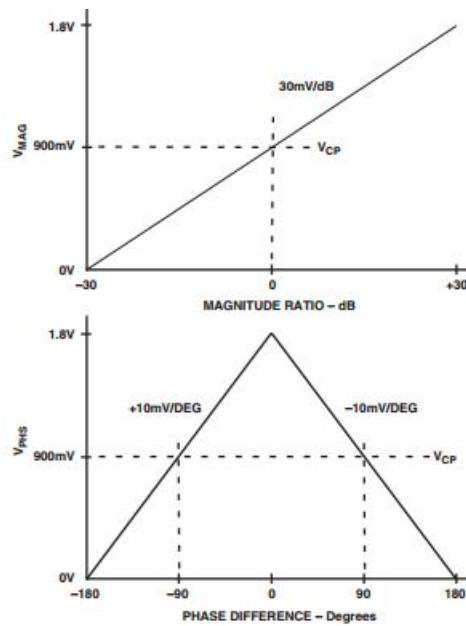
FIGURE 5.9: Idealized Transfer Characteristics for the Gain and Phase Measurement Mode

5.5   Obtaining the Phase in degrees from Voltage Output

Employing the same set up as for the gain adjustment in Figure 5.6 with $L1 = L2$ and $P1 = P2$, the voltage value for the phase difference (A1 pin in the Arduino) is checked with the software.

$$vp = vp\frac{5}{1023} \tag{5.4}$$

where vp is the voltage read in A1 pin of the Arduino corresponding to the phase difference. The value is plotted in Figure 5.10 as a function of the frequency. According to Figure 4.12, if the phase difference between the input signals is $0^{\underline{o}}$, the measured voltage should be around 1.78 V. The measurement and the multimeter verify this value in a quite wide range from 700 MHz up to 2100 MHz with a step of 50 MHz, therefore, no error correction needs to be added.
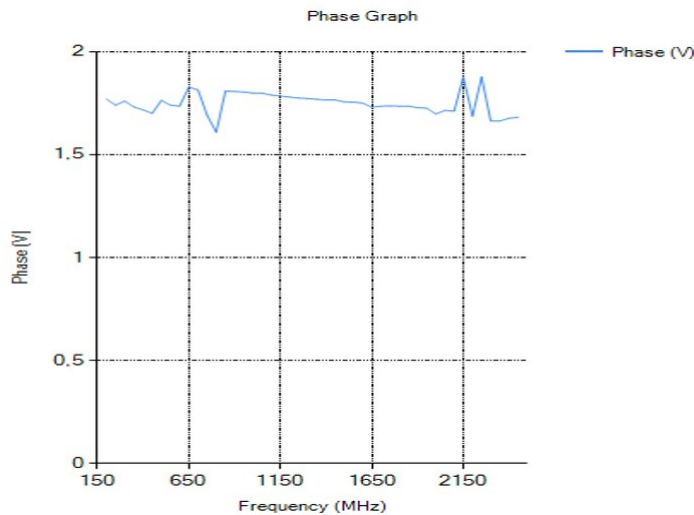
FIGURE 5.10: Measured Phase (V) vs. Frequency graphs from Visual Studio

To convert the voltage into degrees, the linear equation 5.5 is applied.

$$Phase() = \frac{1.78 - vp}{0.01} \tag{5.5}$$

0.01 is the absolute value of the slope of the phase graph on both sides of the curve. The fact that the sign of the phase is not detected adds an extra challenge to the voltage-degree conversion. This is why either the positive or the negative sign of the phase is calculated manually and explained in detail in the next section.

In order to check if the performance of the AD8302 is accurate enough for distinct phase changes and resembles the graph in Figure 4.12, three more demonstrations are done. The length Of one of the wires from the power divider to the gain/phase detector

is increased by a factor of two. This way, $L1 = 2 * L2$ and $P1 = P2$, so the signals arrive to the gain/phase detector with a certain phase difference depending on the frequency of the waveforms.

First of all a frequency sweep is done from 600 MHz up to 750 MHz with a step of 2 MHz. The phase difference that corresponds to this frequency range needs to be calculated.

$$\lambda_{coaxialwire} = \frac{\lambda}{\sqrt{\varepsilon}} = \frac{\lambda}{\sqrt{2.1}} \tag{5.6}$$

where ε is the permittivity of the coaxial wire and λ is the wavelength of the waveform. λ is extracted from one of the limit frequencies of the sweep and the length of one of the wires. In this case, 750 MHz and the longest wire's length, 30 cm, are used.

$$\lambda = \frac{L1}{f} = \frac{0.3 \ \frac{m}{10^9 \ s}}{0.75 \ GHz} = 0.4 \ m \tag{5.7}$$

Plugging this wavelength in equation 5.6,

$$\lambda_{coaxialwire} = \frac{0.4}{\sqrt{2.1}} = 0.276 \ m \tag{5.8}$$

0.28 is the rounded value of the wavelength of the signal in the coaxial wire. Taking into account the length of the shortest wire, 15 cm, it corresponds to a phase difference of 192.85^{o} at the input of the gain/phase detector.

$$\phi(\textit{750 MHz}) = \frac{0.15 \ m}{0.28 \ m}360 = 192.85 \tag{5.9}$$

$$\phi(\textit{600 MHz}) = \phi(\textit{750 MHz})\frac{600MHz}{750MHz} = 192.85 * 0.8 = 153 \tag{5.10}$$

The phase difference for 600 MHz is 153°. Therefore, the graph that refers to the voltage measurements for this sweep should show a straight line with an approximate phase variation of $192 - 153 = 39^{\text{o}}$. From the voltage values it is obtained a change of phase of 40°. Nevertheless, the graph does not show a perfect straight line, but an irregular curve. In the previous graphs plotted over a wider frequency range, some undesired peaks were observed below 700 MHz and above 2100 MHz. Although the cause of the noisy signal is not clear, some changes carried out in order to improve the quality of the signal will be presented in Chapter 8.
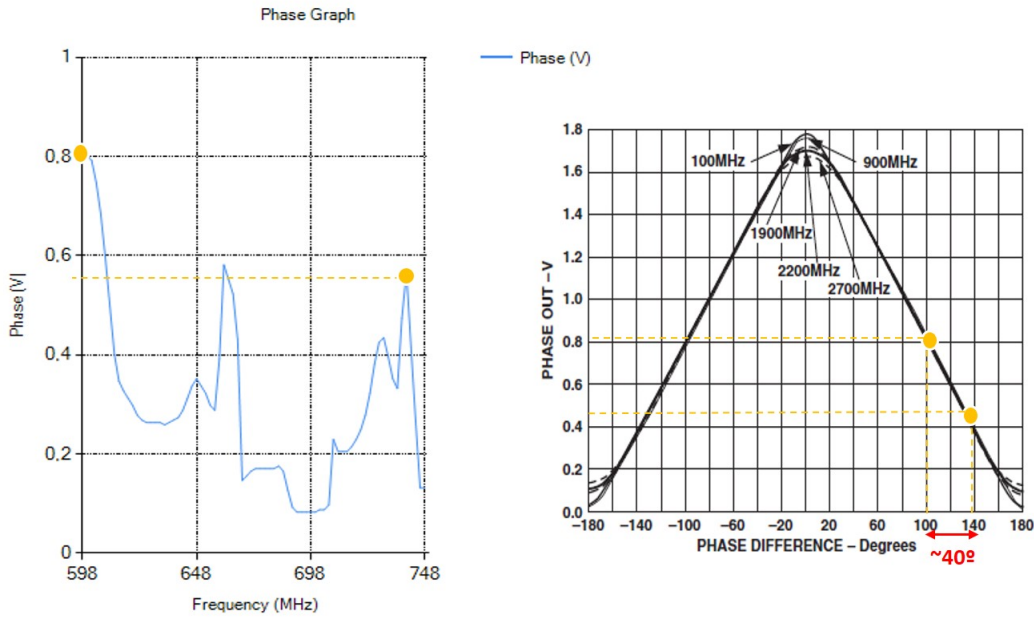
FIGURE 5.11: Phase (V) vs. Frequency graphs from Visual Studio and from AD8302 datasheet

To acquire reliable measurements, a sweep from 1000 MHz to 1250 MHz with a step of 2 MHz is done. The corresponding phase change is calculated below.

$$\lambda = \frac{L1}{f} = \frac{0.3 \; \frac{m}{10^9 \; s}}{1.25 \; GHz} = 0.24 \; m \tag{5.11}$$

$$\lambda_{coaxialwire} = \frac{0.24}{\sqrt{2.1}} = 0.165 \; m \tag{5.12}$$

$$\phi(\text{1.250 GHz}) = \frac{0.15 \; m}{0.165 \; m} * 360 = 327.27 = -32.73 \tag{5.13}$$

$$\phi(\text{1 GHz}) = \phi(\text{1.25 GHz}) * \frac{1 \; GHz}{1.25 \; GHz} =$$
$$327.27 * 0.8 = 261.81 = -98.19 \tag{5.14}$$

$$\phi(\text{1.25 GHz}) - \phi(\text{1 GHz}) = 327.27 - 261.81 = 65.46 \tag{5.15}$$

A phase difference of 65.46º should be observed in the measurements. The plotted curves show smooth ramps without noise. This happens because the sweep covers a range of frequencies in the middle of the working range of the GPD. The result is a significant improvement and it confirms the correct operation of the AD8302 at least in that band.

As a final test, a wider range (700-1900 MHz 50 MHz step) will be covered in order to get a curve centered at a phase difference of 0º and a voltage of 1.78 V. The result is shown in Figure 5.13. It can be observed that from 700 MHz up to 1650 MHz, the curve

resembles the one in the datasheet. Nevertheless, for higher frequencies the line is not monotonically decreasing. For the moment there is no explanation for this anomaly.
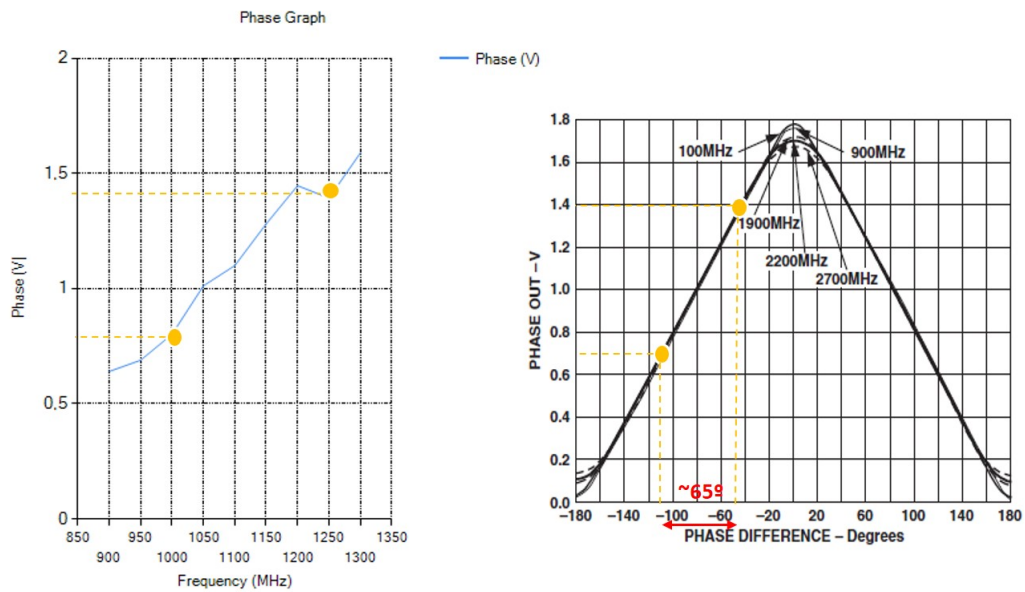
FIGURE 5.12: Phase (V) vs. Frequency graphs from Visual Studio and from AD8302 datasheet
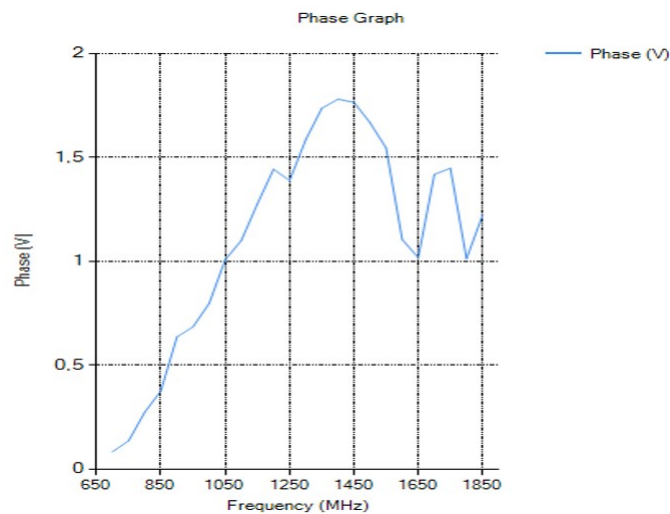
FIGURE 5.13: Phase (V) vs. Frequency graph from Visual Studio

5.5.1 Change of Sign of the Phase

The measured signal has a phase of $\pm 180^\circ$. However, when converting the voltage into degrees in the software, an absolute value is gotten. Therefore, there is a need of a mechanism that distinguishes whether the phase has a positive or a negative value.

According to the calculations in the previous section, the value of the phase always increases when doing a sweep from low frequencies to higher ones.

$$f1 < f2 \Leftrightarrow \phi(f1) < \phi(f2) \tag{5.16}$$

By reading a single voltage value for a certain frequency it is impossible to determine the sign of the phase, it can be deduced by comparing the readings done for two different frequencies though. A procedure that can be followed consists of doing a first reading at a certain frequency. Then, a second voltage value is measured for a second frequency, higher than the previous one. If the voltage is also higher than the previous measurement, this fact will mean that the phase was negative, as the slope of the phase difference graph of the AD8302 was positive for phases between $-180^{\text{o}}$and 0°. On the contrary, if the voltage read for the higher frequency is lower than the previous measurement, this fact will mean that the phase is positive, as the slope of the phase difference graph of the AD8302 is negative for phases between $0^{\text{o}}$and $+180^{\text{o}}$.
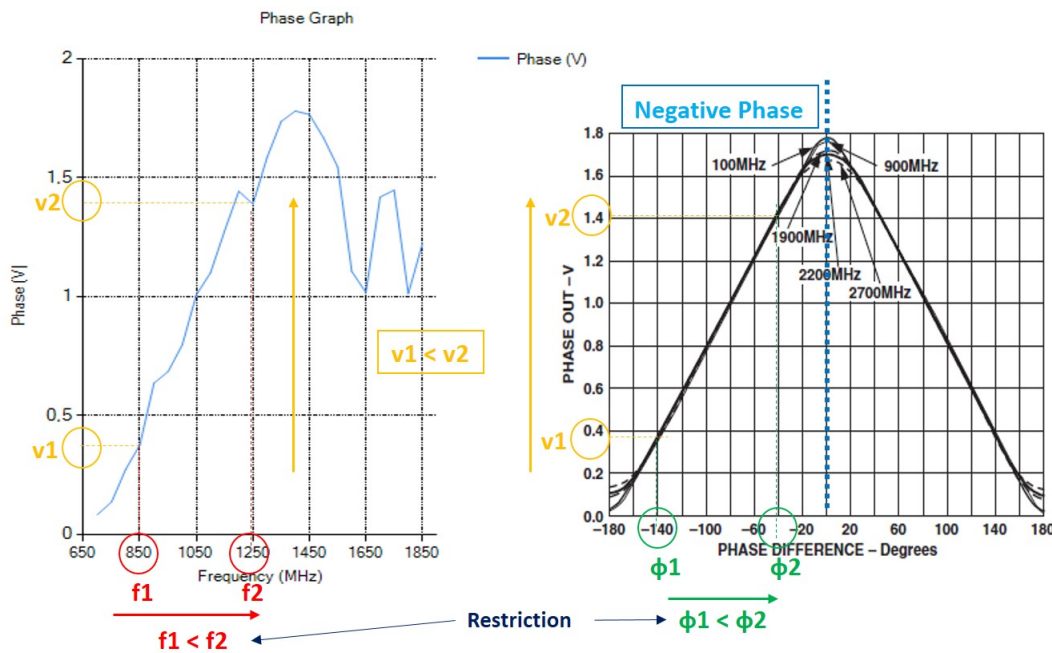
FIGURE 5.14: Principle of negative phase determination

However, the way the change of phase is implemented in the software is slightly different. It is based on the same principle, but the sign of the phase is determined from the absolute value of the measured degrees. As shown in Figure 5.16, if the absolute value of the degrees, $|\alpha|$ increases as the frequency increases, the phase will be positive. The angle will correspond to the upper half of the circumference. If the absolute value

of the phase decreases for higher values of frequency, its sign will be negative and the angle will be part of the lower half of the circle.
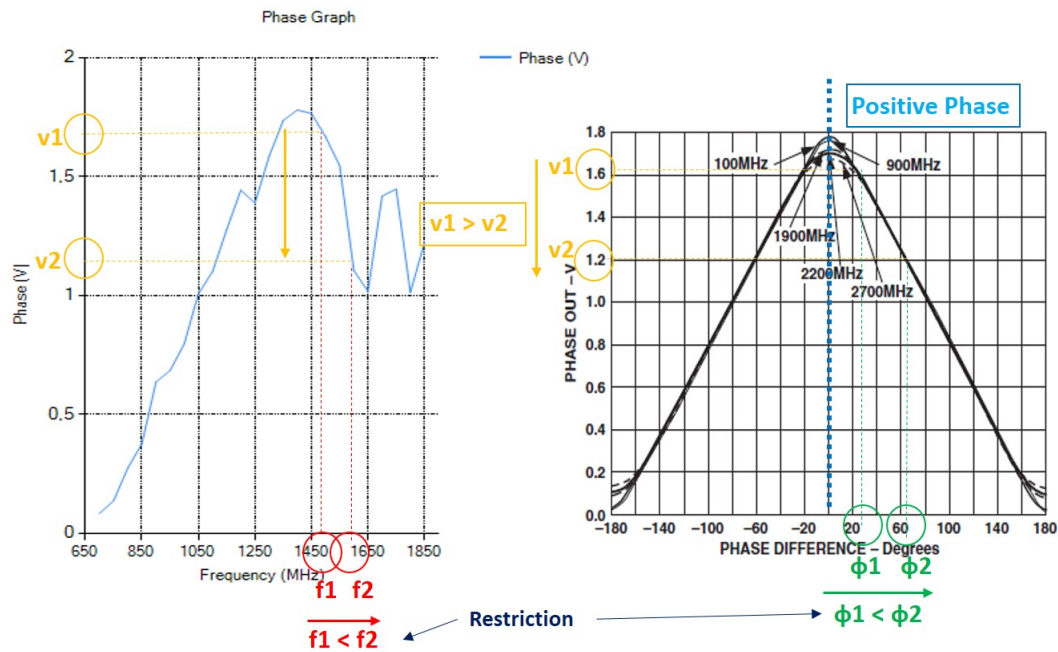
FIGURE 5.15: Principle of positive phase determination
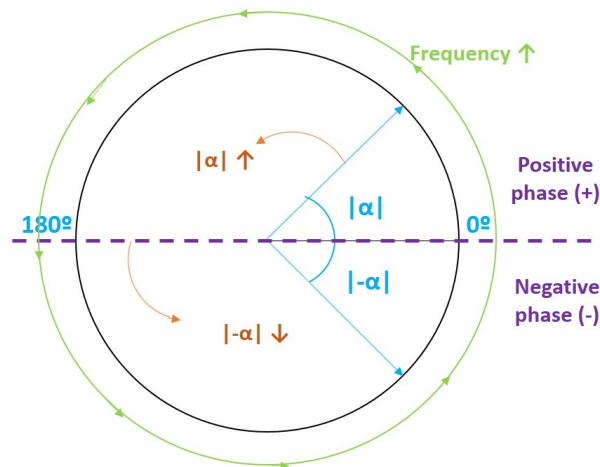
FIGURE 5.16: Principle of phase sign determination

The implementation of the phase sign detection principle in the software is shown in Listing A.4, where matriz_g_g is a 3 column matrix The first column corresponds to each frequency value with a step determined by the spacing, the second column has the gain values in dB and the third column stores the phase values in degrees.

5.6   Calibration of the Measurements

After the basics for the gain (dB) and the phase difference ($^{\underline{o}}$) obtaining are clear, the next step in the software is to process these data stored in the columns of a matrix in order to calculate an accurate value of the normalized S11 or S21.

In Chapter 2 the normalization equations of the S parameters were explained. First, it is compulsory to measure the S11 of the free space. This is done by carrying out a frequency sweep without the tag located in front of the antennas. The software is programmed to wait for 30 seconds after this reference measurement is finished. During this delay, the user counts on with enough time to locate the tag in the right position before an automatic second sweep with the same parameters begins. Listing A.5 implements the operations to calibrate the reader with the environment. The calibration is done each time a new measurement is taken. The system is quite robust for tags located at 20 cm in environments where there are no metal objects facing the antennas that alter the measurements.

There are two different matrices, one with the reference values of gain and phase, and another one with the values of these parameters measured with the tag. The gain is first converted from dB to its corresponding linear value to use it in the calculations. As the S11 is expressed with two numbers (magnitude and angle), it is said that those are its Polar Coordinates.
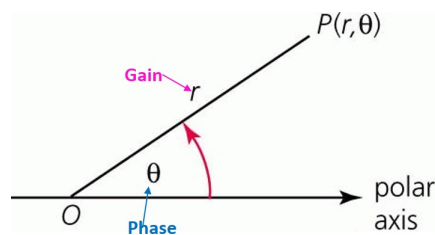
FIGURE 5.17: Polar Coordinates of the S11

In order to subtract the reference from the measurement, the Polar Coordinates need to be converted into Cartesian Coordinates; this is, to x and y values.
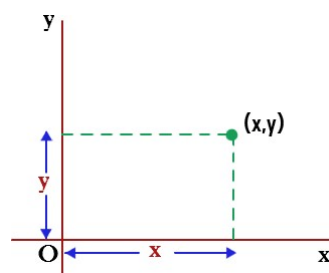
FIGURE 5.18: Cartesian Coordinates of the S11

The relationship between the Polar and the Cartesian Coordinates is shown in Figure 5.19 and expressed in Equation 5.17, where r is the magnitude and θ is the phase.
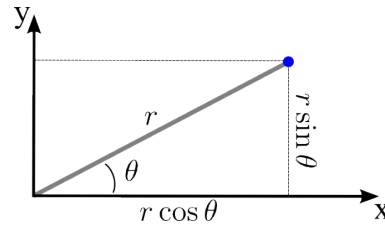
FIGURE 5.19: Relationship between Polar and Cartesian Coordinates of the S11

$$x = rcos(\theta)$$
$$y = rsin(\theta)$$
(5.17)

Once the reference and the tagged S11 are converted to Cartesian Coordinates, the subtraction between the x coordinate and the y coordinate of both can be computed.

$$x_{Normalized} = x_{Tag} - x_{Reference}$$
$$y_{Normalized} = y_{Tag} - y_{Reference}$$
(5.18)

The normalized values are ready to be converted into Polar Coordinates again, so that the S11 values make sense. The equations to reverse the previous conversion are 5.19.

$$r = \sqrt{x^2 + y^2}$$
$$\theta = arctan(\frac{y}{x})$$
(5.19)

This way, the Polar Coordinates of the S11 are ready to be plotted and processed to obtain information about the resonance frequency of the tag from them.

5.7   Plots of the Measurements

With the aim of becoming the identification of the resonance frequency of the chipless tag more visual, there are two extra interfaces in the Visual Studio ADF435x application.

Figure 5.21 shows three different curves of the gain of an S11 measurement (S21 if the configuration of the antennas was bistatic). The blue line corresponds to the first measurement of the environment without the tag, the yellow line represents the measured gain with the tag and finally, the red line is the plot of the magnitude of the normalized S11. The most important curve is the latter, as the most attenuated point will indicate

where the resonance of the tag is in a label. The procedure to determine its value will be explained in the next section.
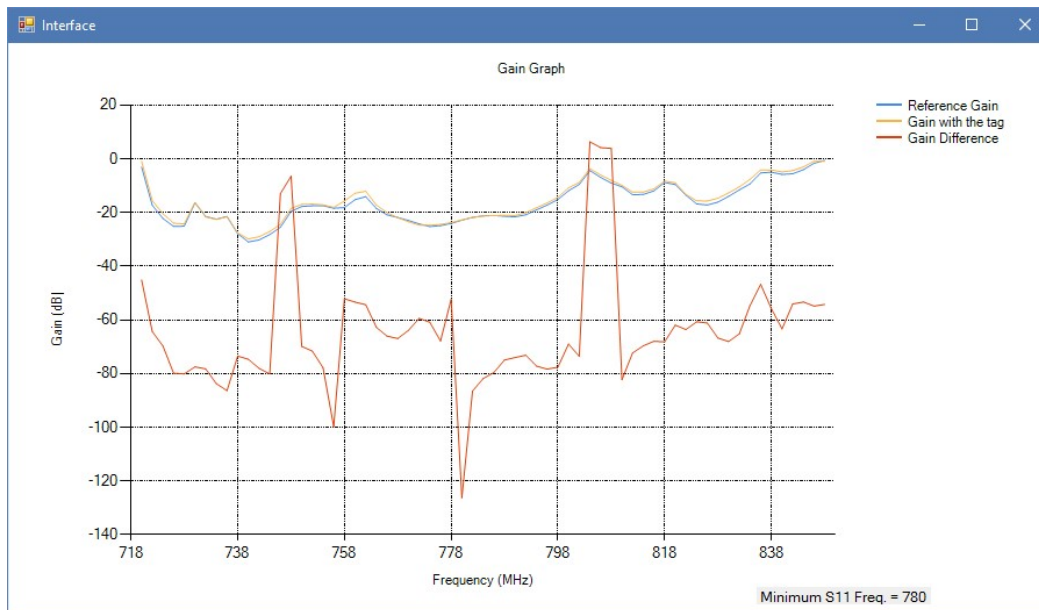
FIGURE 5.20: Plot of the Gain of the S11

The other additional interface in the software is similar to the previous one, with the main difference that this graph displays the phase of the three S11 measurements. The most important curve is the red one as well, which represents the phase of the normalized S11 where the phase jump must be seen at the resonance.
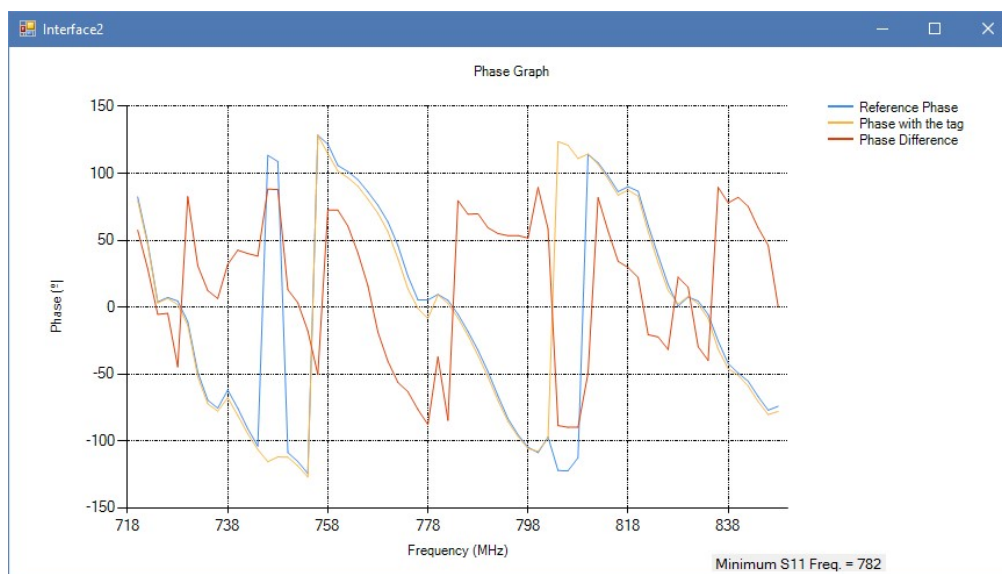
FIGURE 5.21: Plot of the Phase of the S11

The algorithms to implement these interfaces are written in Listings A.6 and A.7. To plot the values stored in the matrices, a loop must iterate through each of the frequency values and plot the gain and phase that correspond to them. As the gain is stored in

the linear form, it is passed to dBs. Moreover, the value of the resonance frequency according to the normalized S11 is written in a label below the graph grids. Some of the properties of the interfaces, such as the colors of the curves and the names of the chart areas are set directly from the Properties tab in the Design View.

5.8 Resonance Frequency Identification

The designed chipless tag reader is based on the identification of the features of frequency signatures. Therefore, the main objective of the software is to detect the value of the resonance frequency of the chipless tag. The signal transmitted towards the tag is directly compared to the one received by the reader, and after normalizing it, data corresponding to the gain and phase of both signals are plotted.

Attenuations and phase jumps are identified in the graphics, which indeed indicate the resonance.

An attenuation is the gradual loss in intensity of any kind of flux through a medium. In the gain graphs, attenuations appear as down peaks in which the measured parameter presents a minimum. As the used resonators have a single resonance frequency, the measured data only show a unique peak. This is why the most accurate method of detecting the resonance is to find the minimum of the gain values of the S11 and determine the frequency at which it occurs.

The basic procedure in order to do so is to set a minimum as the reference ($mini\_g$), and compare every gain measurement with it. If one of the values is smaller than the minimum, it is set as the new minimum and the algorithm continues comparing the following gain values. When the absolute minimum is found, the corresponding frequency ($mini\_i$) is determined and displayed in the interface. The code to do this is written in Listing A.8 in the Appendix A.

On the other hand, a phase jump is a sudden phase change in a signal, ideally passing through a 0 degree phase. Looking at the phase graph after the calibration, it is harder to identify the phase jump at the resonance frequency, and practically, the jump does not even reach 0°. This happens due to the noise introduced by the components of the circuit and because of the inaccuracy of the phase sign change algorithm. The procedure to detect the phase jump is based on the value of the resonance frequency obtained in the gain plot, but it is not very exact yet, so the resonance gotten from the phase will not be taken into account for the results. The code to do this is written in Listing A.9 in the Appendix A.

FIGURE 5.22: Plot of the Gain of the S11 and Minimum Identification

First of all, as the phase jump implies that the phase curve will cross the 0 degree value, every point where the phase changes from positive to negative or *vice versa* is detected. After that, it is checked if the jump occurs inside a range of $\pm 10 MHz$ around the previously detected resonance frequency. In case all these conditions are met, the frequency corresponding to this phase value is determined as the resonance frequency.

The ideal result would be to achieve the same resonance frequency value for the gain and for the phase of the S11, but this does not happen most of the times. However, the numerical results are quite similar, even though the most reliable resonance value is the one obtained from the attenuation in the gain.
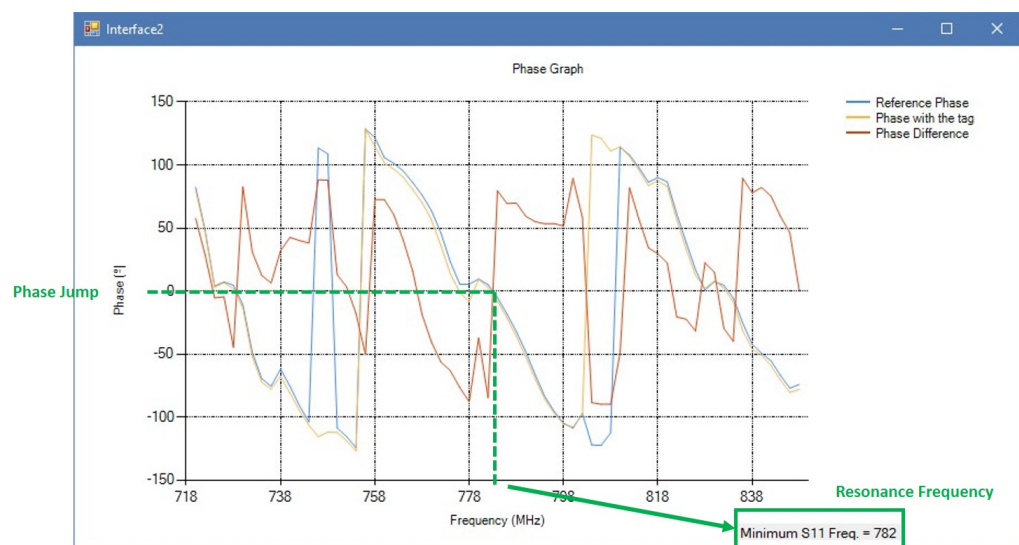
FIGURE 5.23: Plot of the Phase of the S11 and Phase Jump Identification

Chapter 6

Results

This chapter presents the results obtained after doing several S11 and S21 measurements with the designed and developed novel portable version of the reader and with the non-portable one. As it was explained in Chapter 3, depending on the architecture of the device and on the location of the chipless tag with respect to the antennas, the reader can operate in three different modes: Bistatic Transmission Mode, Bistatic Reflection Mode and Monostatic Reflection Mode.

There is a certain set up for each mode, which is utilized for two of the tags presented before. Concretely, the aluminum oxide tag and the FR-4 Tag. The procedure followed to check if the resonance frequency values given by the designed Visual Studio software application are correctly identified consists of first using the non-portable, version of the reader with the signal generator and Matlab to do the measurements, and then comparing the new graphs and values with them. This way, the accuracy and performance of the device and technique will be determined.

6.1 Bistatic Transmission Mode for the Aluminum Oxide Tag

6.1.1 Set Up

The resonance frequency of this resonator must be around 778 MHz when measuring it with any of the configurations and readers. Figure 6.2 and 6.3 show the set up of the reader antennas for the Bistatic Transmission Mode Measurements and Figure 6.1 shows the set up for the calibration. The chipless structure is located at 20 cm from the transmitter antenna and at 20 cm from the receiver antenna, as it is the best distance

according to previous research. The measured parameter is the transmission coefficient S21 that goes through the tag from the Tx to the Rx, but as explained previously, the algorithms implemented in the software are the same either for the S11 or the S21.
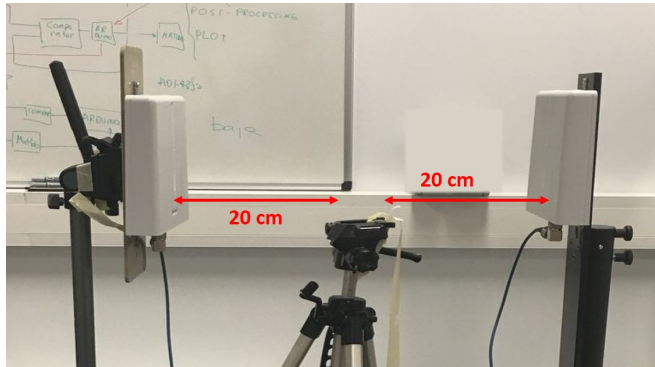
FIGURE 6.1: Set Up for the Bistatic Transmission Mode Calibration
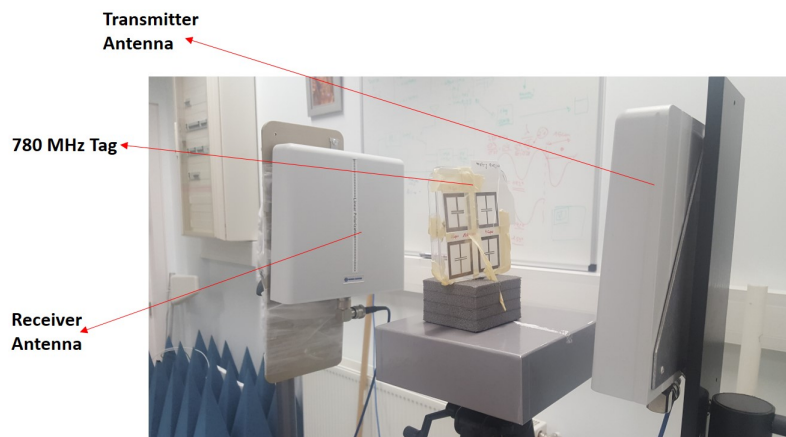
FIGURE 6.2: Set Up for the Bistatic Transmission Mode Measurements
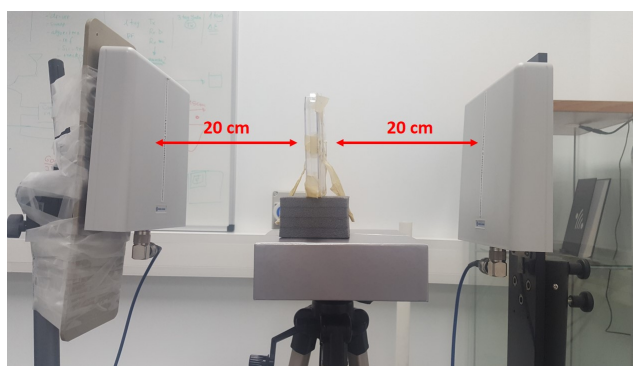
FIGURE 6.3: Set Up for the Bistatic Transmission Mode Measurements

6.1.2   S21 Measurements with the Non-Portable Version of the Reader

The graphs are S21 measurements taken by the non-portable version of the chipless reader in the user interface. The sweep and power parameters are indicated in Table 6.1.

Feature	Value
Start Frequency	720 MHz
Stop Frequency	850 MHz
Step Frequency	2 MHz
Output Power	+5 dBm
Distance from the antenna to the tag	20 cm

TABLE 6.1: Parameters for the Bistatic Transmission Operation

The mean resonance frequency, and the standard error from 6 measurements are shown in Table 6.2.
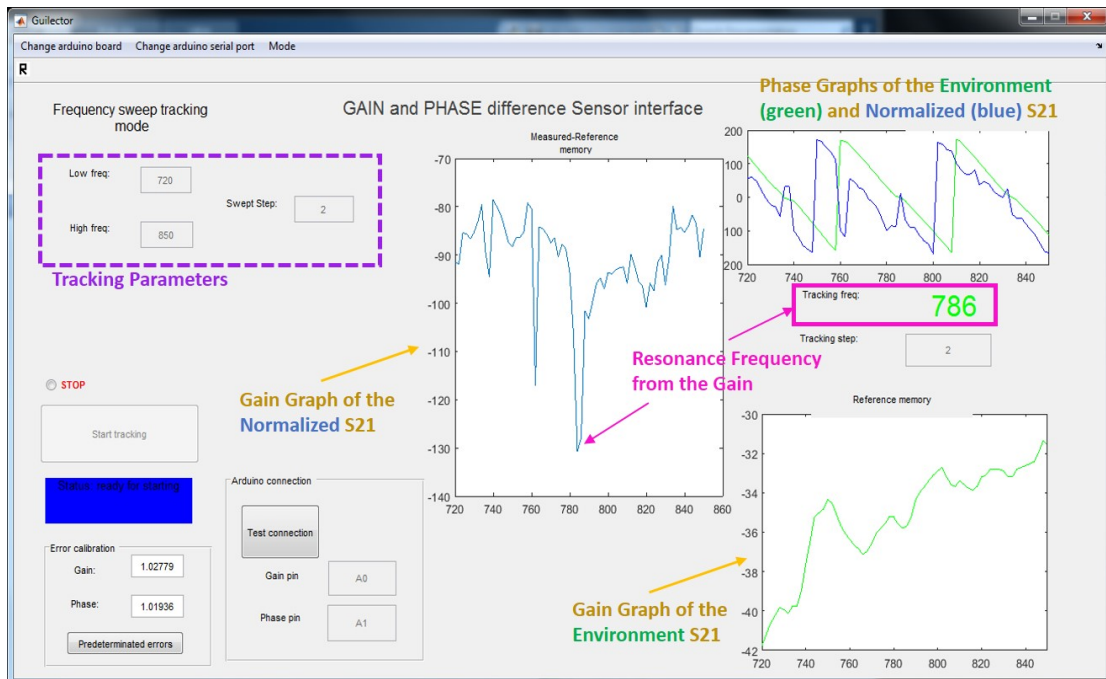
FIGURE 6.4: 780 MHz Tag Bistatic Transmission Mode Measurement

Measurement	Resonance Frequency (MHz)	Mean of the Reson. Freq. (MHz)	Standard Error of Reson. Freq. (MHz)
1	786		
2	770		
3	786	786	±3.46
4	794		
5	788		
6	792		

TABLE 6.2: Resonance Frequency Identified by the Non-Portable Version of the Reader

As the results show, the resonance frequency of this tag when measuring its S11 with the Bistatic Transmission Mode is 786 MHz, with a standard error of ±3.46 MHz.

6.1.3   S21 Measurements with the Portable Version of the Reader

The same procedure was followed with the portable reader. The next gain and phase graphs are S21 measurements taken by the designed reader. The sweep and power parameters are indicated in Table 6.1, just the same as before.

The mean resonance frequency taking into account the gain, as well as the standard error are calculated from 6 measurements shown in Table 6.3. The frequency at which a phase jump crossing the 0 degree axis takes place is indicated, but it is not used for the operations due to the fact that its accuracy is not very clear.
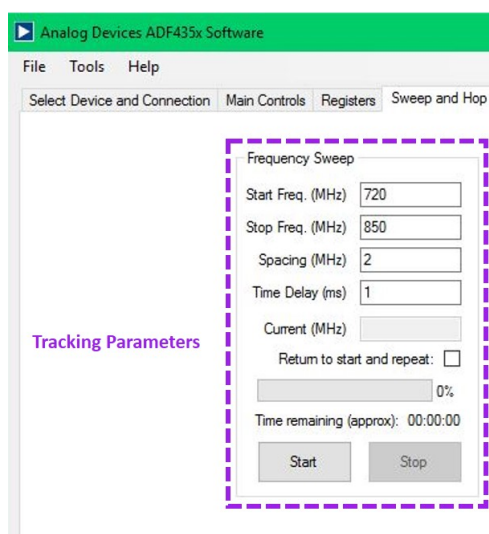
FIGURE 6.5: 780 MHz Tag Bistatic Transmission Mode Parameters

Measurement	Gain Resonance Frequency (MHz)	Phase Resonance Frequency (MHz)	Mean of the Gain Reson. Freq. (MHz)	Standard Error of Gain Reson. Freq. (MHz)
1	780	786		
2	780	788		
3	780	782	780	0
4	780	784		
5	780	782		
6	780	782		

TABLE 6.3: Resonance Frequency Identified by the Portable Version of the Reader

Looking at the resonance frequency identified from the gain graph, the value is constant at 780 MHz. This is a very exact result. Moreover, the attenuation peak is located close to the frequency measured by the VNA in the tag.
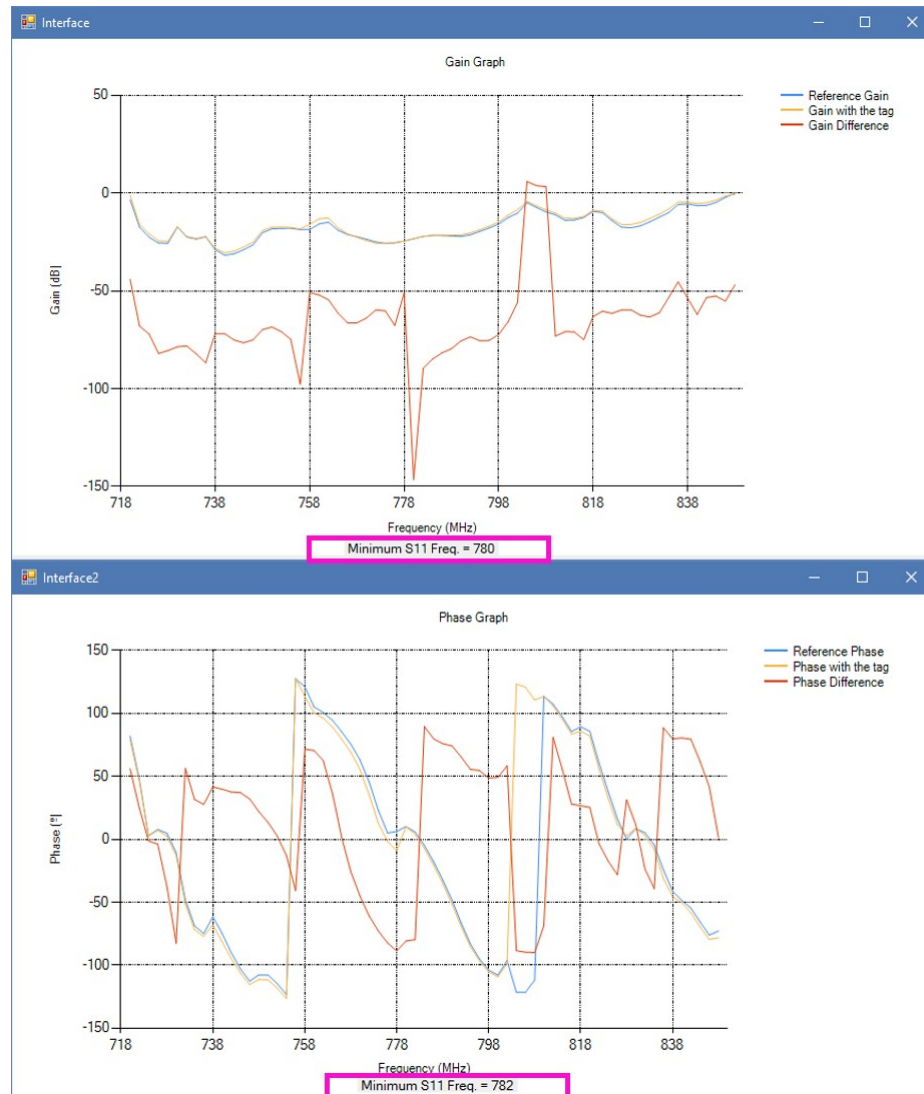
FIGURE 6.6: 780 MHz Tag Bistatic Transmission Mode Measurement

6.1.4 Comparison between the Non-Portable and the Portable Version of the Reader for the Bistatic Transmission Mode

In this section it is intended to compare the performance of the two readers, and to prove that in fact, the portable version is more accurate than the previous.

Table 6.4 presents the mean resonance frequencies identified by each reader, the corresponding standard error and the distance to the expected 778 MHz value.

It can be observed that for the identified resonance frequencies, the distance to the expected 778 MHz value is closer for the portable reader. It differs in 2 MHz with the ideal value if only the gain measurements are analyzed. It is concluded that the improvement in this field is an approaching of 6 MHz to the expected resonance frequency. With respect to the standard error, it decreased by 3.46 MHz among the two readers, which

	Non-Portable Reader	Portable Reader	Improvement
Resonance Frequency (MHz)	786	780	
Distance to 778 MHz (MHz)	8	2	6
Standard Error (MHz)	±3.46	±0	3.46

TABLE 6.4: Comparison of Readers for Bistatic Transmission Mode

means that the measurements are more constant with the portable design. The accuracy of the reader is relevant and it shows an improvement of a 75% between the two versions.

For the Bistatic Transmission Mode, the performance of the portable reader is better than the previous version.

6.2 Bistatic Reflection Mode for the Aluminum Oxide Tag

6.2.1 Set Up

Figure 6.7 shows the set up of the reader antennas for the Bistatic Reflection Mode Measurements with the aluminum oxide tag and Figure 6.8 shows the set up for the calibration without the tag. The chipless structure is located at 20 cm from the transmitter and the receiver antenna. The measured parameter is the reflection coefficient S11, corresponding to the signal sent by Tx and backscattered to Rx.
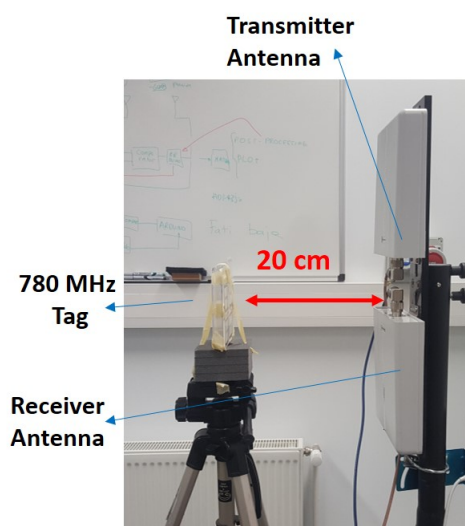
FIGURE 6.7: Set Up for the Bistatic Reflection Mode Measurements

FIGURE 6.8: Set Up for the Bistatic Reflection Mode Calibration

6.2.2 S11 Measurements with the Non-Portable Version of the Reader

Figure 6.9 shows the S11 measurements in the interface of the non-portable reader in Matlab. The sweep and power parameters are indicated in Table 6.5.

Feature	Value
Start Frequency	720 MHz
Stop Frequency	900 MHz
Step Frequency	2 MHz
Output Power	+5 dBm
Distance from the antenna to the tag	20 cm

TABLE 6.5: Parameters Set Up
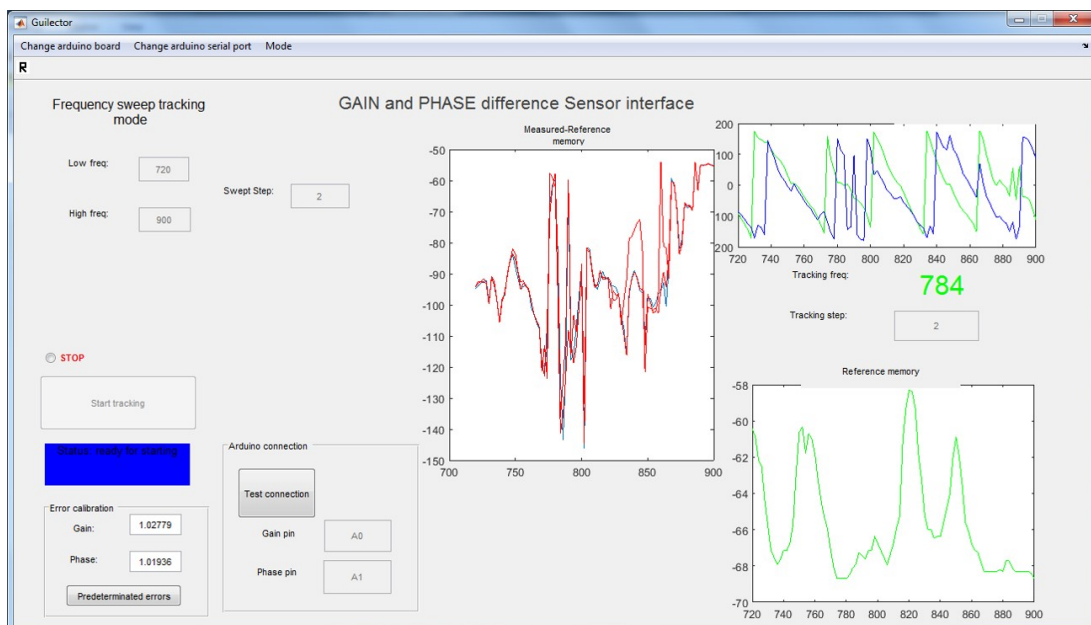
FIGURE 6.9: 780 MHz Tag Bistatic Reflection Mode Measurement

Table 6.6 shows the mean resonance frequency and the standard error of 6 samples.

Measurement	Resonance Frequency (MHz)	Mean of the Reson. Freq. (MHz)	Standard Error of Reson. Freq. (MHz)
1	818		
2	784		
3	786	794.33	±5.81
4	806		
5	786		
6	786		

TABLE 6.6: Resonance Frequency Identified by the Non-Portable Version of the Reader

When operating in the Bistatic Reflection Mode, the mean resonance frequency of this tag is 794.33 MHz, with a standard error of ±5.81 MHz. The accuracy of the set up is not as reliable, so it will be checked if the results improve with the developed reader.

6.2.3   S11 Measurements with the Portable Version of the Reader

To test the performance of the reader, 6 measurements of the S11 have been taken by the designed portable reader. Two gain and phase graphs are of the software application are attached and the sweep and power parameters are indicated in Table 6.12.

Feature	Value
Start Frequency	720 MHz
Stop Frequency	850 MHz
Step Frequency	2 MHz
Output Power	+5 dBm
Distance from the antenna to the tag	20 cm

TABLE 6.7: Parameters Set Up

The mean resonance frequency and the standard error are shown in Table 6.8.

The resonance frequency identified from the gain graph, 782.33 MHz is close to 778 MHz. However, it is not such an exact result as the one obtained for the Transmission Mode. This is also due to the fact that the standard error for the gain resonance frequency is high, ±6.76 MHz, which means that the measurements are more variable.

The result is worse than the one before, but it is closer to the simulated resonance frequency of the chipless tag, so it is valid.

Measurement	Gain Resonance Frequency (MHz)	Phase Resonance Frequency (MHz)	Mean of the Gain Reson. Freq. (MHz)	Standard Error of Gain Reson. Freq. (MHz)
1	770	780		
2	770	784		
3	770	784	782.33	±6.76
4	784	800		
5	788	798		
6	812	814		

TABLE 6.8: Resonance Frequency Identified by the Portable Version of the Reader
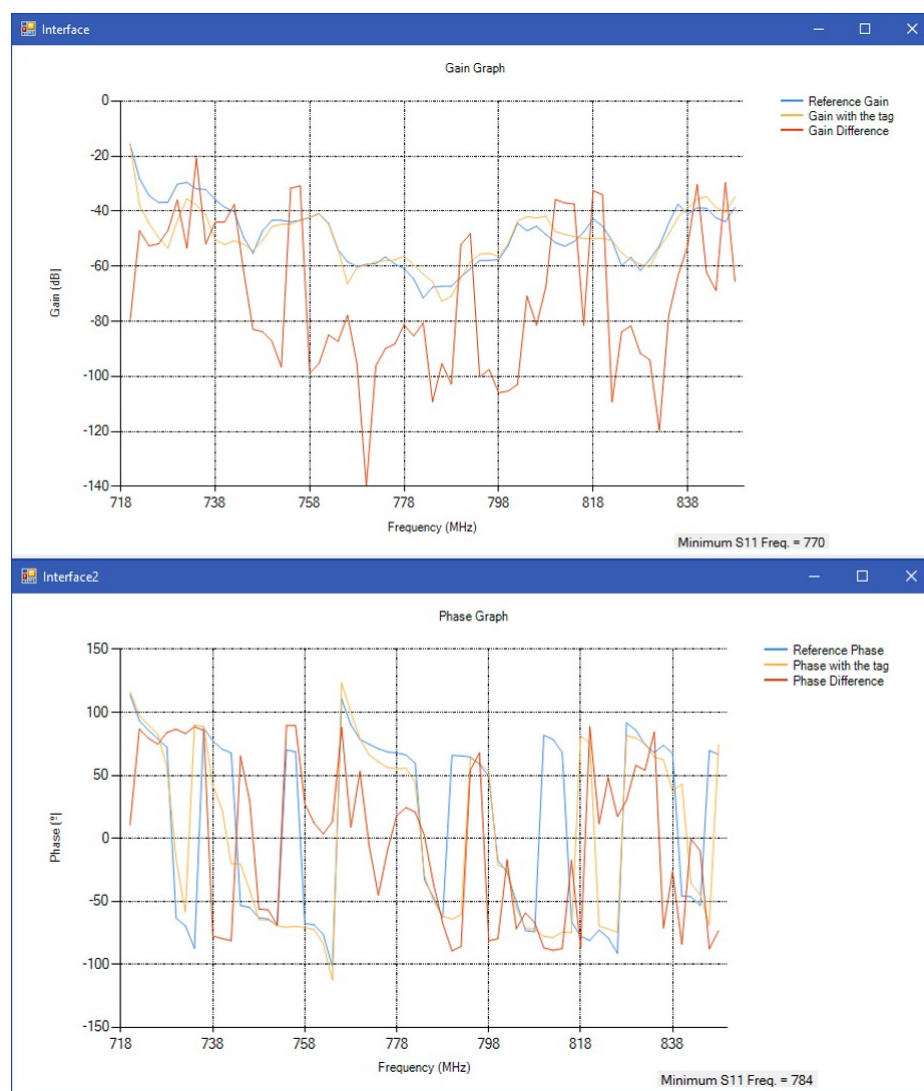
FIGURE 6.10: Aluminum Oxide Tag Bistatic Reflection Mode Measurement

6.2.4   Comparison between the Non-Portable and the Portable Version of the Reader for the Bistatic Reflection Mode

In this section, the performance of the Matlab-based and the portable versions of the chipless Tag reader for the Bistatic Reflection Mode are compared.

Table 6.9 presents the mean resonance frequencies identified by each reader, the corresponding standard error and the distance to the expected 778 MHz value.

	Non-Portable Version of the Reader	Portable Version of the Reader	Improvement
Resonance Frequency (MHz)	794.33	782.33	
Distance to 778 MHz (MHz)	16.33	4.33	12
Standard Error (MHz)	±5.81	±6.76	-0.95

TABLE 6.9: Comparison of Readers for Bistatic Reflection Mode

For the identified resonance frequencies, the distance to VNA value is closer for the portable reader. It differs with the ideal value in 4.33 MHz, if only the gain measurements are analyzed. The distance to 778 MHz in the Matlab-based reader is 16.33 MHz, a very high value, improved by 12 MHz (73.48%) with the Visual Studio-based device. With respect to the standard error, it increased by 0.02 MHz among both readers, which means that the measurements are less constant with the portable design.

For the Bistatic Reflection Mode, the performance of the designed portable chipless RFID reader is better than the previous version according to the resonant frequency mean value identification, but shows more variations in the measurements.

6.3   Monostatic Reflection Mode for Aluminum Oxide Tag

6.3.1   Set Up

Figure 6.12 shows the set up of the single reader antenna for the Monostatic Reflection Mode Operation with the tag that resonates around 778 MHz and Figure 6.11 shows the set up for the calibration without the tag. The chipless structure is located at 20 cm from the antenna. The measured parameter is the reflection coefficient S11, corresponding to the signal sent and backscattered by the same Tx and Rx antenna.

FIGURE 6.11: Set Up for the Monostatic Reflection Mode Calibration
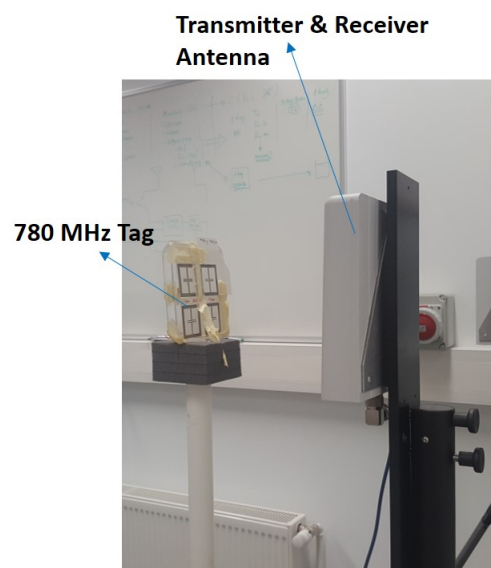
FIGURE 6.12: Set Up for the Monostatic Reflection Mode Measurements
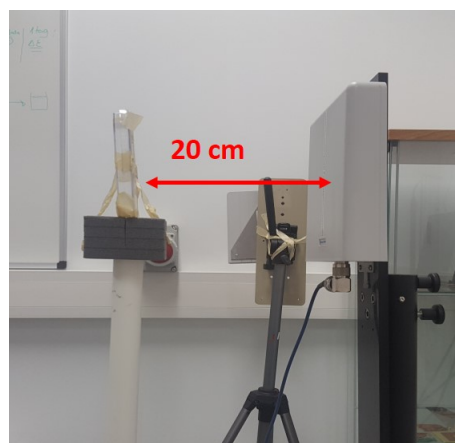
FIGURE 6.13: Set Up for the Monostatic Reflection Mode Measurements

6.3.2 S11 Measurements with the Non-Portable Version of the Reader

S11 measurements in the interface of the Matlab-based version of the reader are in Figure 6.14. The sweep and power parameters are indicated in Table 6.5.

Feature	Value
Start Frequency	720 MHz
Stop Frequency	900 MHz
Step Frequency	2 MHz
Output Power	+5 dBm
Distance from the antenna to the tag	20 cm

TABLE 6.10: Parameters Set Up

The mean resonance frequency and standard error of 6 samples are in Table 6.11.

FIGURE 6.14: 780 MHz Tag Monostatic Reflection Mode Measurement

Measurement	Resonance Frequency (MHz)	Mean of the Reson. Freq. (MHz)	Standard Error of Reson. Freq. (MHz)
1	792		
2	792		
3	792	792	±0
4	792		
5	792		
6	792		

TABLE 6.11: Resonance Frequency Identified by the Non-Portable Reader

When operating in the Monostatic Reflection Mode, the mean resonance frequency of this tag is 792 MHz, with a standard error of ±0 MHz. The accuracy of the set up is constant, so it will be checked if the same happens for the portable reader.

6.3.3   S11 Measurements with the Portable Version of the Reader

To test the operation of the reader in the Monostatic Reflection Mode, 6 measurements of the S11 have been taken. The gain and phase graphs are screenshots of the user interface in the application. The sweep and power parameters are indicated in Table 6.12. The sweeping range is narrower because the results are more accurate within a smaller band.

Feature	Value
Start Frequency	750 MHz
Stop Frequency	830 MHz
Step Frequency	2 MHz
Output Power	+5 dBm
Distance from the antenna to the tag	20 cm

TABLE 6.12: Parameters Set Up

The mean resonance frequency and the standard error are shown in Table 6.28.

Measurement	Gain Resonance Frequency (MHz)	Phase Resonance Frequency (MHz)	Mean of the Gain Reson. Freq. (MHz)	Standard Error of Gain Reson. Freq. (MHz)
1	786	788		
2	786	786		
3	786	778	786.33	±1.67
4	784	788		
5	794	750		
6	782	784		

TABLE 6.13: Resonance Frequency Identified by the Portable Version of the Reader

The resonance frequency identified in the gain graph, is 786.3 MHz. It happens to be further from the resonance than in the previous cases. The standard error for the gain resonance frequency has a value of ±1.67 MHz.

The result is not bad either, and it is close to the expected resonance frequency of the chipless tag, 778 MHz.
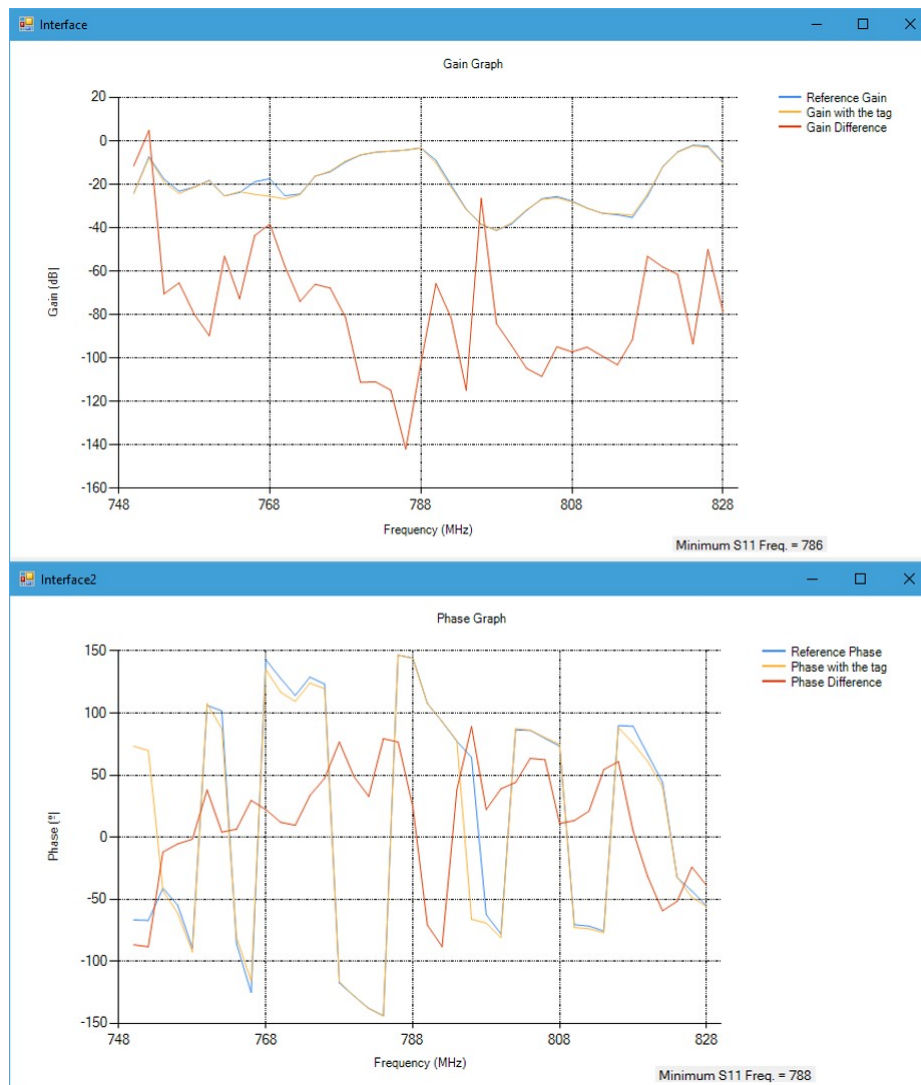
FIGURE 6.15: 780 MHz Tag Monostatic Reflection Mode Measurement

6.3.4 Comparison between the Non-Portable and the Portable Version of the Reader for the Monostatic Reflection Mode

Both versions of the reader for the Monostatic Reflection Mode are compared to determine if there is a significant improvement in the resonance frequency identification. In Table 6.14 the mean resonance frequencies identified by the readers, with their corresponding standard errors and the distance to the expected 778 MHz value are shown.

The distance to the VNA value is closer for the reader with the PLL; it differs in 8.33 MHz. The distance to 778 MHz of the Matlab-based reader is 14 MHz, so it is clear that the 5.67 MHz improvement is worthy. In fact, the accuracy is a 40.50% better. The standard error increased by 1.67 MHz among both readers, which means that the samples are less constant with the portable design, as it happened for the Bistatic Reflection Mode.

	Non-Portable Version of the Reader	Portable Version of the Reader	Improvement
Resonance Frequency (MHz)	792	786.33	
Distance to 778 MHz (MHz)	14	8.33	5.67
Standard Error (MHz)	±0	±1.67	-1.678

TABLE 6.14: Comparison of Readers for Monostatic Reflection Mode

For the Monostatic Reflection Mode, the performance of the portable reader is better than the previous version according to the resonant frequency mean value identification, although it presents a higher standard error.

6.4   Bistatic Transmission Mode for the FR-4 Tag

6.4.1   Set Up

The resonance frequency of the tag is 810 MHz. Figure 6.16 and 6.17 show the set up of the antennas for the Bistatic Transmission Mode Measurements. The chipless structure is located at 20 cm from the transmitter antenna and at 20 cm from the receiver antenna.
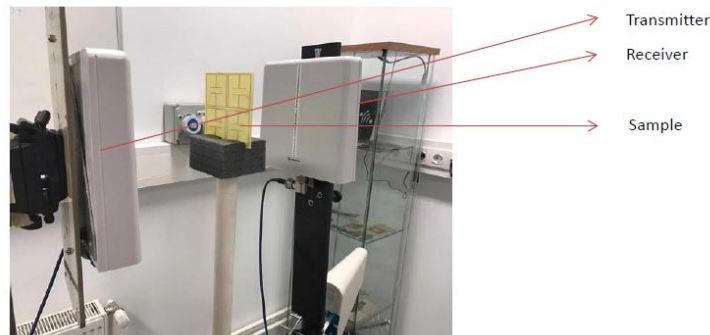
FIGURE 6.16: Set Up for the Bistatic Transmission Mode Measurements
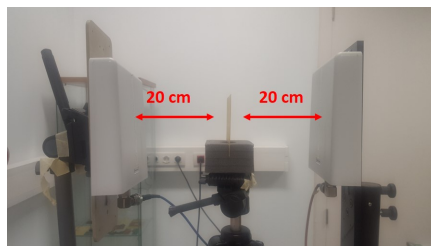
FIGURE 6.17: Set Up for the Bistatic Transmission Mode Measurements

6.4.2 S21 Measurements with the Non-Portable Version of the Reader

S21 measurements taken by the non-portable reader are in Figure 6.18. The sweep and power parameters are indicated in Table 6.15.

Feature	Value
Start Frequency	780 MHz
Stop Frequency	860 MHz
Step Frequency	2 MHz
Output Power	+5 dBm
Distance from the antenna to the tag	20 cm

TABLE 6.15: Parameters for the Bistatic Transmission Operation

The mean resonance frequency, as well as the standard error calculated from 5 measurements are shown in Table 6.16.
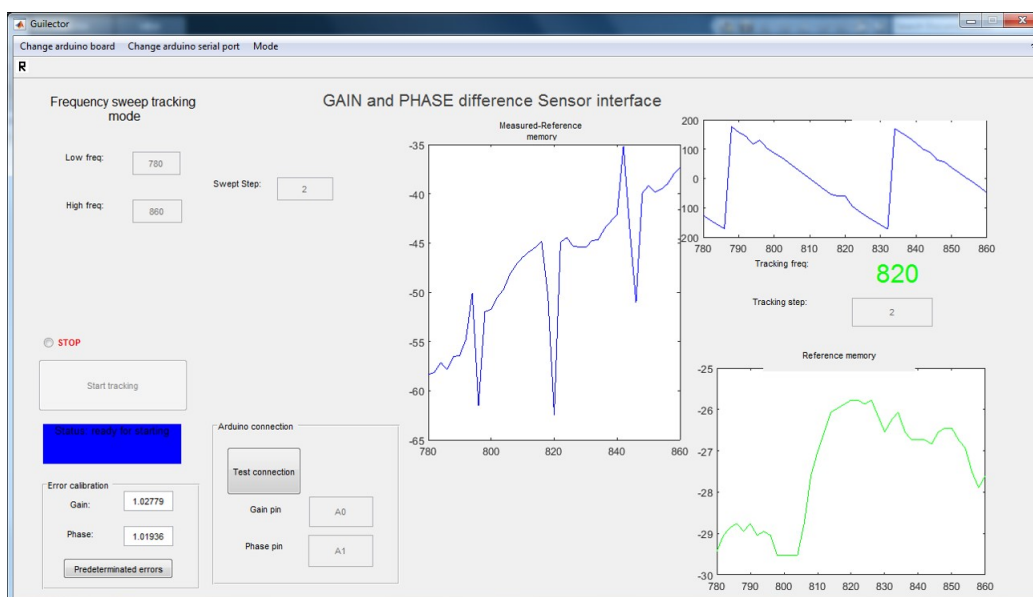
FIGURE 6.18: FR-4 Tag Bistatic Transmission Mode Measurement

Measurement	Resonance Frequency (MHz)	Mean of the Reson. Freq. (MHz)	Standard Error of Reson. Freq. (MHz)
1	820		
2	820		
3	806	817.20	±2.56
4	820		
5	820		

TABLE 6.16: Resonance Frequency Identified by the Non-Portable Reader

As the results show, the resonance frequency of this tag when measuring its S11 with the Bistatic Transmission Mode is 817.2 MHz, with a standard error of ±2.56 MHz. It can be observed that the measurements are very constant, and that only one of the measurements does not detect the correct resonance.

6.4.3   S21 Measurements with the Portable Version of the Reader

The same procedure as before was followed with the Visual Studio-based reader. The next gain and phase graphs are an example of the S21 measurements taken by the designed chipless reader. The sweep and power parameters are the ones indicated in Table 6.17.

Feature	Value
Start Frequency	800 MHz
Stop Frequency	900 MHz
Step Frequency	2 MHz
Output Power	+5 dBm
Distance from the antenna to the tag	20 cm

TABLE 6.17: Parameters for the Bistatic Transmission Operation

The mean resonance frequency, as well as the standard error are calculated from 6 measurements shown in Table 6.18.

Measurement	Gain Resonance Frequency (MHz)	Phase Resonance Frequency (MHz)	Mean of the Gain Reson. Freq. (MHz)	Standard Error of Gain Reson. Freq. (MHz)
1	828	842		
2	804	814		
3	810	816	819.60	±4.77
4	828	842		
5	828	840		

TABLE 6.18: Resonance Frequency Identified by the Portable Version of the Reader

The resonance frequency identified from the gain graph is 819.6 MHz, which is located at a short distance from the expected 810 MHz.

The gain standard error is 4.77. The result is accurate and close to the simulated resonance frequency of the chipless tag.
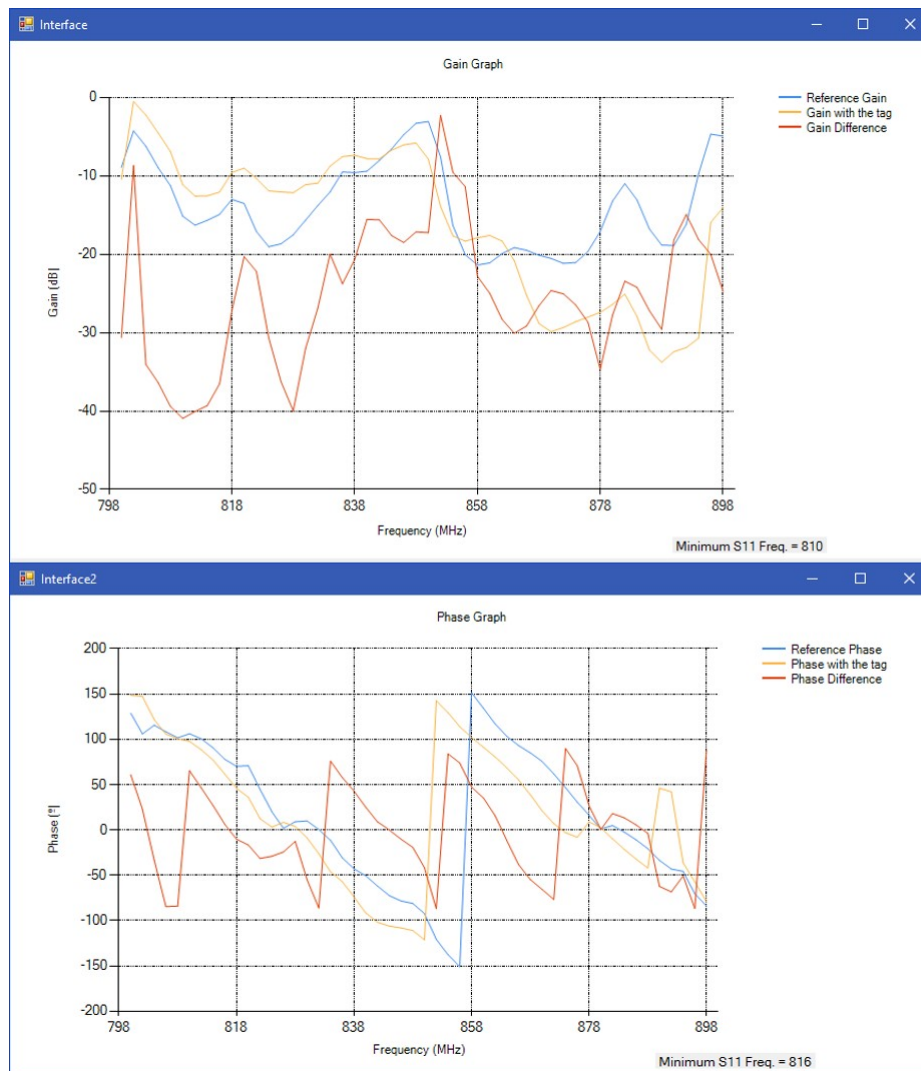
FIGURE 6.19: FR-4 Tag Bistatic Transmission Mode Measurement

6.4.4   Comparison between the Non-Portable and the Portable Version of the Reader for the Bistatic Transmission Mode

In this section the performance of both versions of the reader in the Bistatic Transmission Mode is compared. Table 6.19 presents the mean resonance frequencies identified by each reader, the corresponding standard error and the distance to 810 MHz.

It can be observed that for the identified resonance frequencies, the distance to the value of the VNA is closer for the Matlab-based the reader. It differs with the ideal value in 7.20 MHz. If only the gain measurements are analyzed, the distance to 810 MHz is 9.60 MHz. With respect to the standard error, it increased by 1.97 MHz among the readers, which means that the measurements are less constant with the PLL-based design. The accuracy shows a deterioration of a 33.33% between the two versions. For the Bistatic Transmission Mode, the performance of the designed portable reader is worse.

	Non-Portable Version of the Reader	Portable Version of the Reader	Improvement
Resonance Frequency (MHz)	817.20	819.60	
Distance to 810 MHz (MHz)	7.20	9.60	-2.40
Standard Error (MHz)	±2.56	±4.77	- 1.97

TABLE 6.19: Comparison of Readers for Bistatic Transmission Mode

6.5 Bistatic Reflection Mode for the FR-4 Tag

6.5.1 Set Up

Figure 6.20 shows the set up of the antennas for the Bistatic Reflection Mode Measurements with the tag that resonates around 810 MHz. The chipless structure is located at 20 cm from the transmitter and the receiver antenna.
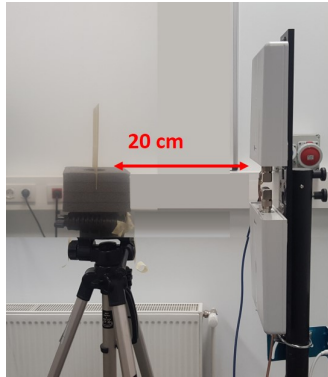
FIGURE 6.20: Set Up for the Bistatic Reflection Mode Measurements

6.5.2 S11 Measurements with the Non-Portable Version of the Reader

S11 measurements in the interface of the non-portable reader are shown in Figure 6.21 and the sweep and power parameters are in Table 6.20. Additionally, the mean resonance frequency, as well as the standard error calculated from 5 measurements are shown in Table 6.21.

When operating in the Bistatic Reflection Mode, the mean resonance frequency of this tag is 808 MHz, with a standard error of 0 MHz, as all the results are constant.

Feature	Value
Start Frequency	780 MHz
Stop Frequency	860 MHz
Step Frequency	2 MHz
Output Power	+5 dBm
Distance from the antenna to the tag	20 cm

TABLE 6.20: Parameters Set Up
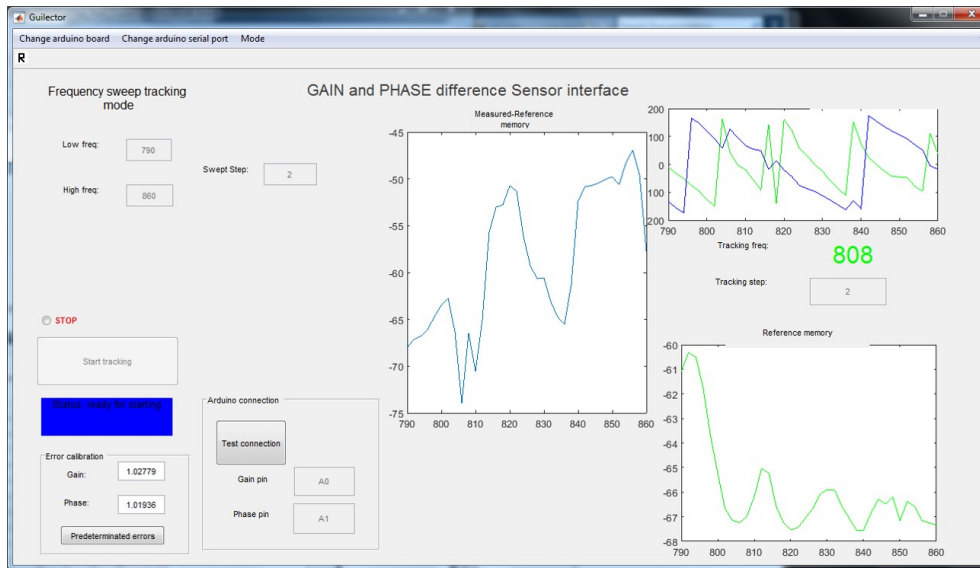
FIGURE 6.21: FR-4 Tag Bistatic Reflection Mode Measurement

Measurement	Resonance Frequency (MHz)	Mean of the Reson. Freq. (MHz)	Standard Error of Reson. Freq. (MHz)
1	808		
2	808		
3	808	808	±0
4	808		
5	808		
6	808		

TABLE 6.21: Resonance Frequency Identified by the Non-Portable Reader

6.5.3 S11 Measurements with the Portable Version of the Reader

In order to test the performance of the reader, 5 measurements of the S11 have been taken by the developed portable reader. The following gain and phase graphs are screenshots of the user interface of the software application. The sweep and power parameters are the ones indicated in Table 6.22.

Feature	Value
Start Frequency	800 MHz
Stop Frequency	900 MHz
Step Frequency	2 MHz
Output Power	+5 dBm
Distance from the antenna to the tag	20 cm

TABLE 6.22: Parameters Set Up

The mean resonance frequency and the standard error are shown in Table 6.23.
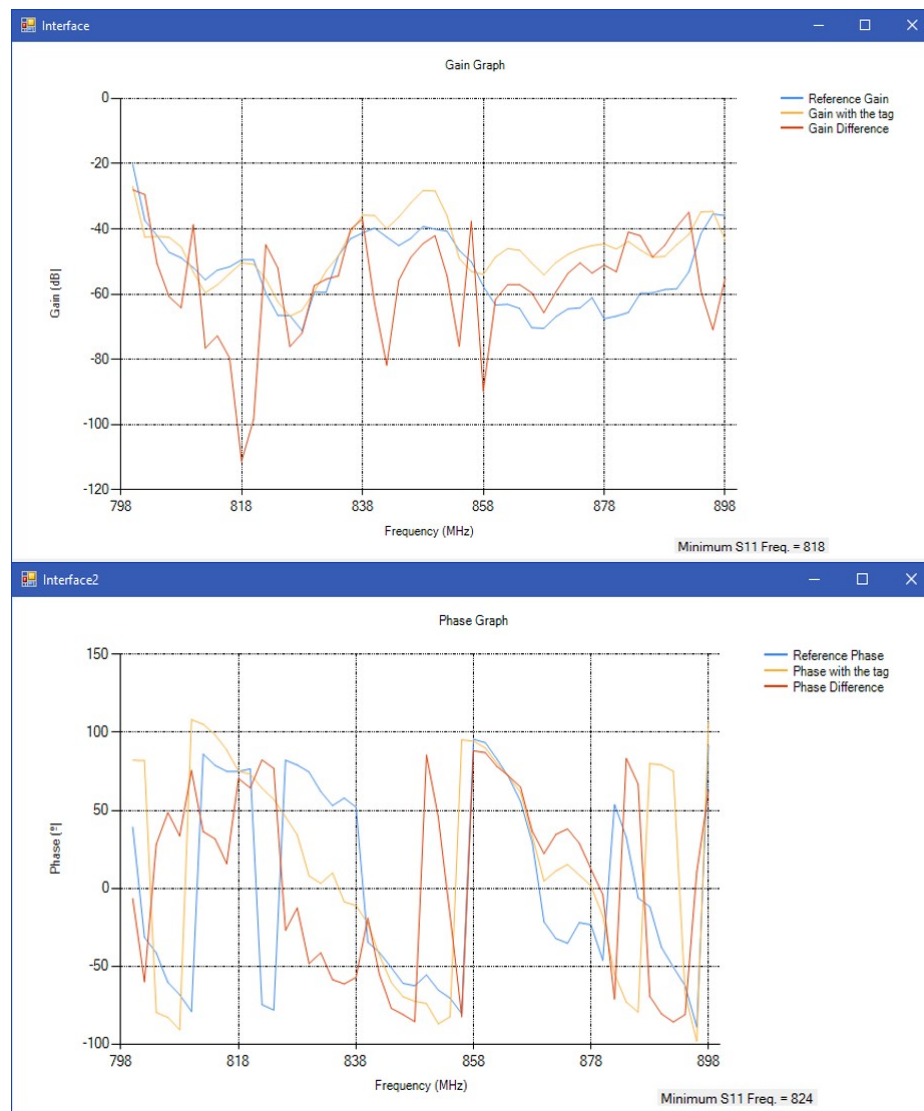
FIGURE 6.22: FR-4 Tag Bistatic Reflection Mode Measurement

The resonance frequency identified from the gain graph, 820.40 MHz is quite far from 810 MHz. It is not such an exact result as the one obtained for the Transmission Mode. The standard error for the gain resonance frequency is ±0.68 MHz, which means that the measurements are not very variable.

Measurement	Gain Resonance Frequency (MHz)	Phase Resonance Frequency (MHz)	Mean of the Gain Reson. Freq. (MHz)	Standard Error of Gain Reson. Freq. (MHz)
1	818	824		
2	822	822		
3	820	826	820.4	±0.68
4	820	824		
5	822	826		

TABLE 6.23: Resonance Frequency Identified by the Portable Version of the Reader

6.5.4   Comparison between the Non-Portable and the Portable Version of the Reader for the Bistatic Reflection Mode

In this section, there is a comparison of the two readers for the Bistatic Reflection Mode.

Table 6.24 presents the mean resonance frequencies identified by each reader, the corresponding standard error and the distance to the expected 810 MHz value.

	Non-Portable Version of the Reader	Portable Version of the Reader	Improvement
Resonance Frequency (MHz)	808	820.4	
Distance to 810 MHz (MHz)	2	10.40	8.40
Standard Error (MHz)	±0	±0.68	-0.68

TABLE 6.24: Comparison of Readers for Bistatic Reflection Mode

For the identified resonance frequencies, the distance to VNA value is closer for the non-portable reader. It differs with the ideal value in 2 MHz. If only the gain measurements of the portable device are analyzed, the distance to 810 MHz is 10.40 MHz, a very high value. The deterioration is 8.40 MHz (76.19%). With respect to the standard error, it increased by 0.68 MHz among both readers, because the measurements were all constant with the first version.

For the Bistatic Reflection Mode, the performance of the portable reader is worse than the previous version according to the resonant frequency mean value identification, and shows more variations in the measurements.

6.6 Monostatic Reflection Mode for the FR-4 Tag

6.6.1 Set Up

Figure 6.23 shows the set up of the antenna for the Monostatic Reflection Mode Operation with the FR-4 tag. The chipless structure is located at 20 cm from the antenna.
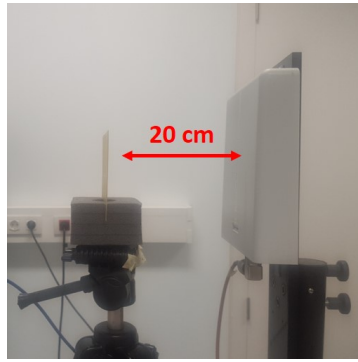

FIGURE 6.23: Set Up for the Monostatic Reflection Mode Measurements

6.6.2 S11 Measurements with the Non-Portable Version of the Reader

S11 measurements in the interface in Matlab are in Figure 6.24. The sweep and power parameters are in Table 6.25.

Feature	Value
Start Frequency	780 MHz
Stop Frequency	860 MHz
Step Frequency	2 MHz
Output Power	+5 dBm
Distance from the antenna to the tag	20 cm

TABLE 6.25: Parameters Set Up

Measurement	Resonance Frequency (MHz)	Mean of the Reson. Freq. (MHz)	Standard Error of Reson. Freq. (MHz)
1	818		
2	818		
3	818	818	±0
4	818		
5	818		

TABLE 6.26: Resonance Frequency Identified by the Non-Portable Reader

The mean resonance frequency, as well as the standard error calculated from 5 measurements are shown in Table 6.26.

FIGURE 6.24: FR-4 Tag Monostatic Reflection Mode Measurement

When operating in the Monostatic Reflection Mode, the mean resonance frequency of this tag is 818 MHz, with a standard error of ± 0 MHz. The accuracy of this set up seems to be very constant and reliable, so it will be checked if the same happens for the reader with the PLL.

6.6.3   S11 Measurements with the Portable Version of the Reader

To test the operation of the reader in the Monostatic Reflection Mode, 1 of the 5 samples of the S11 is shown in the gain and phase graphs. The sweep and power parameters are in Table 6.27 and the mean resonance frequency and the standard error are in Table 6.28.

Feature	Value
Start Frequency	800 MHz
Stop Frequency	900 MHz
Step Frequency	2 MHz
Output Power	+5 dBm
Distance from the antenna to the tag	20 cm

TABLE 6.27: Parameters Set Up
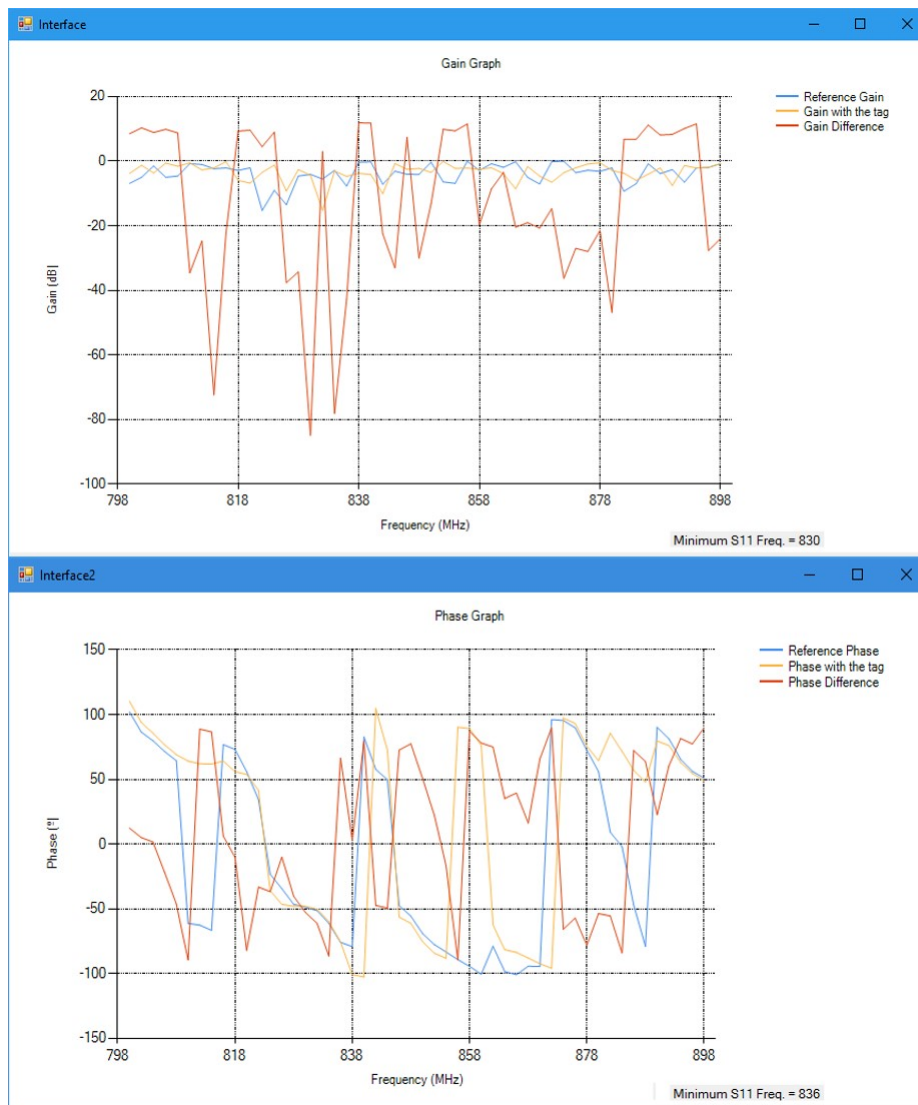
FIGURE 6.25: FR-4 Tag Monostatic Reflection Mode Measurement

Measurement	Gain Resonance Frequency (MHz)	Phase Resonance Frequency (MHz)	Mean of the Gain Reson. Freq. (MHz)	Standard Error of Gain Reson. Freq. (MHz)
1	836	836		
2	836	836		
3	836	836	834.40	±1.06
4	834	834		
5	830	836		

TABLE 6.28: Resonance Frequency Identified by the Portable Version of the Reader

The resonance frequency identified in the gain graph is 834.40 MHz. This result is not very promising, as it is far from the ideal 810 MHz resonance of the tag. The standard error for the gain resonance frequency has a value of ±1.06 MHz.

6.6.4   Comparison between the Non-Portable and the Portable Version of the Reader for the Monostatic Reflection Mode

The operation of the Matlab-based and Visual Studio-based versions of the reader for the Monostatic Reflection Mode are compared in this section. In Table 6.29 the mean resonance frequencies identified by the readers, with their corresponding standard errors and the distance to the VNA value are shown.

	Non-Portable Version of the Reader	Portable Version of the Reader	Improvement
Resonance Frequency (MHz)	818	834.40	
Distance to 810 MHz (MHz)	8	24.4	-16.4
Standard Error (MHz)	±0	±1.06	-1.06

TABLE 6.29: Comparison of Readers for Monostatic Reflection Mode

The distance to 810 MHz is closer for the non-portable reader, as it differs in 8 MHz. If the value of the gain graphs is taken into account, this distance is 24.40 MHz. These results are worse than the ones gotten with the previous system. In fact, the accuracy is a 51.21% worse. The standard error increased by 1.06 MHz among both readers, which means that the measurements are less constant with the design with the PLL.

For the Monostatic Reflection Mode and the FR-4 tag, the performance of the portable reader is worse, according to the resonant frequency identification.

6.7   Monostatic Reflection Mode for Low Frequency Tags

6.7.1   Set Up

The ADF4350 PLL works in a frequency range over 137.5 MHz, and even if it could be replaced with an ADF4351 with an operation band starting at 35 MHz, this frequency is still high for measuring the low frequency tags. Their resonance peak is around 20 MHz, so it is not possible to generate such a low sweep if it is not by using the signal generator. That is why these tags are tested only with the non-portable reader.

It is helpful to explain the set up for this operation mode, based on the block diagram of the Tagsense reader in Section 3.4.3. The set up employed is the one in Figure. 6.26.

The signal generator is connected to the ZFBDC20-61HP-N+ bidirectional coupler. Its output goes to the loop antenna, composed by an inductance. and placed facing a chipless tag. The coupled input is connected to the $INPUT_A$ pin of the gain/phase detector, and the coupled output is wired to the $INPUT_B$.
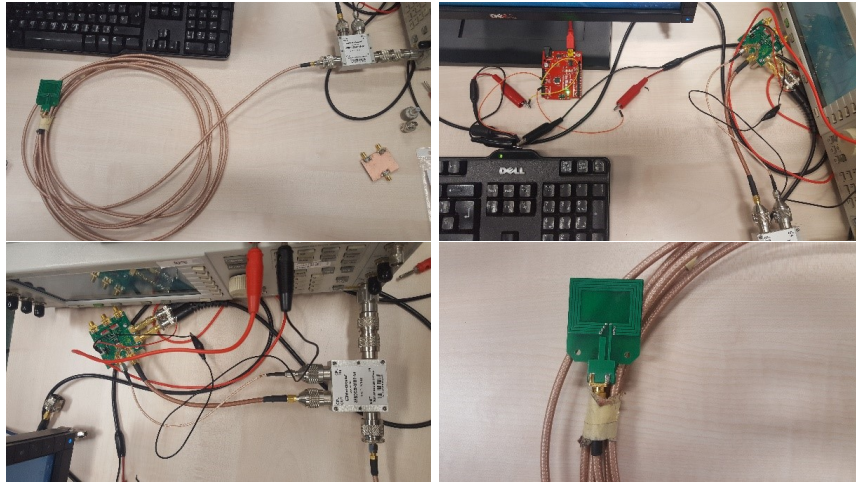
FIGURE 6.26: Set up for the low frequency tags S11 measurement

FIGURE 6.27: Set up of Tag 1 for the measurements

FIGURE 6.28: Set up of Tag 2 for the measurements
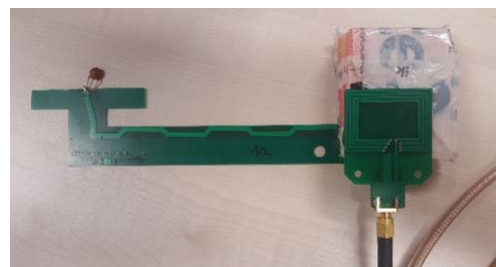
FIGURE 6.29: Set up of Tag 3 for the measurements

6.7.2   S11 Measurements with the Non-Portable Version of the Reader

The sweep and power parameters are in Table 6.30 and the results are shown in Table 6.31.

Feature	Value
Start/Stop Frequency	15 - 30 MHz
Step Frequency	0.2 MHz
Output Power	+5 dBm
Distance from the antenna to the tag	2/2.5 cm

TABLE 6.30: Parameters Set Up

As the measurement procedure for these low frequency tags is slightly different from the previous techniques, it will be explained step by step in a more detailed way.

6.7.3   Measurements with Reference Calibration

First of all, a reference measurement of the loop antenna without a tag is done, although the need of this initial calibration will be discussed later. It is carried out by selecting the frequency parameters and pressing the *Reference Meas.* Button on the left side of the interface. The antenna has a very high impedance, that is why it will reflect the whole transmitted signal back to the wire.

After that calibration, the tag is placed facing the antenna and several trackings are done by selecting the tracking step located between the two graphs on the right side of the interface and pressing the Tracking Button. The tracking consists of doing a frequency sweep, finding the point at which the minimum gain is located and checking if it remains constant. The signal generator sends a signal of a frequency equal to the minimum frequency plus/minus the tracking step and the software checks if the minimum is still the same. The frequency written on the interface updates to the smallest value. This operation is repeated for a fixed time, and then a new frequency sweep takes place to look for the minimum on the whole range of frequencies.

Tag 1

The average value of the resonance frequency is 20.5 MHz, with a standard error of 0.3316. The frequency at which the minimum reflection takes place is lower on each measurement, so a more exact and constant value would be better for the resonating frequency determination.
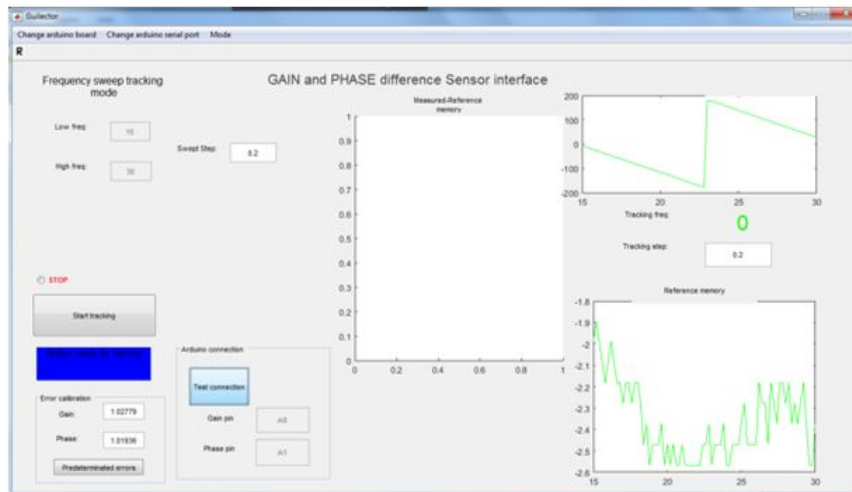
FIGURE 6.30: Reference measurement for Tag 1
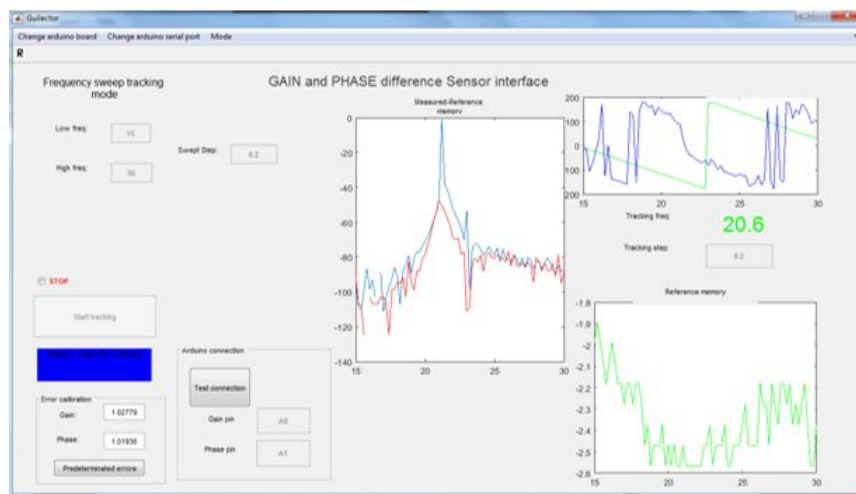
FIGURE 6.31: S11 of Tag 1 with reference measurement subtraction

6.7.4 Measurements without Reference Calibration at 2.5 cm

Due to the fact that the antenna is adapted to 50 Ω, in order to decrease the standard error obtained in the previous measurements, the reference measurement of the antenna without facing the tag is omitted. Therefore, the Tracking Button is pressed after selecting the correct values for the frequency sweep and tracking steps.

Tag 1 at 2.5 cm

The results obtained this time are constant and the peak shows up as a minimum. The resonating frequency of the first tag is 21 MHz. All the trackings detect the same minimum, so it can be concluded that the quality of the measurements without the initial reference calibration is better. Therefore, the mean is 21 MHz and the standard error is 0. The minimum value is extracted from the gain graph, although the phase is also

plotted. However, the phase also gives useful information for detecting the minimum reflection, as it shows a peak around 21 MHz. The Matlab algorithm could be improved and updated to detect that peak in the phase and compare it with the gain.
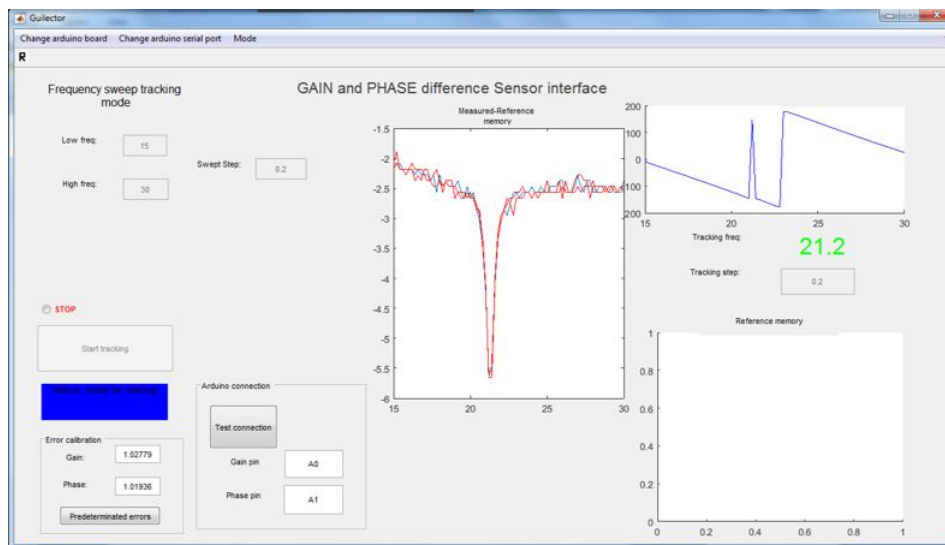
FIGURE 6.32: S11 of Tag 1 without reference measurement subtraction

Tag 2 at 2.5 cm

As it can be observed in Figure 6.33 the resonating frequency is constant and around 20 MHz as expected; exactly 19.8 MHz, with a null standard error. However, the phase graph does not show the peak at the minimum reflection value as before.
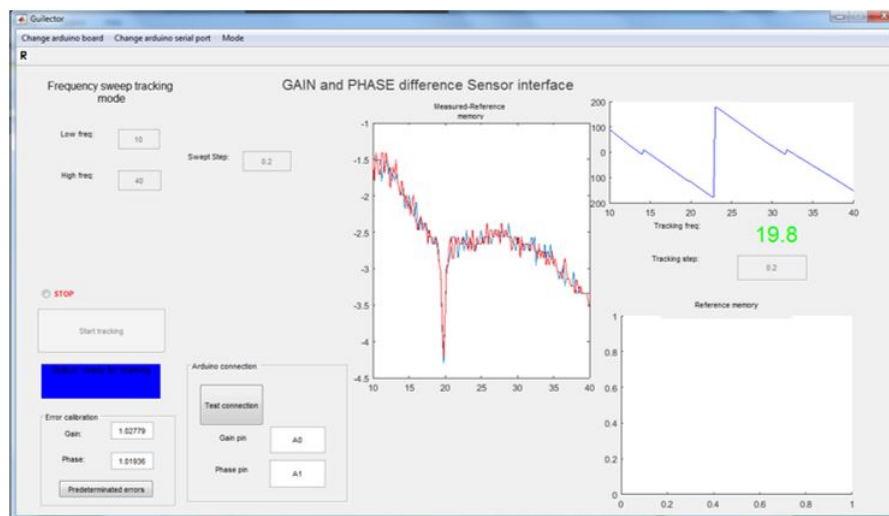
FIGURE 6.33: S11 of Tag 2 without reference measurement subtraction

Tag 3 at 2.5 cm

The results for tag 3 are consistent with the previous ones, as the standard error in the resonance frequency measurement without the reference calibration is zero. The

resonance frequency of the tag is 26.6 MHz, a little bit higher than for Tag 1 and 2, but still constant. The phase on the peak graph appears again at the minimum frequency.
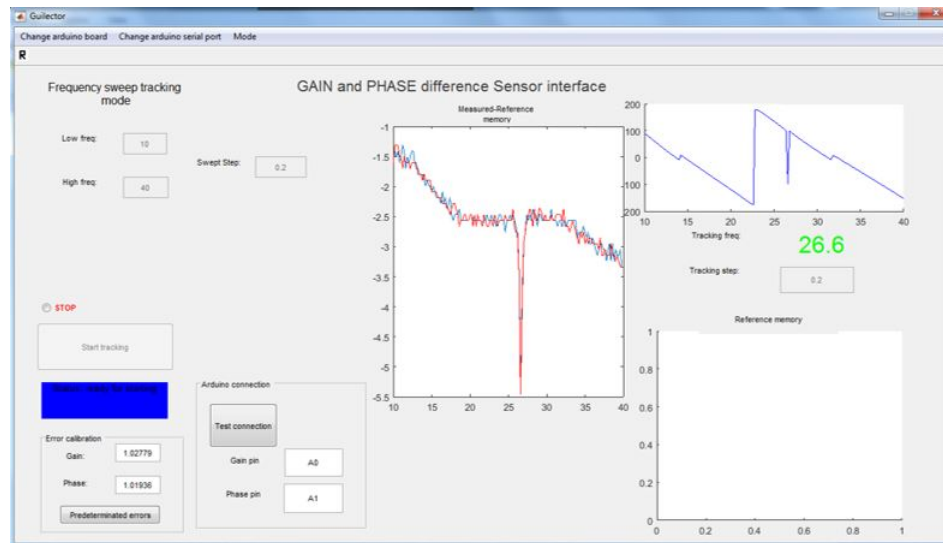
FIGURE 6.34: S11 of Tag 3 without reference measurement subtraction

6.7.5   Measurements without Reference Calibration at 2 cm

Tag 1 at 2 cm

The experiment is repeated with the antenna and the tag at a smaller distance, 2 cm.

The resonance frequency of tag 1 is slightly higher than before, but the result is not that significant, as the value is around 20 MHz and the standard error is null.
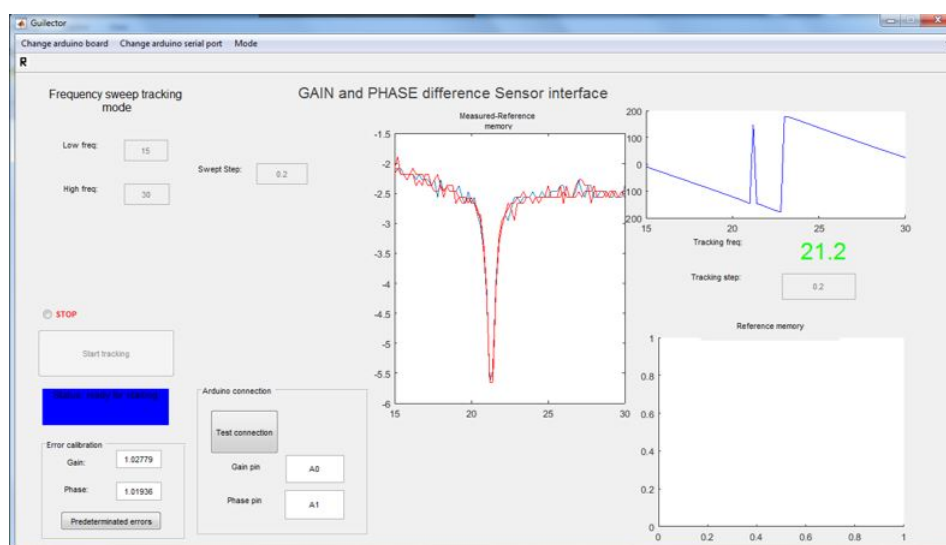
FIGURE 6.35: S11 of Tag 1 without reference measurement subtraction at 2 cm

Tag 2 at 2 cm

With tag 2, the resonance frequency is 19.8 MHz at a distance of 2 cm. When measured at 2.5 cm, the minimum reflection coefficient was at 19.8 as well, so it remains constant.
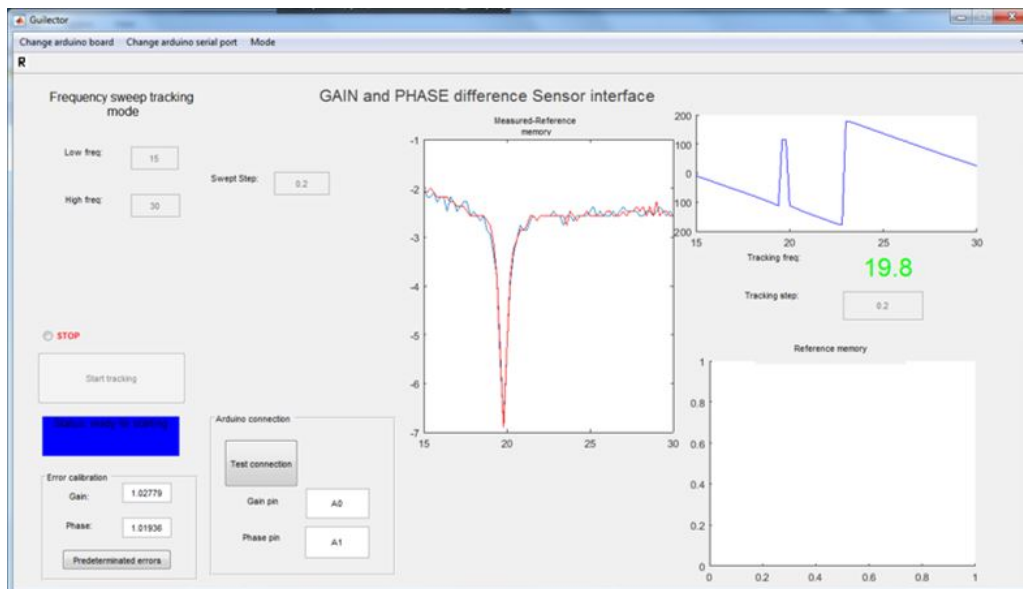
FIGURE 6.36: S11 of Tag 2 without reference measurement subtraction at 2 cm

Tag 3 at 2 cm
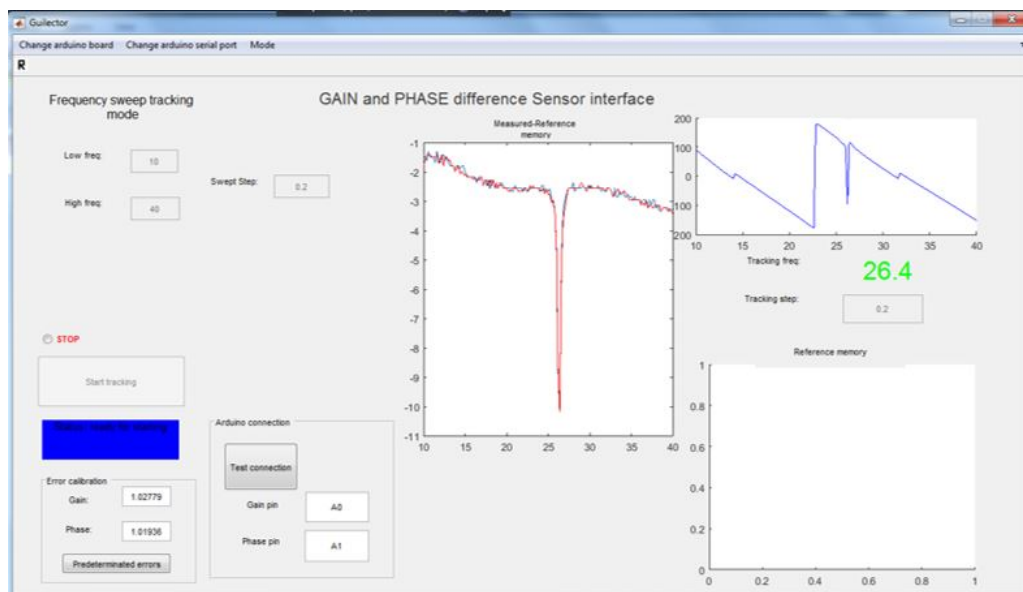
FIGURE 6.37: S11 of Tag 3 without reference measurement subtraction at 2 cm

According to the experimental results obtained for tag 3, the resonance frequency of the third tag is 26.4 MHz. The previous measurements showed that the minimum S11 was at 26.6 MHz. There is a difference of 0.2 MHz between both measurements.

Resonance Frequency of Tag 1 with calibration						
Tag	Distance (cm)	Frequency Sweep Range (MHz)	Step (MHz)	Resonance Frequency (MHz)	Mean (MHz)	Standard Error
1 (with ref.meas)	2	15-30	0.2	21.2 20.6 20.6 19.6	20.5	0.3316
1 (without ref.meas)	2.5	15-30	0.2	21 21 21 21	21	0
2 (without ref.meas)	2.5	10-40	0.2	19.8 19.8 19.8 19.8	19.8	0
3 (without ref.meas)	2.5	10-40	0.2	26.6 26.6 26.6 26.6	26.6	0
1 (without ref.meas)	2	15-30	0.2	21.2 21.2 21.2 21.2	21.2	0
2 (without ref.meas)	2	15-30	0.2	19.8 19.8 19.8 19.8	19.8	0
3 (without ref.meas)	2	15-30	0.2	26.4 26.4 26.4 26.4	26.4	0

TABLE 6.31: Measured values for tags 1, 2 and 3

Chapter 7

Conclusions

After identifying the resonance frequency of two chipless tags with the designed portable reader and setting up the device for three operation modes (Bistatic Transmission, Bistatic Relection and Monostatic Reflection Mode), the obtained values are analyzed to characterize the reader. Once the resonance frequency is identified, it will be concluded which of the modes has the best performance and if the device is fast enough.

7.1 Operation Mode Comparison

In this section, the three operation modes of the chipless tag reader are compared, taking into account the calculated parameters for the two tags. The numbers are shown in Table 7.1, and they are analyzed and commented below.

	VNA	Bistatic Transmission Mode	Bistatic Reflection Mode	Monostatic Reflection Mode
Resonance Frequency (MHz)	778 810	780 819.6	782.33 820.40	786.33 834.40

TABLE 7.1: Comparison of Operation Modes

The detected resonance frequencies are notably close to the expected ones for both tags in the three modes. This fact is evaluated in Table 7.2 where the distance from the measured frequency to the VNA value are calculated.

The most relevant values are the three numbers in the Overall Mean Column of the table. It is observed that the Bistatic Transmission Mode approaches the most to the

theoretical resonance, as it only differs on 5.80 MHz. The Bistatic Reflection Mode presents results that are 10.40 MHz away from the expected resonance, which is an acceptable result too. The Monostatic Reflection Mode has a higher value, 16.36 MHz, which is the most inaccurate operation mode.

The performance of the modes is similar for both tags. However, even if some of the differences are higher than others, they are all below 20 MHz. Taking into account that the S11 and S21 of the tags were measured in a 100/130 MHz frequency range, this is not such a significant difference.

Distance to 778/810 MHz (MHz)	VNA	Bistatic Transmission Mode	Bistatic Reflection Mode	Monostatic Reflection Mode
Mean for tag (MHz)	778 MHz	2	4.33	8.33
	810 MHz	9.60	10.40	24.40
Overall Mean (MHz)	**Mean**	5.80	7.36	16.36

TABLE 7.2: Comparison of Distances to the Expected Resonance

The measurements of the standard error of each operating mode are in Table 7.3.

Standard Error (MHz)	Tag	Bistatic Transmission Mode	Bistatic Reflection Mode	Monostatic Reflection Mode
Mean for Tag (MHz)	780 MHz	±0	±6.76	±1.67
	820 MHz	±4.77	±0.68	±1.06
Overall Mean (MHz)	**Mean**	±2.38	±3.72	±1.36

TABLE 7.3: Comparison of Standard Errors

According to the standard error, it can be stated that the Monostatic Reflection Mode is the one that presents the lower error. The error of the Bistatic Transmission Mode has a similar value. This time, the Bistatic Reflection Mode presents the most varying, this is, less constant numbers.

7.2 Sweep Time Comparison

The time of a sweep of 130 MHz was counted both for the non-portable reader and for the portable device, in order to determine which one is faster. The most interesting result would be a significant reduction of the time it takes to send the interrogation signal; this is, to do the frequency sweep. Apart from delay of the connection to the Arduino, this parameter depends exclusively on the signal generator in the case of the first version of the reader and on the PLL in case the novel version is being used. The time of a sweep is not dependant on the mode of operation of the reader. The measured timings are shown in Table 7.4 and Table 7.5.

Measurement	Sweep Time (ms)	Mean of the Sweep Time (ms)	Standard Error of Sweep Time (ms)
1	41.93		
2	42.13		
3	37.80	38.89	±1
4	36.73		
5	37.17		
6	37.59		

TABLE 7.4: Sweep Time Measurements with the Non-Portable Version of the Reader

Measurement	Sweep Time (ms)	Mean of the Sweep Time (ms)	Standard Error of Sweep Time (ms)
1	26.93		
2	27.26		
3	28.26	28.02	±0.3
4	28.69		
5	28.61		
6	28.38		

TABLE 7.5: Sweep Time Measurements with the Portable Version of the Reader

It can be observed that the mean time of a 130 MHz sweep is 38.89 ms in the Matlab-based reader. Additionally, the mean time of a 130 MHz sweep is 28.02 ms in the portable equipment.

This fact implies a reduction of the sweeping time of 10.87 ms, a great advantage, because more measurements will be done in less seconds. Concretely, the designed chipless tag reader is a 27.95% faster.

7.3   Analysis of Low Frequency Measurements

The results of the low frequency tags are analyzed apart from the previous ones, because the reader antennas are not the same, and the operation of the Matlab software is slightly different, as the calibration is not taken into account.

All the tags have the resonance around 20 MHz, as the measurements confirm. If the numbers obtained for distinct distances from the antenna to the tags are analyzed, according to the obtained experimental results for tag 3, there is a difference of 0.2 MHz between the measurements carried out. The same happened for tag 1, so two conclusions can be deduced.

1. There is a measurement error when doing the frequency sweep, as it is done with a step of 0.2 MHz.

2. The resonance frequency varies slightly with the distance between the antenna and the tag.

These results can be improved by detecting the peak present on the phase plot and calculating a more exact resonance frequency value. Moreover, if a smaller step is used, 0.1 MHz for instance, the numbers could be more accurate.

Table 6.31 in the previous chapter contains the measured values for the three tags at different distances and the calculation of the standard error for each one.

Chapter 8

Improvements in the Chipless RFID Reader and Future Work

From the conclusions chapter it can be deduced that the designed resonance frequency identification reader works properly for the three possible operation modes and for two different tags. Moreover, it sends an interrogation signal in a reduced time. However, there are some aspects of the device that could be improved, such as the accuracy of the detection and identification of the resonance frequency of the resonator and the speed of the sweep. In this chapter, several techniques employed to change the desired parameters are described. Some of them have already been implemented, and some others still need to be tested and will be left as future work.

8.1   Reduce of the number of measurements for each frequency

Each time the PLL generates a tone at a certain frequency, the Arduino Driver sends a request to the hardware and reads the gain and phase voltage values from the corresponding pins. As it was explained in Section 5.3, *vg* and *vf* in Listing A.10 are the variables that store a mean of four measurements done consequently in the A0 (*ping*) and A1 (*pinf*) pins in a respective way.

The improvement in the speed of the reader consists of doing a single reading instead of four. This way, the time the arduino is requesting voltage values is reduced significantly, therefore, the frequency sweep of the PLL as well. The time of one sweep is reduced from 28.02 ms to 20.23 ms.

8.2   Increase the step between frequencies in the sweep

Increasing the step between frequencies in the interrogation signal does not require any change in the C language code, neither in the hardware of the device. The spacing can be directly modified in the user interface of the ADF435x application.
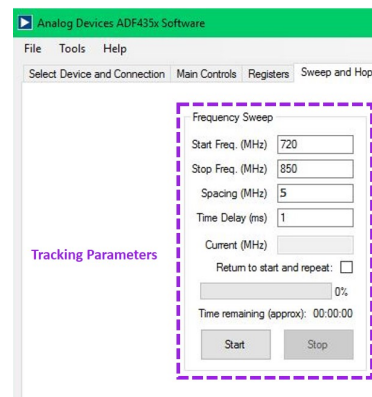
FIGURE 8.1: 5 MHz Step Parameters

If the step is increased to a higher value, for instance, from 2 MHz to 5 MHz, the time of one sweep is reduced from 28.02 ms to 12.43 ms. This happens because if the same frequency range is maintained, there are less steps between the limits of the sweep. Indeed, the resonance frequency value can be more inexact, but at the same time have a smaller standard error, as the results are more constant.

Figure 8.2 and 8.3 show the gain and phase graphs of a measurement done with a 5 MHz step for the 780 MHz tag. The curve is not as smooth as for 2 MHz, but the value still approaches the required one, it is 765 MHz from the gain and 775 MHz from the phase.
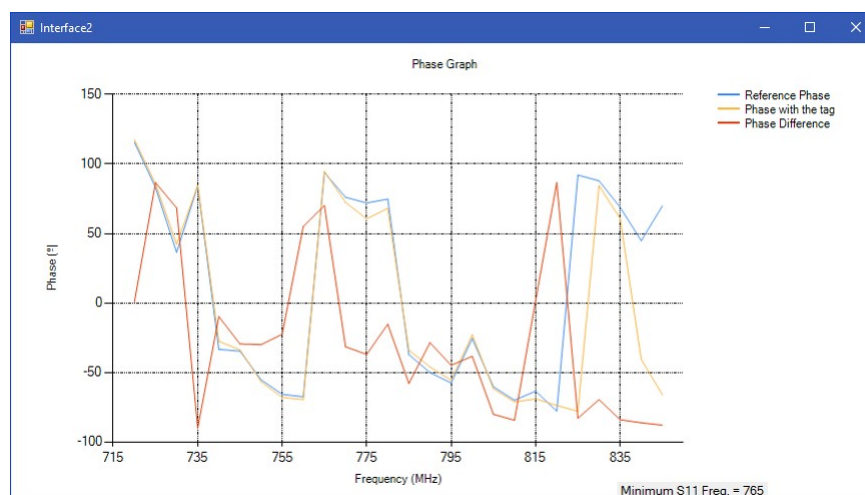
FIGURE 8.2: Aluminum Oxide Tag Gain Measurement with 5 MHz step
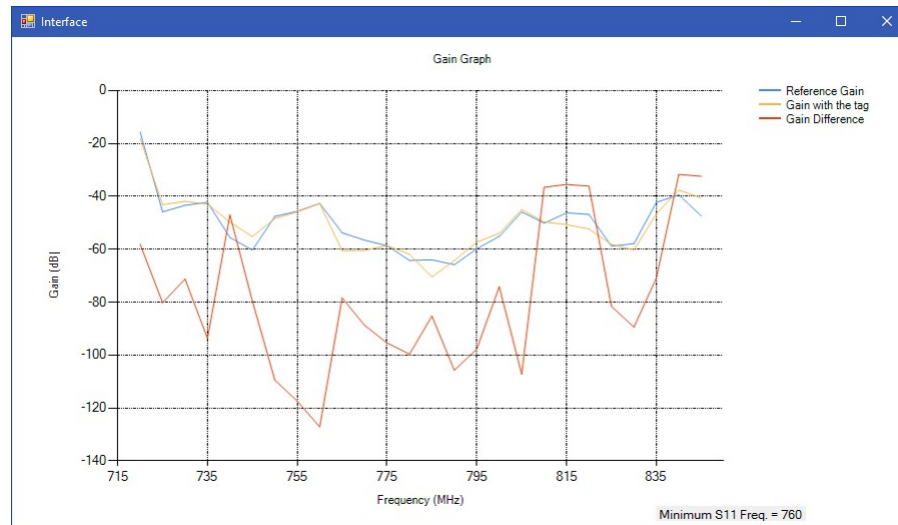
FIGURE 8.3: Aluminum Oxide Tag Phase Measurement with 5 MHz step

8.3   Change of speed of the Arduino

It is interesting to have the fastest reader as possible, so one of the improvements in the device is changing the speed settings of the Arduino UNO in order to read analog voltages at a higher bit rate.

In this section, it is explained how to change this feature from the Arduino IDE, the open-source software provided with the platform.

First, the software of Arduino Programming (Arduino IDE) needs to be downloaded from the official website of Arduino.
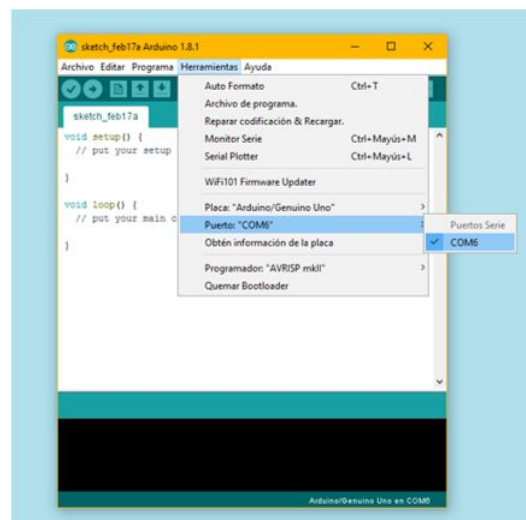
FIGURE 8.4: Arduino IDE Interface Screenshot of COM Port Settings
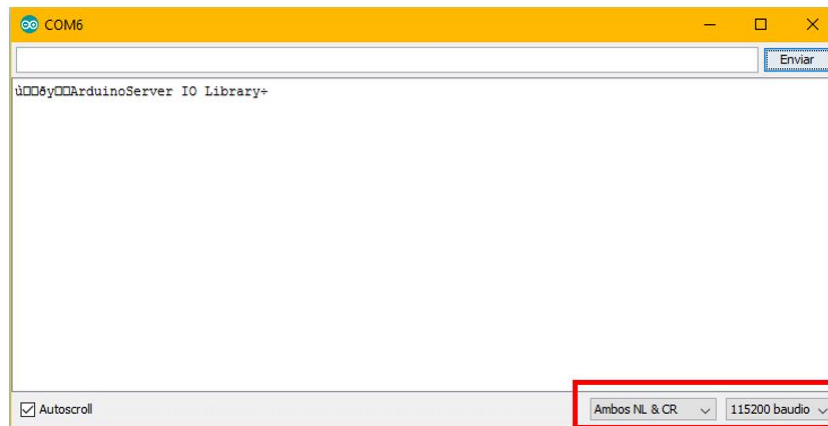
FIGURE 8.5: Arduino IDE Interface Screenshot of Speed Settings

If the arduino.exe file is opened and the RedBoard is connected to the laptop via USB, some communication tests can be carried out, as the program includes a serial message sending /receiving tool.

When opening the mentioned file, a blank example pops up on the screen. It is not necessary to open any specific Arduino project. When selecting Tools>Port, the COM Port to which the device is connected must be chosen. After that, if the icon with the magnifying glass is clicked, whose name is Serial Monitor, the serial communication tool will be opened. On the bottom of the screen, the speed must be set at 115.200 and the option Both NL and CR (both New Line and Carriage Return) activated.

This way, the communication of the Arduino will be faster than before, but as mentioned, the methodology of connecting all over again with the computer and with the Arduino, makes the system still slow.

Once the features of the Arduino are changed, the measurements can be taken properly at a slightly higher speed.

8.4 Use the ADF4351 Wideband Synthesizer with Integrated VCO

In the gain and phase graphs shown in Section 5.5, it is observed that there is not a perfect straight line as the datasheet stated, but an irregular curve. In previous graphs plotted over a wider frequency range, some undesired peaks are also observed below 700 MHz and above 2100 MHz, which might cause the wrong identification of the gain and phase values in dB and degrees. Although the cause of the noisy signal is not clear, it could be due to the reduced working range of the ADF4350, 137.5 MHz-2700 MHz.

Therefore, if the device is replaced with a PLL of its family that works with the same software, several changes may be appreciated. The working range of the ADF4351 is 35 MHz-2700 MHz. When the *ADF4351* radio button is selected in the front panel of the user interface, the operation of the software and device is equal to the previous one.

The plots with the ADF4350 and ADF4351 are attached in order to compare the smoothness of the curves. However, the shape of both lines still presents the undesired peaks, so they are not caused by the PLL, but by another factor in the circuit.
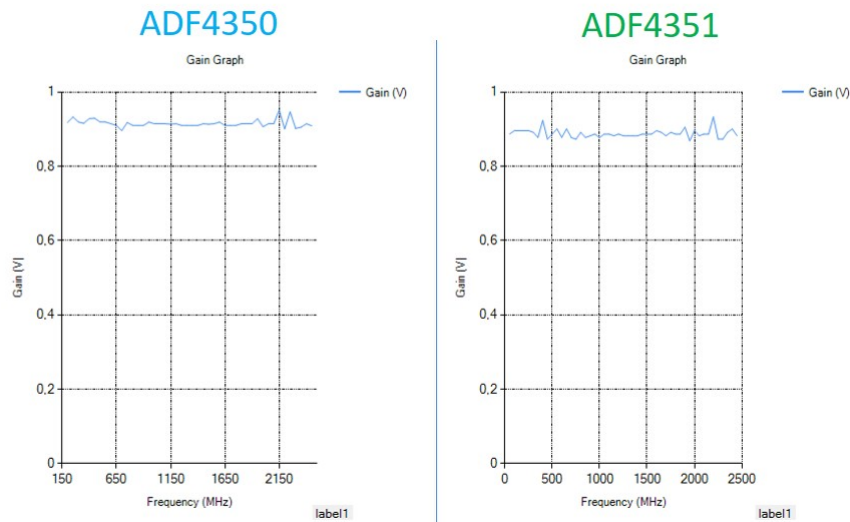
FIGURE 8.6: Gain Graphs for the same Input Power
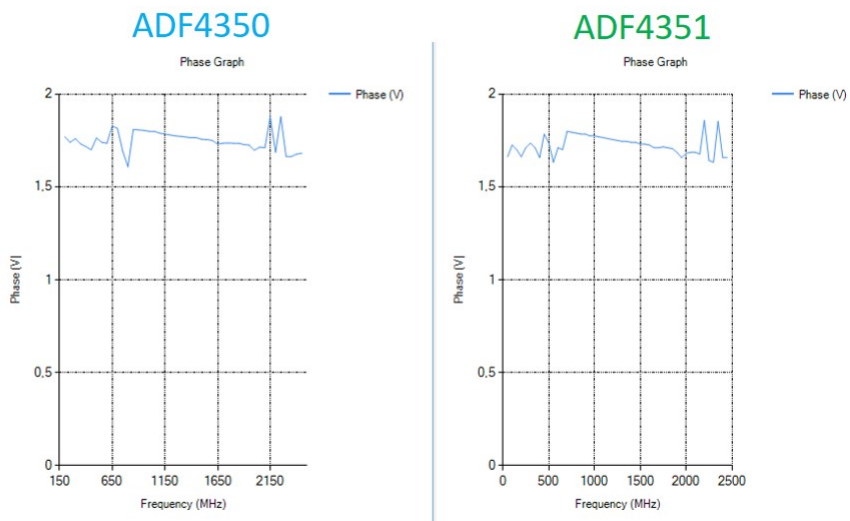
FIGURE 8.7: Phase Graphs for a phase change of 0 degrees

Despite the ADF4351 does not solve the spurs issue, it is useful to widen the read range of the technology, because it has the capability to generate tones at lower frequencies than the ADF4350.

8.5 Do a tracking around the resonance frequency

As it was done for the Matlab software in the chipless reader, a way of assuring that the minimum in the gain graph of the S11 resonates constantly at a certain frequency is doing a tracking around this value.

Once the minimum peak is identified, the PLL must send a signal of a frequency equal to the minimum frequency plus/minus a tracking step set by the user (2 MHz for example) to check if the value of the minimum gain has changed. If this last statement happens to be true, the frequency written on the interface will update and the tracking will be done around that new value. This operation is repeated during a fixed time or for several iterations of a loop. This way, the last value displayed in the interface will be the most accurate identified resonance frequency.

A first testing version of the tracking has been incorporated to the Visual Studio software, but it needs to be tested and characterized.

8.6 Implement a new phase sign detection method

The current reader implements a *homemade* phase sign detection method, based on the next voltage measurement of the AD8302. The method is explained in Section 5.5.1. It is a good technique but when the compared waveforms have a phase difference of 0 degrees, the voltage value outputted by the gain/phase detector depends strongly on the operating frequency, as it is confirmed in the datasheet of the device. It varies around 1.8 V, which causes a confusion when determining if the slope is positive or negative.
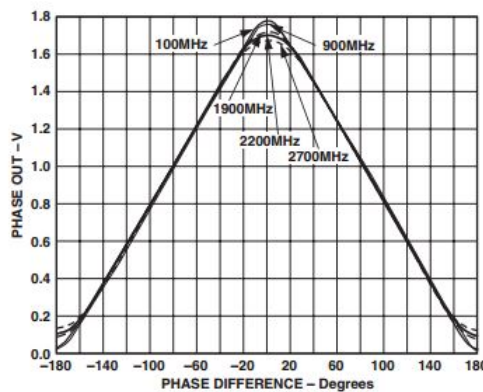
FIGURE 8.8: Phase Graph from the AD8302 Datasheet

In addition, according to the method used so far, if a voltage measurement is followed by a higher number, it is automatically set as a negative phase and if it is followed by a

lower value, the phase is determined as positive. However, if the sweeping step is not very large, consequent voltage measurements can be almost equal or vary only in a decimal. This variation can be randomly either above or below the previous reading, which does not mean that the phase difference is decreasing or increasing that way.

In order to correct this error, it exists the possibility of setting a threshold above which the voltage reading is considered to have increased or decreased. The software will ignore slight variations and the number of wrongly detected phase signs is expected to decrease. The challenge would be to decide the value of that threshold. It can be approximated with some calculations taking into account the wavelength of the waveforms sent and the distance from the antennas to the chipless tag.

8.7   Further Work

The design of the chipless tag reader is successful according to the results obtained after its characterization. Furthermore, one of its main objectives was achieved: it is fully portable if the Power Supply is replaced by a commercial battery of 2.7 V.

The development of the device is based on a non-portable version of a reader, which was used for the redaction of the paper *Chipless Wireless sensor sensitivity analysis for IoT applications*, presented in the European Antenna Conference *EuCap 2017* in Paris, attached to the report.

Furthermore, the reader can be potentially used in numerous applications, such as industrial tools or biomedical instruments to identify the characteristics of tags located under the human skin.

Appendix A

Codes of the ADF435x Application in Visual Studio in C Language

```
1  var driver = new ArduinoDriver(ArduinoModel.UnoR3, true);
```

LISTING A.1: Code to create an ArduinoDriver for Arduino UNO in Visual Studio

```
2      function measurefreespace_Callback(hObject, eventdata, handles)
3
4          if (exist('obj1','var'))==1
5              if isempty(obj1)==0
6                  delete(obj1);
7                  clear obj1
8              end
9          end
10
11          if (exist('obj1','var'))==1
12              delete(obj1);
13          end
14
15          obj1 = instrfind('Type', 'visa-gpib', 'RsrcName', 'GPIB0::17::INSTR', 'Tag', '')
16
17          % Create the VISA-GPIB object if it does not exist otherwise use the object that
18          if isempty(obj1)
19              obj1 = visa('AGILENT', 'GPIB0::17::INSTR');
20              fopen(obj1);
21          else
22              fclose(obj1);
23              obj1 = obj1(1);
24          end
25
26          % Communicating with instrument object, obj1.
27          fprintf(obj1, ':FREQUENCY 868 MHZ');
```

```
28
29          [    ] % Operations to carry out the frequency sweep.
30
31          fclose(obj1);
32          delete(obj1);
33          clear obj1
34      end
```

LISTING A.2: Matlab Code for the Connection to the Signal Generator

```
35  //————————————————Read Analog Voltage Values————————————————//
36      vg = 0;  vf = 0;
37      for (int i = 0;  i < 4;  i++){
38          var ping = driver.Send(new AnalogReadRequest(0));
39          aveg[0, i] = ping.PinValue;
40          vg = aveg[0, i] + vg;
41          var pinf = driver.Send(new AnalogReadRequest(1));
42          aveg[1, i] = pinf.PinValue;
43          vf = aveg[1, i] + vf;
44      }
45      vg = vg / 4;
46      vf = vf / 4;
```

LISTING A.3: Code for the Analog Voltage Readings with the Arduino

```
47  //————————————————————Change of sign of the phase————————————————————
48
49      for (int i = 0;  i < freq - 1;  i++)
50      {
51          if (matriz_g_g[i, 2] < matriz_g_g[i + 1, 2])
52          {
53              matriz_g_g[i, 2] = -matriz_g_g[i, 2];
54          }
55      }
56      if (Math.Sign(matriz_g_g[freq - 1, 2]) == -1)
57      {
58          matriz_g_g[freq, 2] = -matriz_g_g[freq, 2];
59      }
```

LISTING A.4: Code for the Implementation of Phase Sign Detection in C Programmming Language

```
61  //————————————————————Subtraction of the reference————————————————————
62      for (int i = 0;  i < freq - 1;  i++)
63      {
64          // Gain of Tag
65          matriz_g_g_m[freq, 1] = Math.Pow(10, dB / 20);
66          double li_m = matriz_g_g_m[i, 1];
67          //Gain of Reference
```

```
68              matriz_g_g[freq, 1] = Math.Pow(10, dB / 20);
69              double li = matriz_g_g[i, 1];
70
71              // Phase of Tag
72              double deg_m = matriz_g_g_m[i, 2];
73
74              //Phase of Reference
75              double deg = matriz_g_g[i, 2];
76
77              //Polar to Cartesian Coordinates
78              // x
79              matriz_cart[i, 0] = li_m * Math.Cos(deg_m * (Math.PI / 180)) −
80              − li * Math.Cos(deg * (Math.PI / 180));
81              // y
82              matriz_cart[i, 1] = li_m * Math.Sin(deg_m * (Math.PI / 180)) −
83              − li * Math.Sin(deg * (Math.PI / 180));
84
85              //Cartesian to Polar Coordinates
86              // Gain
87              matriz_pol[i, 0] = Math.Sqrt(Math.Pow(matriz_cart[i, 0], 2) +
88              +Math.Pow(matriz_cart[i, 1], 2));
89              // Phase
90              matriz_pol[i, 1] = (180/ Math.PI)*
91              *Math.Atan(matriz_cart[i, 1] / matriz_cart[i, 0]);
92          }
```

LISTING A.5: Code for the Implementation of Calibration

```
93  //————————————————Interface Initialization ————————————————
94      Interface form = new Interface();
95      Interface2 form2 = new Interface2();
96
97  //Dashed−Line Grid on Background
98      form.chart_gain.ChartAreas[0].AxisX.MajorGrid.LineDashStyle = System.Windows.Forms.D
99
100     form.chart_gain.ChartAreas[0].AxisY.MajorGrid.LineDashStyle = System.Windows.Forms.D
101
102     form2.chart_phase.ChartAreas[0].AxisX.MajorGrid.LineDashStyle = System.Windows.Forms
103
104     form2.chart_phase.ChartAreas[0].AxisY.MajorGrid.LineDashStyle = System.Windows.Forms
105
106
107 //Axis Titles
108     form.chart_gain.ChartAreas["Gain (dB)"].AxisX.Title = "Frequency (MHz)";
109     form.chart_gain.ChartAreas["Gain (dB)"].AxisY.Title = "Gain (dB)";
110
111     form2.chart_phase.ChartAreas["Phase (  )"].AxisX.Title= "Frequency (MHz)";
112     form2.chart_phase.ChartAreas["Phase (  )"].AxisY.Title= "Phase (  )";
```

LISTING A.6: Initialization of the Interfaces with the Graphics

```
114  //————————————Plot the values in the Interface.cs————————————
115      for (int i = 0; i < freq − 1; i++)
116      {
117          form.chart_gain.Series["Reference Gain"].Points.AddXY(matriz_g_g[i, 0], 20 ∗ Math.Log(m
118
119          form2.chart_phase.Series["Reference Phase"].Points.AddXY(matriz_g_g[i, 0], matriz_g_g[i
120      }
121
122      form.label_gain.Text = "Minimum S11 Freq. = " + matriz_g_g_m[mini_i, 0];
123      form2.label_gain.Text = "Minimum S11 Freq. = " + matriz_g_g_m[mini_p, 0];
124
125      form.Show();
126      form2.Show();
```

LISTING A.7: Plot of one of the Measurements

```
127  //————————————————Minimum Calculation ————————————————————
128      double mini_g = 1;
129      int mini_i = 0;
130      for (int i = 0; i < freq − 1; i++)
131      {
132          if (matriz_pol[i, 0] <= mini_g)
133          {
134              mini_g = matriz_pol[i, 0];
135              mini_i = i;
136          }
137      }
```

LISTING A.8: Code for the Minimum Detection in the Gain

```
138  //————————————————————Phase Jump Detection ————————————————————
139      double mini_p = 0;
140      int mini_1 = 0;
141      for (int i = 0; i < freq − 1; i++){
142          if (matriz_pol[i, 1] >= 0 && matriz_pol[i+1, 1] <= 0) {
143              mini_1 = i;
144              if ((matriz_g_g_m[mini_1, 0] <= (matriz_g_g_m[mini_i, 0] + 10))
145              && (matriz_g_g_m[mini_1, 0] >= (matriz_g_g_m[mini_i, 0] − 10)))
146              {
147                  mini_p = i;
148              }
149          }else if (matriz_pol[i, 1] <= 0 && matriz_pol[i + 1, 1] >= 0) {
150              mini_1 = i;
151              if ((matriz_g_g_m[mini_1, 0] <= (matriz_g_g_m[mini_i, 0]))
152              && (matriz_g_g_m[mini_1, 0] >= (matriz_g_g_m[mini_i, 0] − 10)))
```

```
153                 {
154                     mini_p = i ;
155                 }
156             }
157         }
```

LISTING A.9: Code for the Phase Jump Detection

```
158    //————————————Read Analog Voltage Values————————————//
159        vg = 0; vf = 0;
160        var ping = driver.Send(new AnalogReadRequest(0));
161        aveg[0, 0] = ping.PinValue;
162        vg = aveg[0, 0] + vg;
163        var pinf = driver.Send(new AnalogReadRequest(1));
164        aveg[1, 0] = pinf.PinValue;
165        vf = aveg[1, 0] + vf;
```

LISTING A.10: Voltage Readings with 1 measurement

Appendix B

Chipless Wireless Displacement Sensor Sensitivity Analysis for IoT Applications

Chipless Wireless Displacement Sensor Sensitivity Analysis for IoT Applications

Ruben Campo[1], Fátima Villa[1], Josu Catalina[1], Lucía Merino[1], Miguel Sanz[1], Daniel Valderas[2]

[1]Electricity, Electronics and Control Department, Tecnun, University of Navarra, San Sebastian, Spain

[2]Electronics and Communications Department, Ceit and Tecnun, University of Navarra, San Sebastian, Spain, dvalderas@ceit.es

Abstract - **This paper shows a wireless chipless displacement sensor for IoT applications. It is designed for environments where only an on-off position detection is required. The results shows that an oscillation of 30 mm can be detected at a 30 cm distance giving a 10% resolution. Static and dynamic tests demonstrate that the number of oscillations around a certain position can be counted.**

Index Terms - **wireless chipless sensors, radar, passive sensors, CPW**

I. INTRODUCTION

WIRELESS Passive sensors based on backscattered signals have arisen as a promising add-on to RFID technology[1][2]. Even if no battery is present in RFID tags, the IC provides information for identification and sensing with digital resolution. However, quite often only an on-off threshold detection is required in many low resolution applications. In these cases, the way is paved for the elimination of tag electronics by chipless technology based on backscattered signal analysis. Furthermore, this technology could be a solution for high temperature environments (not compatible with silicon) and will reduce price for massive numbers of tags.

When it comes to designing displacement sensors, it must be taken into account that these devices typically operate at DC, translating a change in magnitude (e.g. position) to a difference in voltage at their terminals. However, for the desired application and due to the fact that the sensors are chipless and wireless, they need to work at RF [3]. The aim of this paper is to show the results obtained on the research of a wireless chipless displacement sensitive element useful for these environments where only an (ON-OFF) position is needed. The sensitive element has been designed in order to work at a frequency of 868 MHz due to its similarity to the European RFID frequency. It is demonstrated that when acting as load of a patch antenna it becomes a chipless, wireless displacement sensor.

The paper also provides the necessary theoretical background required to analyze the sensitivity of such a system and it assesses the displacement oscillations in a dynamic regime based on the changes of the phase of the backscattered signal at that frequency.

II. METHODOLOGY

A. Wireless phase detection principle

Reflection coefficient (S_{11}) is extracted by a VNA when its port is connected through a cable to a transmitting antenna facing a possible target or chipless sensor. (See Fig. 1)

Fig. 1 System overview

This S_{11} from the VNA on the reader side includes the reflection not only from the transmitting antenna itself but also from the surrounding environment, even in the absence of a target (sensor side). This value is taken as a normalization factor S_{11} extracted by the reader when the target is not present. When a target is added, e.g., a patch antenna or a dipole antenna with a changing load, a new S_{11}' is measured so that the normalized result will be:

$$S_{11N} = S_{11}' - S_{11}$$
$$|S_{11N}|\angle \varphi_N = |S_{11}'|\angle \varphi' - |S_{11}|\angle \varphi \qquad (1)$$

1) Reference plane for phase measurement

The value of the normalized phase of the S11, φ_N, at the operating frequency depends on the calibration of the VNA and therefore on the distance between the target and the transmitting antenna. Although the φ_N value changes with the calibration and the distance, the relative difference between two values corresponding to two states would remain constant (Fig.2)
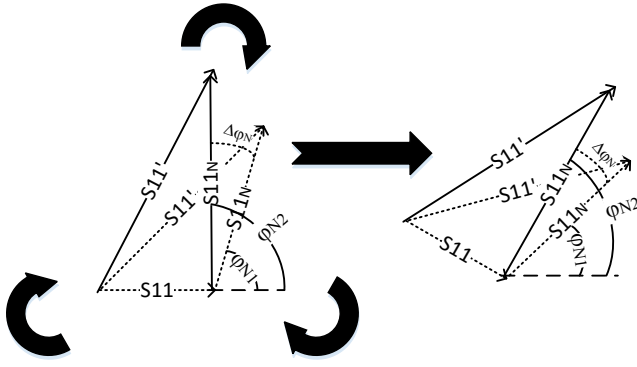
Fig.2. Effect of the change in reference plane (calibration) in the measured ΔφN

Therefore, the parameter to be analyzed is

$$\Delta\varphi_N = \varphi_{N1} - \varphi_{N2} \qquad (2)$$

That is why the ideal sensor will consist on the comparison between two states. And $\Delta\varphi_N$ should be independent on distance, calibration and even setup.

2) Theoretical backscattered phase

This effect is also analyzed theoretically, based on the power transfer given by the Friis equation.

The power budget for a monostatic setup in free space is calculated according to the following formula in dB:

$$P2 = P1 + Gt + 10\log\frac{1}{4\pi d^2} + RCS + 10\log\frac{1}{4\pi d^2} + \frac{\lambda^2}{4\pi} * Gt$$

$$S11 = Gt + 10\log\frac{1}{4\pi d^2} + RCS + 10\log\frac{1}{4\pi d^2} + \frac{\lambda^2}{4\pi} * Gt \quad (3)$$

Where P_2 is the backscattered power by the chipless sensor at the transmitter side, P_1 is the transmitting power, both terms $10\log\frac{1}{4\pi d^2}$ correspond to the free space losses in the incidence way and in the reflection way, d is the distance between the reader and the chipless sensor, Gt is the gain of the reader antenna and RCS is the Radar Cross Section of the target, given by:

$$RCS = \frac{\lambda^2 Gr^2 Ra^2}{\pi|Za+Zc|^2} \qquad (4)$$

Where Gr is the gain of an antenna put as a target at the receiver side, Ra is that antenna's resistance, Za is its impedance and Zl (is the impedance of the sensitive element).

Expression (4) comes from the fact that P_a is the power collected by the target antenna and P_{re-rad} is the power re-radiated by the same antenna [3] [4].

$$Pa = S * Ae \qquad\qquad Pa = Pt\frac{\lambda^2 GrGt}{(4\pi)^2 d^2} \qquad (5), (6)$$

$$P_{re-rad} = K * Pa * Gr \qquad (7)$$

S refers to the power density and Ae to the effective area

$$K = (1 - \tau *)^2 = \frac{4Ra^2}{|Za+Zl|^2} \qquad (8)$$

K is the power dissipated in the antenna resistance and $\tau *$ is the reflection coefficient between the target and the sensitive element.

$$RCS = \frac{P_{re-rad}}{S} = K * Ae * Gr = \frac{\lambda^2 Gr^2 Ra^2}{\pi|Za+Zl|^2} \qquad (9)$$

The only parameter in equation (3) that has an effect on the phase $\Delta\varphi_N$ of the S11 is K. If this constant is analyzed from the point of view of the signal, instead of power, the equation that defines K is:

$$(1 - \tau *) = \sqrt{K} = \frac{2Ra}{|Za+Zl|} \qquad (10)$$

Therefore, the phases of K can be calculated with the Euler's formula.

$$\Delta\varphi_N = \arctan\left(\frac{Im(\sqrt{K})}{Re(\sqrt{K})}\right) \qquad (11)$$

The term "1" in the expression $(1 - \tau *)$ corresponds to the reflection for a dipole. If the general expression for any other antenna is taken, the equation would be the following:

$$(As - \tau *) = \frac{2Ra}{|Za+Zl|} \qquad (12)$$

As is a complex parameter independent of the load that only depends on the antenna.

The influence of As is clearly important in the phase of the S11, which is present when it comes to comparing the results obtained in the measurements and the theoretical ones.
As can been calculated using equation (13)

$$As = \frac{\left(\frac{S11N,Zl2}{S11N,Zl1}\right)}{\left(\frac{S11N,Zl2}{S11N,Zl1}\right) - 1} \qquad (13) [5]$$

S11N are readouts taken by normalizing by free space (eq 1) and using two measurements of the sensor.

III. CHIPLESS DISPLACEMENT SENSOR DESIGN

1) Displacement sensor

A co-planar waveguide (CPW) with a length of $\lambda/4$, working at a frequency of 868 MHz and with an impedance of 50 Ω is designed in CST Microwave Studio and manufactured in FR4 thickness of 1.6mm.

The CPW has a ground plane beneath (Fig.3). The metal strip that short-circuits the CPW in (Fig.3) models the contact point of a sliding metal object. We want to get high impedance variation at the input port when one sliding object that short-circuits the CPW moves. When the short-circuit it is at the further end is an open circuit at the input port; and as the sliding object progresses over the surface, the impedance turns to a short-circuit.

Fig. 3 Target based on a CPW at 868 MHz

2) Used antenna

The used antenna is a patch one with impedance of 40,44 – 24,4i Ω implemented in FR4 with a thickness of 1.6mm .The antenna is designed to work at 868 MHz as we can see the S11 is less that -10dB at the desired frequency with bandwidth of 12 MHz. That bandwidth is between 856,5 MHz and 868,7 MHz.

IV. IMPLEMENTATION AND RESULTS

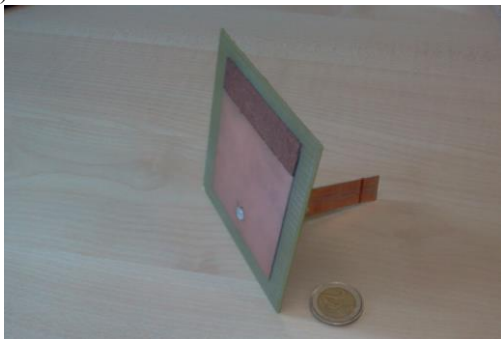The sensor is connected as a target to the patch antenna (Fig. 4)

Fig. 4 Position sensor implementation to the patch antenna

1) Static set up

The objective is to measure the reflection coefficient (S11) with a VNA, locating the setup at a fixed distance from the reader antenna (50 cm) (Fig 1), and analyzing the changes on its phase φ_N.

When the sensor is short circuited at different positions along its length (λ/4 track), the load of the sensor varies for the different intermediate states. This change has a direct influence on the measured S11's phase at the reader.

The analyzed intermediate states of the short circuits are schematically shown in the sketch:
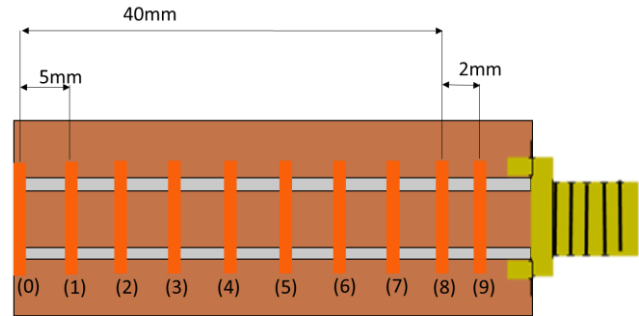

Fig. 5 Intermediate states of metallic pieces in the sensor

The input impedances of the sensor in the considered positions are shown in the following table:

State of the metallic piece	Distance from the side without connector to the metallic piece	Real part of the impedance	Imaginary part of the impedance
(0)	0	45	-356
(1)	5	2,72 k	1,4 k
(2)	10	16,6	262,3
(3)	15	3,72	137,55
(4)	20	1,44	90,05
(5)	25	668 m	63,7
(6)	30	280 m	44,18
(7)	35	180 m	31,7
(8)	40	110 m	22,6
(9)	42	97,05 m	17,84

Table. 1 Input impedances for the CPW for shortcircuit positions illustrated in Fig.5

It can be observed that the impedance of the sensor with the metallic piece located at a distance of 5mm measured from the further end is very close to the open circuit. As the metallic pieces moves, from (0) to (9), the sensor's impedance moves progressively in a counter-clock wise way in the smith chart from the open circuit (1) to positions closer to the short circuit (9). The sensor has the behavior shown in Fig.6
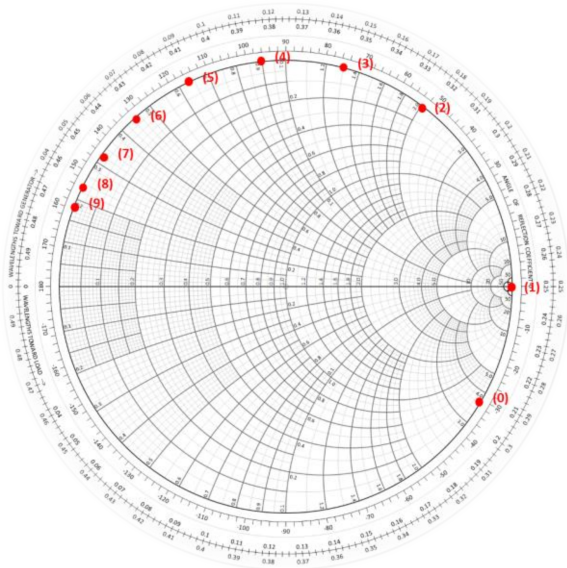
Fig. 6 Smith Chart with the impedances of the sensor

As has been calculated using equation (13). Comparing states 3 and 4, the obtained value is *As*= 0, 54295 + 0,60405i. With the new value, the theoretical phase of √*K* within the sensor has been plotted (Fig.7).
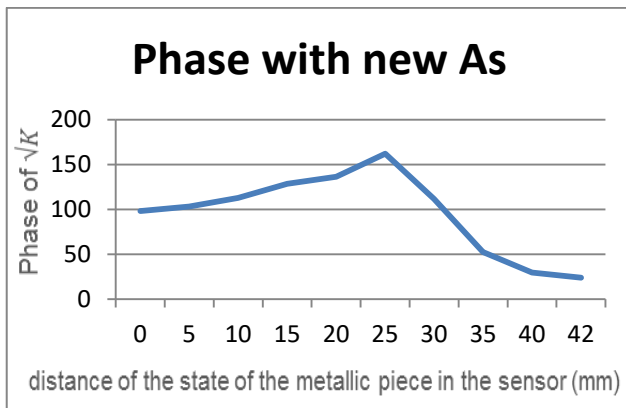

Fig. 7 Theoretical phase with As as comparison of state 3-4

With the Agilent E5062A VNA the experimental phase was measured when the sensor is short circuited at different positions (Fig.8)
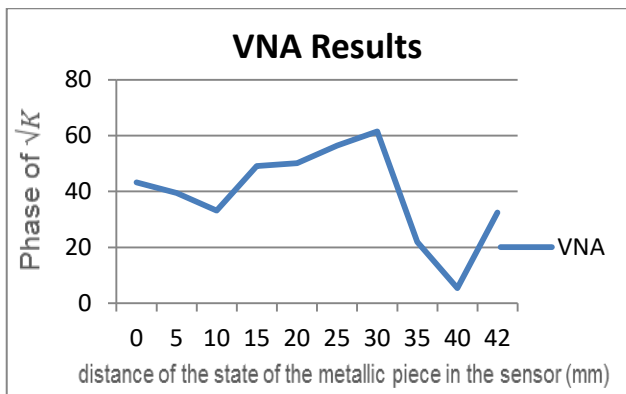

Fig. 8 Measured phase with VNA

We can see that both, the theoretical and experimental phases, follow the same tendency with a useful region between 5 and 40 mm.

2) Dynamic test set up

In this section a real time displacement is dynamically monitored. With that in mind a wider sensor was built to enable a sliding object moving along. A finger contact between strips was used instead of a metallic contact for the difficulty to implement a sliding metallic piece as a reliable short-circuit. Due to mechanical needs a SMA male-male adapter was introduced. The sensor element input impedances under these circumstances are the following:

State of the contact	Distance from the side with adapter to the finger contact	Real part of the impedance	Imaginary part of the impedance
(0)	0	80	120
(1)	5	56	112
(2)	10	36	100
(3)	15	25	87
(4)	20	25,6	89
(5)	25	17	67
(6)	30	5,9	59,3
(7)	35	7,2	79
(8)	40	5,3	48,7
(9)	42	2,91	41,7

Table. 2 Input impedances for the CPW for shortcircuit with connector positions illustrated in Fig.5

Eq 13 allows calculating As by taking load pairs. In our case, three pairs are taken:

- Comparing state (2 and 3) *As*: 0,54295 + 0,60405i
- Comparing state (6 and 7) *As*: 0,77916 + 1,222i
- Comparing state (7 and 8) *As*: 0,28489 + 2,3007i

As it can be seen, there is uncertainty of repeatability as we are using a finger as contact.
With these *As* the theoretical phase has been plotted for each *As,* Fig.9 for 2-3 comparison, Fig.10 for 6-7 and Fig.11 for 7-8.
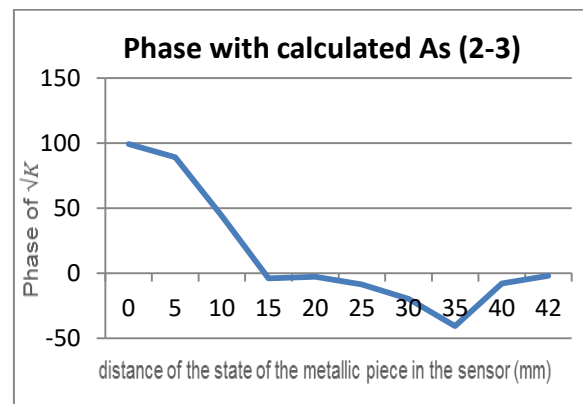

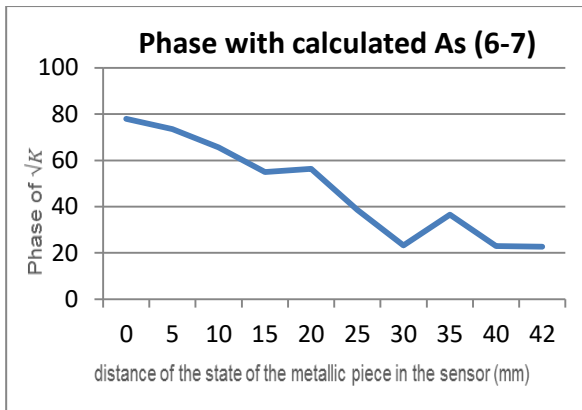*Fig. 9 Theoretical phase with As as comparison of state 2-3*

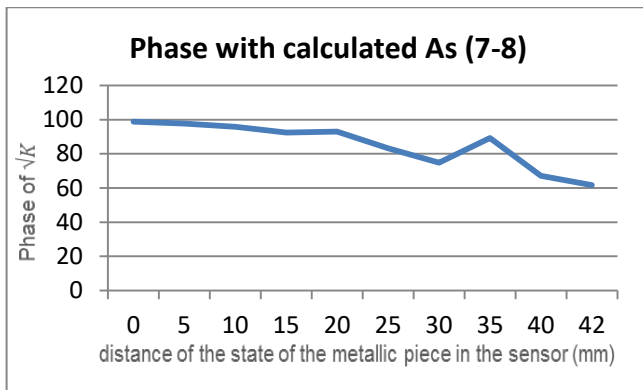Fig. 10 Theoretical phase with As as comparison of state 6-7

Fig. 11 Theoretical phase with As as comparison of state 7-8

As it can be observed, the linearity in 30mm (position 6) changes and therefore the experimental measurements have been taking this fact into account. A bistatic reader is built that consists of an AD8302 gain and phase comparator, Arduino, PA MAX2235 and two high gain antennas (8dBi) (not shown for brevity). The parameter φ_N is recorded in real time while a finger oscillates three times within 30 mm over the sensor at a distance of 30cm between the reader and the wireless chipless sensor. Results are shown in Fig.12.
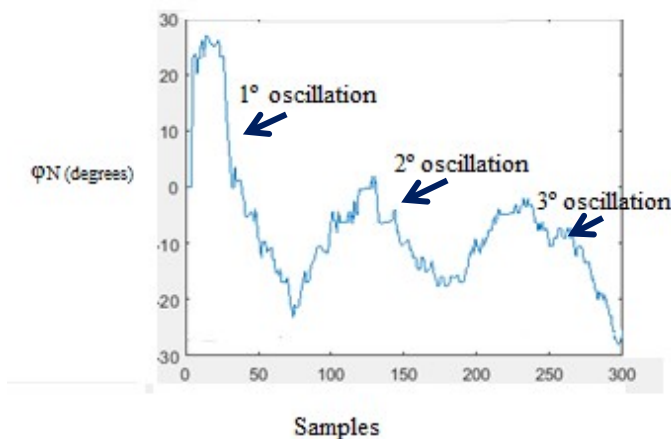
It is possible to see that every phase cycle corresponds to an oscillation back and forth over the CPW sensor. Once the signal is filtered we can count oscillations of sliding objects at a distance defined as predicted by the theoretical analysis.

V. CONCLUSIONS

A chipless wireless displacement sensor has been introduced that can cover a wide range of IoT applications, even with low-resolution. It is accurate for environments with harsh conditions when high resolution is not required. The methodology employed has been the wireless phase detection principle, based on the measurement of the backscattered signal. The obtained results have been compared with theoretically calculated data. The results show that an oscillation of 30 mm can be detected and the number of cycles counted at a 30 cm distance giving a 10% resolution.

REFERENCES

[1] S. Capdevila, L. Jofre, J. Romeu. Passive RFID based sensing.
[2] Abdul Ali Babar, , Sabina Manzari, ,Lauri Sydänheimo, , Atef Z. Elsherbeni, and Leena Ukkonen,. Passive UHF RFID Tag for Heat Sensing Applications
[3] Impedance Matching concepts in RFID Transponder Design. Article by K.V.S. Rao, Pavel V. Nikitin, Sander F. Lan
[4] Theory and Measurement of Backscattering from RFID Tags. Article by Pavel V. Nikitin and K.S.V. Rao
[5] Huan-Yang Chen, Yue Weng Mak, Sangchul Bae, Atul Bhadkamkar, and Daniel W van der Weide. Wireless Impedance Measurement of UHF RFID Tag Chips
[6] Mario J. Cazecaa, Joey Meada, Julie Chenb, Ramaswamy Nagarajana. Passive wireless displacement sensor based on RFID technology
[7] N. C. Karmakar, "Chipless RFID Reader Architecture", Artech House,   2013, p 71 ,
[8] Constantine A. Balanis. Antenna Theory Analysis and design. Third Edition

Fig. 12 Experimental phase vs samples with finger and 30mm limit

Bibliography

[1] Rubayet E-Azim, Prasanna Kalansuriya, Nemai Chandra Karmakar, Randika Koswatta. *Chipless RFID Reader Architecture*. Artech House Publishers, 2013.

[2] Dominique Paret. *RFID at Ultra and Super High Frequencies: Theory and application*. Wiley, November 2009.

[3] Stevan Preradovic, Isaac Balbin, Nemai Chandra Karmakar and Gerhard F. Swiegers. *Multiresonator-Based Chipless RFID System for Low-Cost Item Tracking*. IEEE Transactions on Microwave Theory and Techniques, Vol. 57, No. 5, May 2009.

[4] Stevan Preradovic, Isaac Balbin, Nemai Chandra Karmakar and Gerhard F. Swiegers. *Exploring Arduino: Tools and Techniques for Engineering Wizardry*. Wiley, August 2013.

[5] Miren Azkarate, Josu Catalina, Lucía Merino, Miguel Sanz, Fátima Villa, Rubén Campo, Noemí Pérez, Daniel Valderas. *Chipless Wireless sensor sensitivity analysis for IoT applications*. Antennas and Propagation, 2017. EuCAP 2017. The Second European Conference on

[6] Rattapong Suwalak, Chuwong Phongcharoenpanich, Prayoot Akkaraekthalin and Danai Torrungrueng. *A Radar-Cross Section of a passive tag on dielectric material in an RFID sensor application*. Electrical Engineering/Electronics, Computer, Telecommunications and Information Technology (ECTI-CON), 2015 12th International Conference on

[7] Nemai Chandra Karmakar. *Tag, You're It!*. IEEE Microwave Magazine, July 2016.

[8] Audrey Pouzin, Tan-Phu Vuong, Smail Tedjini, Jacques Perdreau, Lionel Dreux *Measurement Of Radar Cross Section For Passive UHF RFID Tags*. Antennas and Propagation, 2007. EuCAP 2007. The Second European Conference on

[9] Audrey Pouzin, Tan-Phu Vuong, Smail Tedjini, Maxime Pouyet, Jacques Perdereau. *Determination of the Activation Range of Passive UHF RFID Transponders by Radar Cross-Section Measurements*. Microwave Conference, 2009. EuMC 2009. European

[10] *RFID Reader for Multiscatterer Based Chipless RFID Tags.* Cochin University of Science and Technology.

[11] Rubén Campo Nogales. *Chipless Wireless Displacement and Proximity Radar Sensors by Backscattered Phase Modulation.* Tecnun-University of Navarra, San Sebastián, 2016.

[12] Cao Wenda. *Chipless wireless sensor reader design and characterization.* Queen Mary University of London and Beijing University of Posts and Telecommunications (BUPT), June 2017.

[13] Data sheet of PLL (ADF4350) Available at:
`http://www.analog.com/media/en/technical-documentation/data-sheets/ADF4350.pdf`

[14] Data sheet of PLL Eval Board (EVAL-ADF4350EB1Z) Available at:
`http://www.analog.com/media/en/technical-documentation/user-guides/UG-109.pdf`

[15] User Guide of PLL Software Available at:
`http://www.analog.com/media/en/technical-documentation/user-guides/UG-476.pdf`

[16] Data sheet of Gain/Phase Comparator (AD8302) Available at:
`http://www.analog.com/media/en/technical-documentation/data-sheets/AD8302.pdf`

[17] Data sheet of Gain/Phase Comparator Eval Board (EVAL-AD8302EB) Available at:`http://pdf.eicom.ru/datasheets/analog_devices_pdfs/ad8302eb/ad8302eb.pdf`

[18] Data sheet of Arduino Redboard (SparkFun RedBoard) Available at:
`https://cdn.sparkfun.com/datasheets/Dev/Arduino/Boards/Redboardv1.pdf`

[19] Power Divider Available at:
`https://www.microwaves101.com/encyclopedias/wilkinson-power-splitters`

[20] Datasheet of ZGBDC6-362HP+ Bidirectional Coupler Available at:
`http://www.datasheets360.com/pdf/-6467931768890326631`

[21] Datasheet of ZFBDC20-61HP+ Bidirectional Coupler Available at:
`https://www.minicircuits.com/pdfs/ZFBDC20-61HP+.pdf`

[22] Standard Error Calculations:
`http://es.wikihow.com/calcular-el-error-est%C3%A1ndar`

[23] SparkFun RedBoard Information Available at:

`https://learn.sparkfun.com/tutorials/redboard-vs-uno` and

`https://learn.sparkfun.com/tutorials/redboard-hookup-guide?_ga=2.95434713.419480221.`

[24] Arduino Driver Available at:

`https://github.com/christophediericx/ArduinoDriver`

[25] Tutorial of Redboard Available at:

`https://learn.sparkfun.com/tutorials/redboard-vs-uno`

`https://learn.sparkfun.com/tutorials/redboard-hookup-guide?_ga=2.95434713.`

`419480221.1496516852-552318429.1489996411`

[26] ADF435x Software Available at:

`https://ez.analog.com/thread/13743`